Construction of Artificial Metalloproteins: Noncovalent Insertion of Metal Complex Catalysts into Protein Cavities

Masataka Ohashi

DOCTOR OF PHILOSOPHY

Department of Structural Molecular Science
School of Mathematical and Physical Science
The Graduate University for Advanced Studies

2002

CONTENTS

PART I

GENERAL INTRODUCTION

In the past decade, several approaches for the construction of artificial proteins have been reported. For example, utilization of catalytic antibody[1] and molecular evolution of enzymes by random mutagenesis have been developed.[2-4] Although those approaches have succeeded in constructing artificial biocatalysts, it is still difficult to get their catalytic activities as high as the native enzymes. Therefore, alteration and/or improvement of enzymatic functions of metalloproteins and metalloenzymes have been a subject of intense studies.

Construction of artificial metalloproteins is one of the most interesting subjects in inorganic biochemistry since metalloproteins play important roles in biological system. Among the metalloproteins, heme proteins have been investigated very well because of the importance and variety of their enzymatic reactions. For instance, myoglobin (Mb) realizes reversible fixation of an oxygen molecule with imidazole of His64 and heme iron (Fig. 1 a). Cytochrome $P450_{cam}$ catalyzes selective oxidation of *d*-camphor (cam) by utilizing Tyr96 to fix it (Fig. 1 b). Furthermore, His105 and Glu183 play a role of the acid-base catalyst in Chloroperoxidase (CPO) (Fig. 1 c). If we are able to control their chemical functions, it will be possible to use them as biocatalysts or sensors in medical and industrial fields. Therefore, the conversion of the biological functions of metalloproteins, especially heme proteins, has been performed by different approaches; direct evolution of heme enzymes, exon shuffling of hemoglobin, rational design of metalloproteins, modification of a heme prosthetic group, and interaction of proteins with metal complexes.

Directed evolution of heme enzymes

Recently, a number of heme enzymes have been the targets of directed evolution. The functional conversion of $P450_{cam}$, P450 BM-3, CPO and cytochrome *c* peroxidase (CcP) has been challenged and oxidations of substrates that the wild-type enzymes are incapable of oxidizing were reported. In addition, the stability of a fungal peroxidase (CiP) at high pH and high temperature as well as oxidative degradation has been dramatically improved. For example, Joo *et al*. have reported a successful application of the directed evolution.

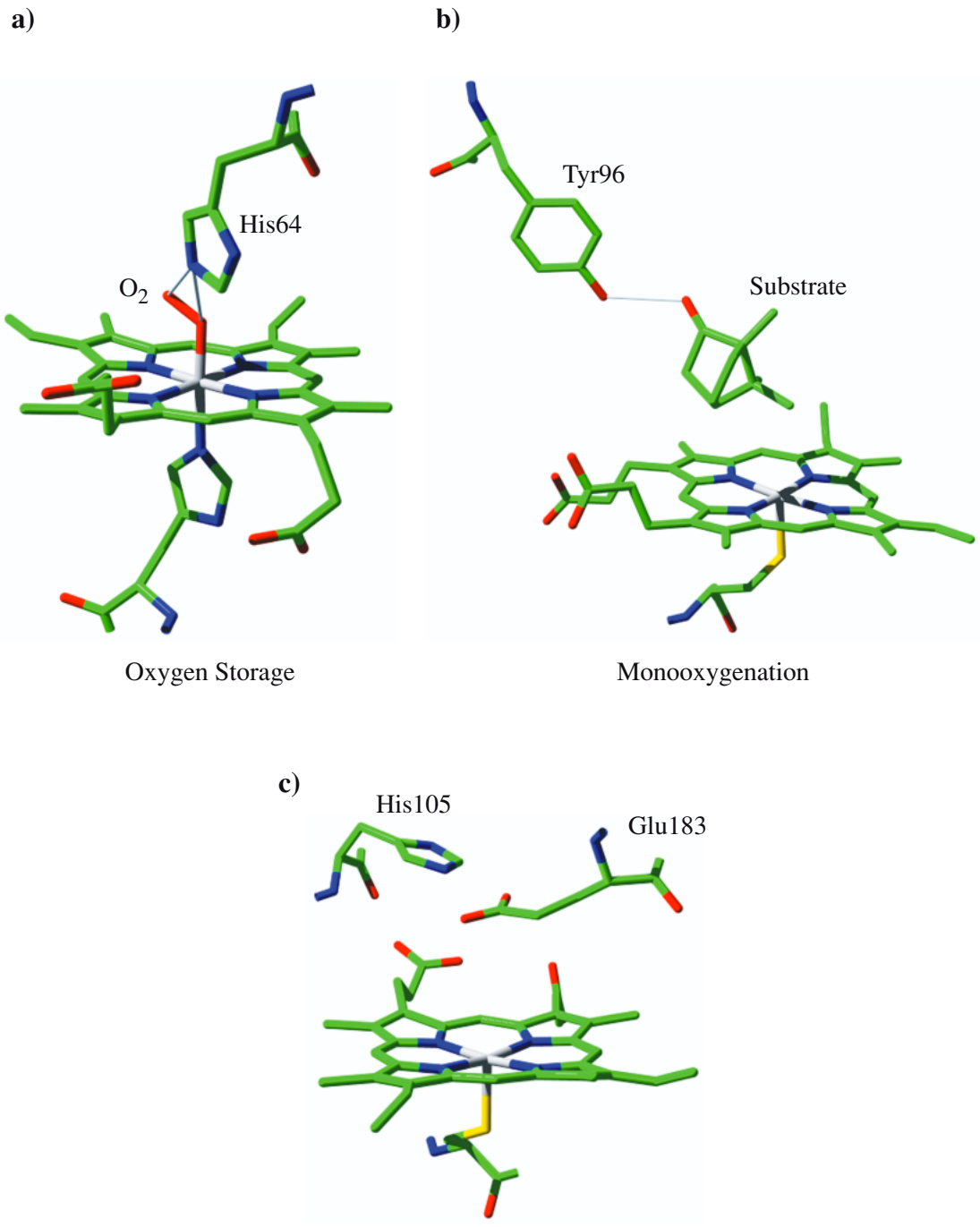

Figure 1. Active site structures of heme proteins; a) Mb, b) $P450_{cam}$, and c) CPO

They have prepared approximately 200,000 random mutants of $P450_{cam}$ co-expressed with horseradish peroxidase (HRP1A6) were screened for H_2O_2-dependent naphthalene hy-

droxylation by fluorescence digital imaging. The resulting mutant has shown 20-fold improvement in naphthalene hydroxylation activity over the wild type.[5] Li *et al*. have developed P450 BM-3 mutants, engineered by a combination of the rational design and directed evolution, that are capable of hydroxylation of indole to produce indigo and indirubin.[6] Rai *et al*. have developed CPO mutants by directed evolution that are resistant to the suicide inactivation. Mutants resistant to the inactivation were identified by the chlorination activity of the CPO mutants immediately after the styrene oxidation by H_2O_2.[7] Johnson *et al*. have prepared CcP mutants having efficient activity either for guaiacol or for ABTS oxidation by directed evolution. The most active mutant shows 23-fold increase in ABTS oxidation, whereas the activity against guaiacol is within 20% of the activity of wild-type CcP.[8] Although the catalytic activities of these heme enzyme mutants increased for non-natural substrates, the catalytic activities for native substrates such as *d*-camphor, cytochrome *c*, and so on were dramatically decrease.

On the other hand, Cherry *et al*. have also employed two parallel approaches; site-directed mutagenesis based on the structure-function consideration and directed evolution for the heme peroxidase from CiP, to prepare a mutant suitable for use as a dye-transfer inhibitor in laundry detergent. The best of them shows 174-fold increase in thermal stability and 100-fold increase in peroxide dependent heme destruction than the native enzyme.[9] An important goal for the directed evolution method is to prepare heme protein mutants whose activities for non-native substrates are comparable to or exceed that for the native substrates.

Exon shuffling of Hemoglobin

Exon shuffling is also an attraction approach for constructing artificial metalloproteins. The exon in DNA is the part in DNA for the transcription into RNA and finally affording the protein. Go investigated the correlation of a DNA exon region with a protein structure unit in hemoglobin.[10] On the basis of Go's conclusion, Wakasugi *et al*. have replaced the M4 module in the β-globin of human hemoglobin with that in the α-globin by mutagen-

esis and the resulting chimera βα-subunit was prepared. They showed that the chimera βα-subunit binds exclusively to the β-subunit instead of the α-subunit without large structural change in the heme vicinity.[11] Thus, the exon shuffling has been demonstrated to be a powerful method to construct artificial proteins.

Rational design of heme enzymes

While directed evolution and exon shuffling of heme enzymes have been focused on evolutional aspects of natural proteins, studies on the rational design of the heme proteins have been emphasizing the development of biocatalysts. There are two directions for the rational design of heme enzymes: one is the construction of enzyme active sites by mimicking the active site structures of peroxidases and the other is the enhancement and alteration of enzymatic reactions. Several studies have been made on the functional alteration of Mb by site-directed mutagenesis. Mb is a small globular heme protein that serves as an oxygen carrier/storage in many biological systems. Since the system for the preparation, purification, and characterization of Mb and their various mutants is well established, it has been often used for the construction of artificial enzyme. For instance, in order to express peroxidase activities into Mb, a general acid-base catalyst was introduced into the distal site of Mb, i.e., Phe43 and His64 were replaced by histidine and leucine, respectively (F43H/H64L Mb). As expected, the double mutation increases the oxidation activity by 11-fold relative to that of wild-type Mb. Furthermore, the distal histidine was replaced with aspartate (H64D Mb) to mimic the active site of CPO and to terminate the electron flow from oxidizable amino acids such as tyrosine and tryptophan to a porphyrin radical. The resulting mutant gave its compound I as the active intermediate species by the reaction with H_2O_2 (Fig. 2 a) and exhibits high reactivity than the wild type.[12] Very recently, Hara *et al*. have succeeded in oxidizing the aromatic ring of tryptophan by introducing tryptophan close to the heme (Fig. 2 b). The oxidation proceeded almost stoichiometrically, indicating that compound I of Mb mutants is capable of carrying most of the P450-catalyzed monooxygenations.[13] On the other hand, Lu *et al*. have constructed a

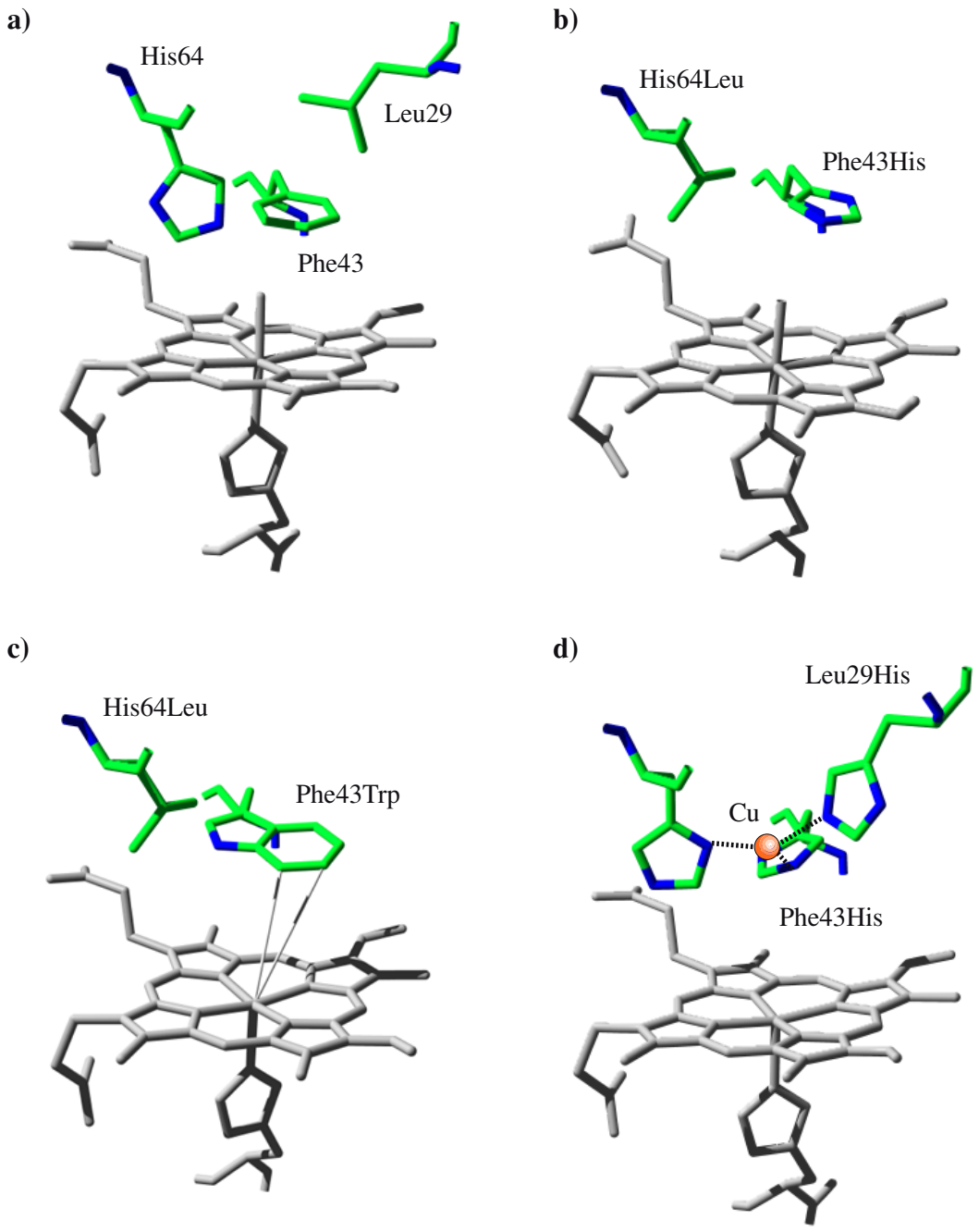

Figure 2. Site-directed mutagenesis of Mb; a) crystal structure of wild-type Mb, b) crystal structure of F43H/H64L Mb mutant, c) calculated structure of F43W/H64L Mb mutant based on computer modeling and energy minimization, and d) model of Heme-Cu oxidase by L29H/F43H Mb mutant based on computer simulation

heme-Cu oxidase active site into Mb by introducing two histidines at position -29 and -43. Distal histidine 64 in Mb worked together with two histidines (His29 and 43) to bind a Cu ion (Fig. 2 c).[14] These concepts are very instructive to design artificial metalloproteins.

Modification of the heme prosthetic group

Heme modification has also been recognized as an approach for the introduction of new functions into hemoproteins. Since the heme in Mb has been fixed in the cavity by noncovalent interaction, it is possible to take the heme out of Mb under denature conditions.[15] Thus, it is possible for Mb to reconstitute with metal substituted or chemically modified hemes in order to add a new function or improve the oxygen affinity. By these modifications, the heme iron in Mb was replaced with Mn,[16] Co,[17] Zn,[18] Ru,[19] and so on. Structural, spectroscopic, and electrochemical properties of metal substituted Mbs have been investigated. In particular, the crystal structure of Co substituted Mb has shown its structure similar to the native Mb structure.[20] Redox potential and its slow electron transfer suggested that it can be used as a catalyst for C-C bond formation (Fig. 3 a).[21] Furthermore, chemically modified hemes have been attempted to introduce new functions to Mb. For instance, to create an artificial binding domain on the Mb surface, a modified heme bearing eight carboxylates bound to the propionate side chains has been inserted into apo-Mb (Fig. 3 b). The eight branched carboxylates have worked as an interface to interact with other proteins or small molecules. The reconstituted Mb has shown a peroxidase activity since the branched carboxylates construct the hydrophobic substrate-binding site on a surface of Mb. In the case of zinc substituted carboxylates branched heme, the electron transfer has occurred from the reconstituted Mb to methyl viologen or cytochrome *c* through the branched carboxylates interface.[22,23] On the other hand, Neya *et al*. have reported the first analysis for iron etiocorrphycene substituted Mb to reveal the effect of the porphyrin skeleton deformation on oxygen binding. The etiocorrphycene reconstituted Mb exhibits extremely lower affinities for O_2 and CO as compared with the native protein. The functional anomaly was ascribed to the geometric strain on the iron (II) atom in the

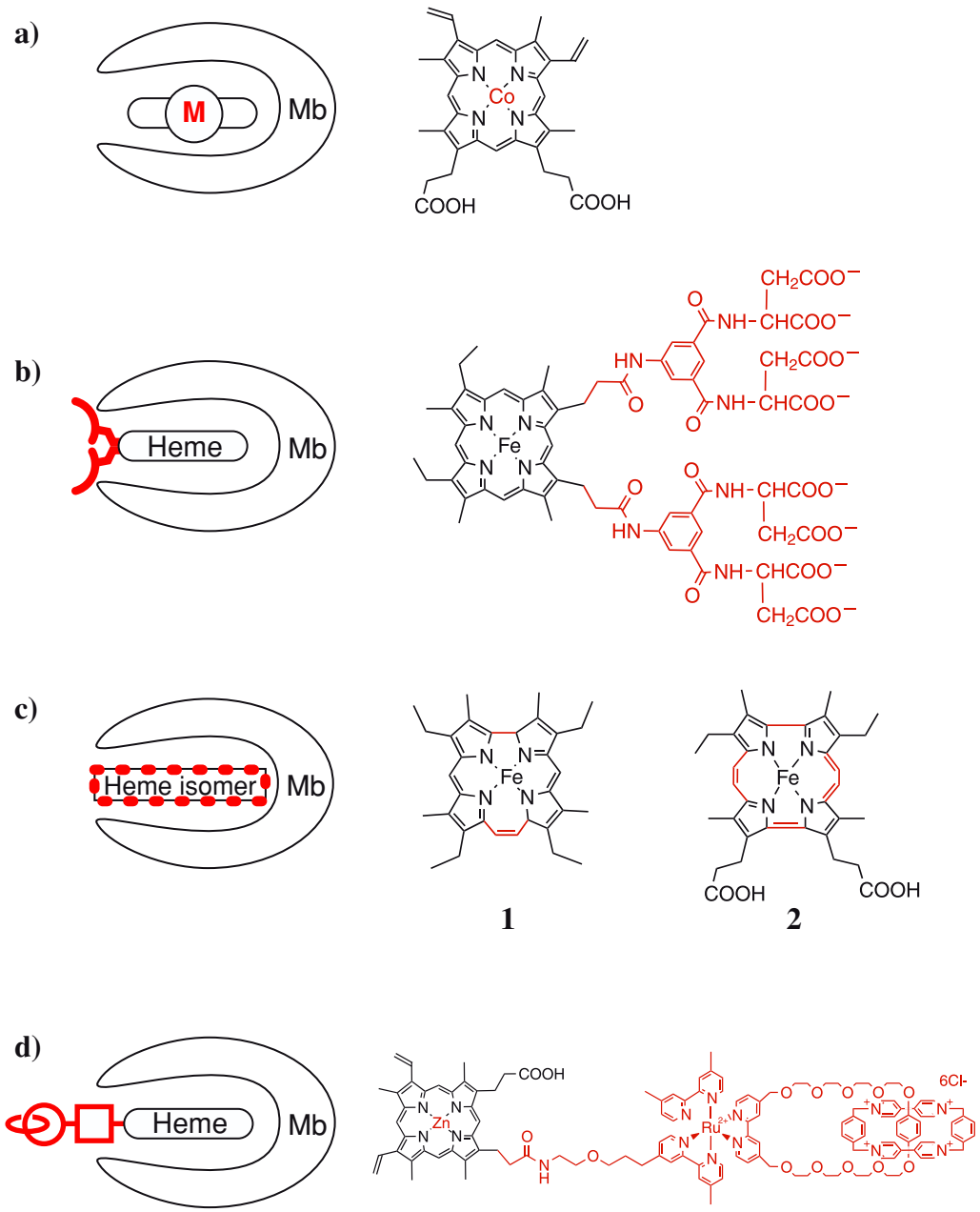

Figure 3. Reconstitution of heme proteins; a) metal substitution heme, b) heme ligand modification, c) heme structural isomer, and d) electron donor-sensitizer-acceptor triads

trapezoidal coordination core of corrphycene (Fig. 3 c-1).[24,25] Hayashi *et al*. have also reported artificial Mbs reconstituted with iron porphycene, a structural isomer of iron porphyrin. The reconstituted Mb indicated a 1,400-fold increase in oxygen affinity (Fig. 3

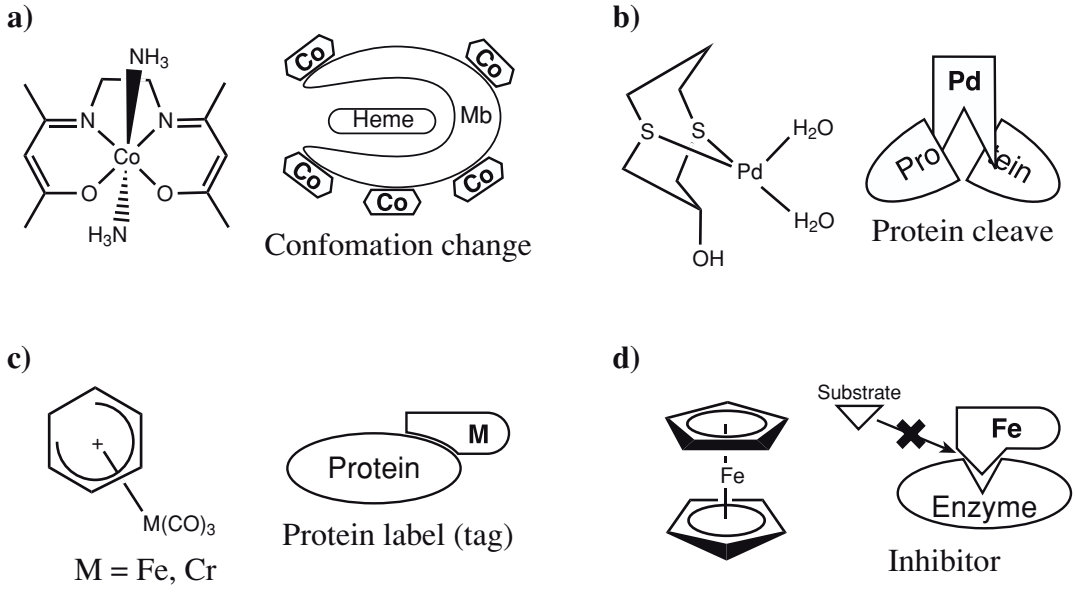

Figure 4. Interaction between metal complexes with proteins

c-2).[26] In order to construct artificial photosynthetic reaction centers (PRCs) on a Mb surface, a chemically modified Zn heme having ruthenium tris(2,2'-bipyridine) moiety as a sensitizer was mechanically linked (in catenane-type) with a cyclobis(paraquat-*p*-phenylene) unit as an acceptor. The donor-sensitizer-acceptor triad was reconstituted with apo-Mb and it has shown a long-lived charge-separated state similar to natural PRCs.[27,28] The reconstitution approach by metal substituted or chemically modified hemes is, therefore, a powerful method, and there are several successful examples in the functional conversion of Mb. However, syntheses of very complicated modification parts are sometimes very hard to proceed.

Utilization of a noncovalent interaction of metal complexes with proteins

Although there are many reports on the interaction between metal complexes and proteins, most of them have focused on structural perturbation, site-specific cleavage, protein labeling, inhibition of enzymatic activities (Fig. 4).[29-33] In order to construct asymmetric catalysts, complexation of metal complexes and proteins has been recently examined as

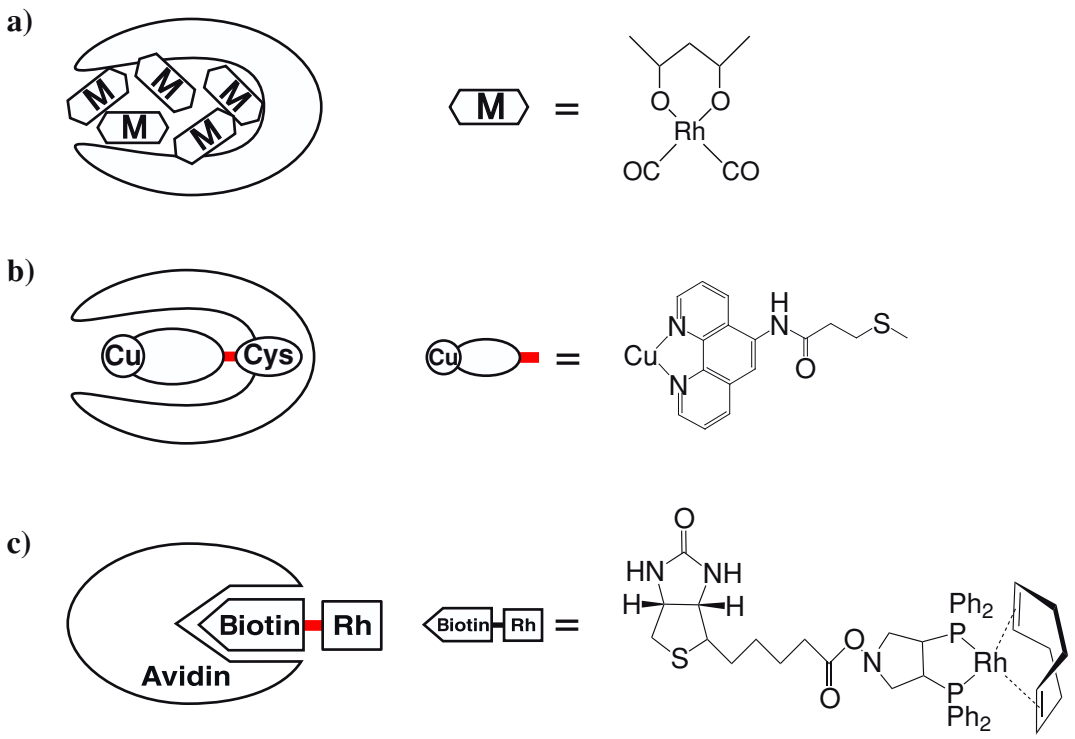

Figure 5. Effect of proteins to catalytic reaction of metal complexes

an innovative approach. Highly efficient and chemoselective biphasic hydroformylation of olefin has been accomplished by using Human Serum Albumin (HSA) complexed with a water soluble $Rh(CO)_2(acac)$, a readily available water soluble protein. Although this system catalyzes the olefin hydroformylation in water, it is difficult to improve the catalytic activity since many rhodium complexes binds to HSA at random (Fig. 5 a).[34] To develop of an asymmetric hydrolytic cleavage catalyst, a copper complex is bonded to a cysteine residue of an adipocyte lipid binding protein (Fig. 5 b).[35] The covalent linkage of pyrophos-Rh complex and modified biotin, which strongly binds to avidin, has been attempted for asymmetric hydrogenation in water (Fig. 5 c).[36] However, these systems have required arduous synthesis in order to fix the metal complexes into protein cavities with site-specificity. If we could reconstitute various metal complexes with protein matrixes without the modification, we will be able to prepare novel metalloenzymes more easily.

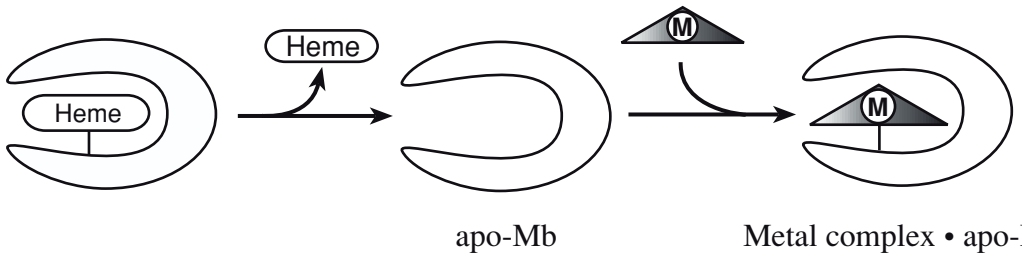

Scheme 1. Schematic representations of preparation of artificial metalloenzymes by noncovalent insertion

This thesis focuses on the establishment of a new methodology for the construction of artificial metalloproteins by noncovalent insertion of metal complex catalysts into protein cavities. Our strategy is more convenient for the preparation and design of artificial metalloenzymes and it will endue various functions by only changing the inserted metal complexes. Furthermore, it is possible to regulate the reactivity by site-directed mutagenesis since metal complex catalysts work inside of the protein cavity. Thus, this method can be applicable to many proteins, and construct various bio composite materials (Scheme 1).

In order to fix synthetic metal complexes in the heme cavity of apo-Mb, it is very important to optimize the ligand structure for the protein cavity. At the same time, mutation of the protein cavity for the accommodation of metal complexes will be helpful. According to the X-ray crystal structures of apo-Mb reconstituted with both heme derivatives and billiverdin, their protein foldings are very similar to met-Mb.[37,38] The results may imply that apo-Mb is capable for binding synthetic metal complexes if one could prepare metal complexes having a proper structure. In addition, Hunter *et al*. have reported that heme is fixed in the Mb cavity by three factors; 1) hydrophobic interaction of the heme ligand with the cavity (50 %), 2) proximal histidine ligation to the heme iron (25 %), and 3) hydrogen bonds between the heme side chains and amino acid residues (25 %) (Figure 6).[39] Therefore, the hydrophobic interaction has been controlled by the ligand

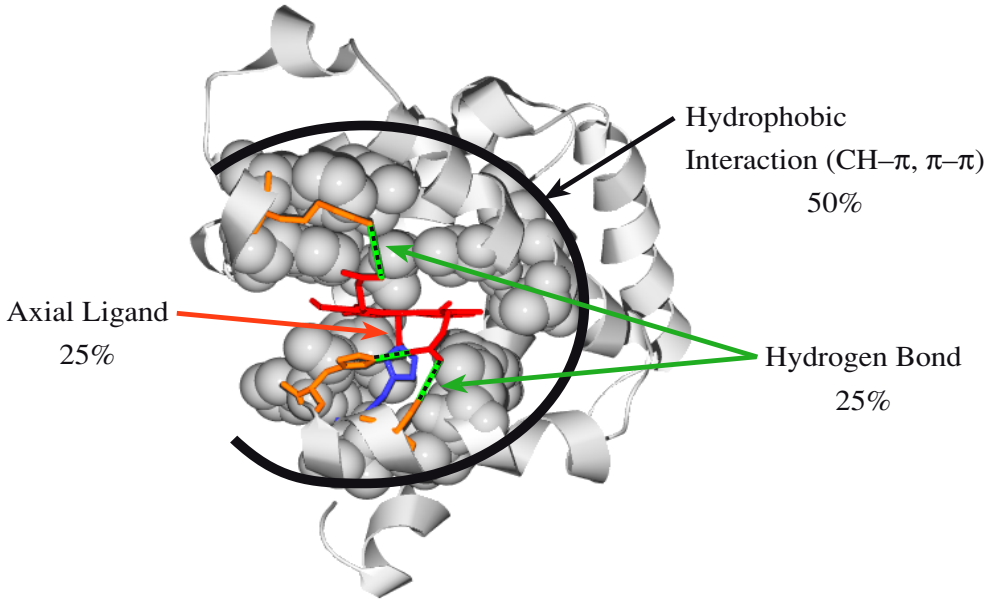

Figure 6. Stabilization factors of heme in Mb cavity

modification as well as amino acid replacement in the active site.

Actually, Schiff base complexes have been selected as candidates for the insertion into Mb because they can be easily synthesized and the metal substituted complexes catalyze various chemical reactions. For instance, Mn and Cr complexes have been prepared as asymmetric oxidation catalysts by Katsuki, Jacobsen, and Kochi (Fig. 7 a, b, and c). Salophen and its derivatives were used as Schiff base ligands to be inserted into Mb (Fig. 7 d). Salophen complexes have a plane structure without asymmetric center. Although salophen structure is very different from the heme structure, it can be inserted to the apo-Mb cavity since its molecular size is similar to heme (Fig. 7 e). In this study, Fe^{III}, Cr^{III} and Mn^{III} salophen complexes have been chosen as the prosthetic group of artificial metalloproteins. Fe^{III}(salophen) complexes could be used as a probe of small molecule binding such as O_2, CO, and CN^- to compare with heme. In order to construct the artificial monooxygenase, Mn^{III} and Cr^{III} salophen were employed.[40-42]

Amino acid residues, which are close to the inserted metal complex, could influence

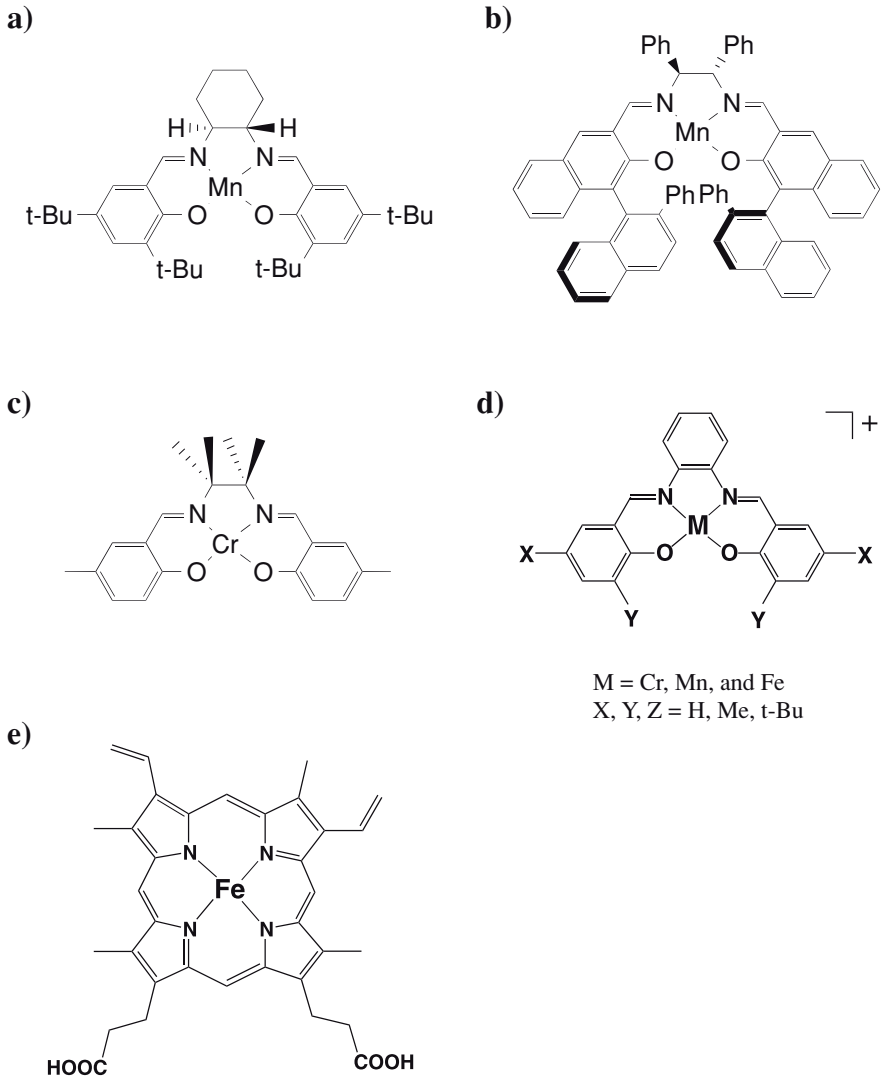

Figure 7. Schiff base complexes and heme; a) Jacobsen's ligand, b) Katsuki's ligand, c) Kochi's ligand, d) salophen complex, and e) heme

the catalytic reactivity of the metal complex. In the case of Mb, replacement of His64, which serves for the capture of molecular oxygen worked with heme iron, by aspartate (H64D Mb) was shown to dramatically increase the peroxidase and peroxygenase activity.[43] Furthermore, mutation of Val68 in H64D Mb to alanine (H64D/V68A Mb) indicates remarkable improvement of *R, S* selectivity in enantioselective sulfoxidation of thioanisole (6% $\rightarrow$ 86%).[44] The X-ray crystal structure of H64D/V68A Mb shows that the side chain

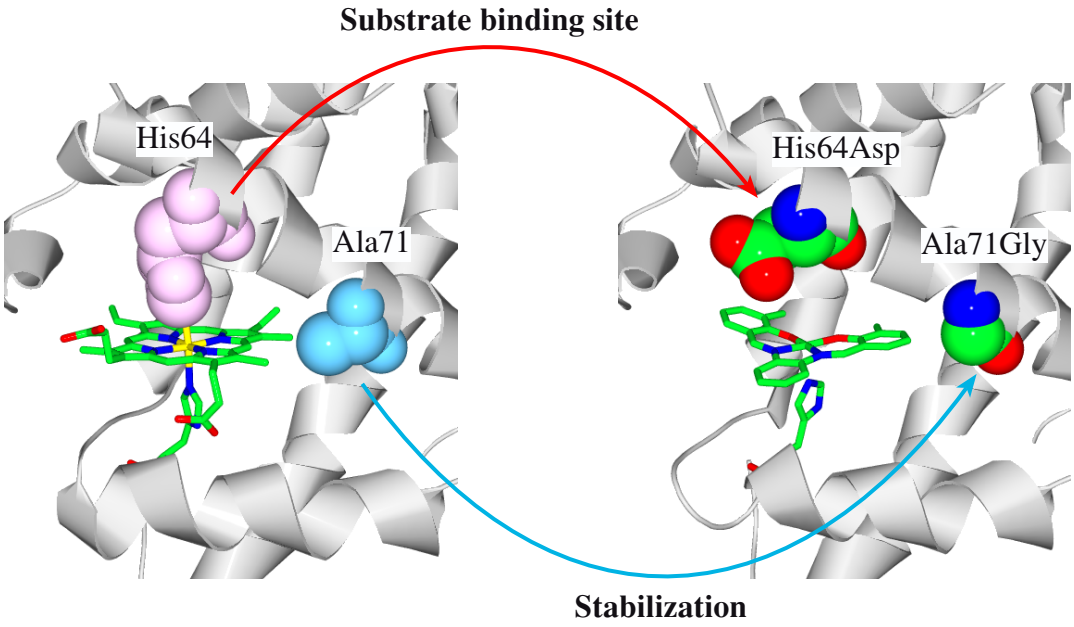

Figure 8. Design of Mb cavity

of aspartate at the position 64 participates in a hydrogen-bonding network with Arg45 and the reaction space immediately above the heme is expanded by this mutation.[45] Thus, apo-H64D Mb and its related mutants have been used for the construction of artificial metalloenzymes. In order to improve the reactivity and thermal stability of metal Schiff base•apo-Mb, molecular dynamics calculations were performed by using an Insight II/ Discover 3 program. The calculated structure of Fe^{III}(salophen)•apo-Mb indicated that the steric interaction between the salophen ligand and Ala71. Thus, Ala71 of H64D Mb is replaced by glycine (H64D/A71G Mb) (Fig. 8).

In order to apply the method to other metal complexes, the author has examined several organometallic compounds. In the past few years, organometal complexes embedded in proteins have been examined as water soluble catalysts. In fact, $Rh(CO)_2(acac)$ has been included in HSA as a catalyst for the hydroformylation of olefin in water.[34] In this case, it is very difficult for $[Rh]_n$•HSA (n = *ca.* 30) to improve the catalytic activity because of the random binding of the Ru complexes on the protein surface. In the second

example, organometal complexes have attached to a biomolecule with a covalent linkage. Whiteside and Chan have employed specific interaction between avidin and biothin. They have synthesized a Rh complex which has chiral phosphine ligand linked to biothin and reconstituted it as an asymmetric hydrogenation catalyst by embedding to avidin.[36,46] On the other hand, it seems much easier if one takes a noncovalent insertion method to synthesize organometalloprotein. Furthermore, it can be possible to regulate activities such as selectivity and reaction rate by the rational design of protein mutants because organometal complexes are inserted into the specific protein site.

This thesis focuses on the construction of artificial metalloproteins by the noncovalent insertion approach and aims to control their functions with combination of design of metal complexes and site-directed mutagenesis of protein. In Part II, the author discusses Schiff base complexes inserted into an apo-Mb cavity in order to construct the artificial metalloproteins. In chapter 1, the author reports the preparation and crystal structure determination of Fe^{III}(3,3'-Me_2-salophen)•apo-Mb and Fe^{III}(3,3'-Me_2-salophen)•apo-A71G Mb to understand the detailed three dimensional structures. Furthermore, the role of A71G in apo-Mb on Schiff base fixation and cyanide association was discussed on the basis of the crystal structures. In chapter 2, the author describes the design and screening of salophen ligands to improve the thermal stability and function of Fe^{III}(Schiff base)•apo-Mb. The salophen ligand whose 3, 3' or 5, 5' positions were modified with methyl or tertiary-butyl group was used. The thermal stability of a series of Fe^{III}(salophen)- derivatives•apo-Mb was examined by measuring of melting temperature (T_m) of proteins. Furthermore, the effect of the modification of the salophen ligand on cyanide accociation was examined by stopped flow analysis. In chapter 3, the author focuses on the construction of an artificial monooxygenase by the noncovalent insertion method. Therefore, Cr^{III}(salophen) complexes, which catalyzes oxidation reactions in organic solvent, were inserted into apo-Mb mutants. Furthermore, we chose wild type, H64D, A71G, and H64D/A71G Mb to introduce Cr^{III}(salophen) based on the structural calculation by Insight II/Discover 3. Catalytic

oxidation activity of each Cr^{III}(salophen)•apo-Mb mutant was evaluated by sulfoxidation of thioanisole. The effect of mutation on the reaction rate and enatioselectivity is discussed. In Part III, the author describes the synthesis of organometalloproteins by utilizing a noncovalent binding of Ru complexes to apo-Mb. At the same time, a vacant site of the protein is used for the synthesis of metal complexes, i.e., organometalloprotein are planned to construct by mixing all components in one portion. In order to evaluate formation of organometalloproteins, we have employed electrospray ionization time-of-flight mass spectrometry (ESI-TOF MS).

Reference

(1) Schultz, P. G.; Lerner, R. A. *Science* **1995**, *269*, 1835-1842.

(2) Wilson, C.; Szostak, J. W. *Nature* **1995**, *374*, 777-782.

(3) Wright, M. C.; Joyce, G. F. *Science* **1997**, *276*, 614-617.

(4) Wrighton, N. C.; Farrell, F. X. *Nature* **1996**, *273*, 458-463.

(5) Joo, H.; Lin, Z.; Arnold, F. H. *Nature* **1999**, *399*, 670-673.

(6) Li, Q. S.; Schwaneberg, U.; Ficher, P.; Schmid, R. D. *Chem. Eur. J.* **2000**, *6*, 1513-1536.

(7) Rai, G.; Zong, Q.; Hager, L. *Israel J. Chem.* **2000**, *40*, 63-70.

(8) Iffland, A.; Tafemeyer, P.; Saudan, C.; Johnsson, K. *Biochemistry* **2000**, *39*, 10790-10798.

(9) Cherry, J. R.; Lamsa, M. H.; Schneider, P.; Vind, J.; Svendsen, A.; Jones, A.; Pedersen, A. H. *Nat. Biotechnol.* **1999**, *17*, 379-384.

(10) Go, M. *Nature* **1981**, *291*, 90-92.

(11) Wakasugi, K.; Ishimori, K.; Imai, K.; Wada, Y.; Morishima, I. *J. Biol. Chem.* **1994**, *269*, 18750-18756.

(12) Ozaki, S.; Roach, M. P.; Matsui, T.; Watanabe, Y. *Acc. Chem. Res.* **2001**, *34*, 818-825.

(13) Hara, I.; Ueno, T.; Ozaki, S.; Itoh, S.; Lee, K.; Ueyama, N.; Watanabe, Y. *J. Biol. Chem.* **2001**, *276*, 36067-36070.

(14) Sigman, J. A.; Kwok, B. C.; Lu, Y. *J. Am. Chem. Soc.* **2000**, *122*, 8192-8196.

(15) Teale, F. W. J. *Biochem. Biophys. Acta.* **1959**, *35*, 543.

(16) Mondal, M. S.; Mazumdar, S.; Mitra, S. *Inorg. Chem.* **1993**, *32*, 5362-5367.

(17) Yonetani, T.; Yamamoto, H.; Woodrow1, G. V. *J. Biol. Chem.* **1974**, *249*, 682-690.

(18) Hoffman, B. M. *J. Am. Chem. Soc.* **1975**, *94*, 1688-1694.

(19) Srivastaveq, T. S. *Biochem. Biophys. Acta.* **1977**, *491*, 599-604.

(20) Brucker, E. A.; Olson, J. S.; Phillips, G. N.; Dou, Y.; IkedaSaito, M. *J. Biol. Chem.*

1996, *271*, 25419-25422.

(21) Gao, J. X.; Rusling, J. F. *J. Electroanal. Chem.* **1998**, *449*, 1-4.

(22) Hayashi, T.; Hisaeda, Y. *Acc. Chem. Res.* **2002**, *35*, 35-43.

(23) Hayashi, T.; Hitomi, Y.; Ando, T.; Mizutani, T.; Hisaeda, Y.; Kitagawa, S.; Ogoshi, H. *J. Am. Chem. Soc.* **1999**, *121*, 7747-7750.

(24) Neya, S.; Funasaki, N.; Hori, H.; Imai, K.; Nagatomo, S.; Iwase, T.; Yonetani, T. *Chem. Lett.* **1999**, 989-990.

(25) Neya, S.; Nakamura, M.; Imai, K.; Funasaki, N. *Chem. Pharm. Bull.* **2001**, *49*, 345-346.

(26) Hayashi, T.; Dejima, H.; Matsuo, T.; Sato, H.; Murata, D.; Hisaeda, Y. *J. Am. Chem. Soc.* **2002**, *124*, 11226-11227.

(27) Hu, Y. Z.; Takashima, H.; Tsukiji, S.; Shinkai, S.; Nagamune, T.; Oishi, S.; Hamachi, I. *Chem. Euro. J.* **2000**, *6*, 1907-1916.

(28) Hu, Y. Z.; Tsukiji, S.; Shinkai, S.; Oishi, S.; Hamachi, I. *J. Am. Chem. Soc.* **2000**, *122*, 241-253.

(29) Blum, O.; Haiek, A.; Cwikel, D.; Dori, Z.; Meade, T. J.; Gray, H. B. *Proc. Natl. Acad. Sci. USA* **1998**, *95*, 6659-6662.

(30) Douglas, K. T.; Ejim, O. S.; Taylor, K. *J. Enzym. Inhib.* **1992**, *6*, 233-242.

(31) Qiao, F.; Hu, J.; Zhu, H.; Luo, X.; Zhu, L.; Zhu, D. *Polyhedron* **1999**, *18*, 1629-1633.

(32) Salmain, M.; Gorfti, A.; Jaouen, G. *Eur. J. Biochem.* **1998**, *258*, 192-199.

(33) Shrivastave, H. Y.; Nair, B. U. *Biochem. Biophys. Res. Commun.* **2000**, *270*, 749-754.

(34) Marchetti, M.; Mangano, G.; Pagenelli, S.; Botteghi, C. *Tetrahedron Letters* **2000**, *41*, 3717-3720.

(35) Davies, R. R.; Distefano, M. D. *J. Am. Chem. Soc.* **1997**, *119*, 11643-11652.

(36) Lin, C. C.; Lin, C. W.; Chan, A. S. C. *Tetrahedron: Asymmetry* **1999**, *10*, 1887-

1893.

(37) Hata, T.; Hata, Y.; Sato, T.; Tanaka, N.; Neya, S.; Funasaki, N.; Katsube, Y. *Bull. Chem. Soc. Jpn.* **1991**, *64*, 821-828.

(38) Wagner, U. G.; Müller, N.; Schmitzberger, W.; Falk, H.; Kratky, C. *J. Mol.Biol* 1**995**, 2*47,* 326-337.

(39) Hunter, C. L.; Lloyd, E.; Eltis, L. D.; Rafferty, S. P.; Lee, H.; Smith, M.; Mauk, A. G. *Biochemistry* **1997**, *36*, 1010-1017.

(40) Jacobsen, E. N.; Zhang, W.; Muci, A. R.; Ecker, J. R.; Deng, L. *J. Am. Chem. Soc.* **1991**, *113*, 7063-7064.

(41) Katsuki, T. *Coord. Chem. Rev.* **1995**, *140*, 189-214.

(42) Samsel, E. G.; Srinivasan, K.; Kochi, J. K. *J. Am. Chem. Soc.* **1985**, *107*, 7606-7617.

(43) Ozaki, S.; Matsui, T.; Roach, M. P.; Watanabe, Y. *Coord. Chem. Rev.* **2000**, *198*, 39-59.

(44) Kato, S.; Yang, H. J.; Ueno, T.; Ozaki, S.; Phillips, G. N.; Fukuzumi, S.; Watanabe, Y. *J. Am. Chem. Soc.* **2002**, *124*, 8506-8507.

(45) Watanabe Y. Unpublished data.

(46) Wilson, M. E.; Whitesides, G. M. *J. Am. Chem. Soc.* **1978**, *100*, 306-307.

PART II

CONSTRUCTION OF ARTIFICIAL METALLOPROTEINS BY NONCOVALENT INSERTION OF METAL SCHIFF BASE COMPLEXES TO APO-MYOGLOBINS

Chapter 1. The Role of Ala71 in Apo-Myoglobin on Schiff Base Binding and Cyanide Association to Fe^{III}(Schiff Base)•Apo-Myoglobins

Chapter 2. Regulation of Cyanide Binding to Fe^{III}(Schiff Base)•Apo-Myoglobin by the Schiff Base Ligand Structure

Chapter 3. Preparation of Artificial Metalloenzymes by Noncovalent Insertion of Cr^{III}(Schiff Base) Complexes into Apo-Myoglobin Mutants

Chapter 1.

The Role of Ala71 in Apo-Myoglobin on Schiff Base Binding and Cyanide Association to Fe^{III}(Schiff Base)•Apo-Myoglobins

Introduction

Reconstitution of proteins with synthetic metal complexes is one of the most exiting subjects in the field of protein engineering because the reconstituted metalloproteins (artificial metalloproteins) could serve as catalysts, biosensors and electronic devices.[1-5] Recently, several research groups have reported interesting methods for the design of artificial metalloproteins; i) introduction of metal ion binding site in a small protein by computational rational design,[6,7] ii) alteration of metalloprotein functions by site-directed mutagenesis,[3,8] and iii) chemical modification of protein scaffold, natural cofactors, and substrates.[5,9-15] For example, Hellinga and his co-workers have constructed several metal binding sites in a thioredoxin scaffold.[2] The Cu_B binding site of cytochrome *c* oxidase has been introduced immediately above the heme of myoglobin (Mb) by replacing Phe43 and Leu29 to His.[16] Peroxygenase and peroxidase activities have also been introduced into Mb by mutation of His64.[8,17] While utilization of organometallic compounds as artificial cofactors of metalloproteins are attractive, it is very hard to fix the organometallic compounds at the desired position in a protein matrix.

Recently, we have reported the insertion of Cr^{III}(Schiff base) complexes into apo-myoglobin (apo-Mb) by considering three factors, i.e., i) hydrophobic interaction, ii) ligation of the complex to proximal histidine, and iii) deletion of steric hindrance between the ligand and protein matrix by site-directed mutagenesis.[18] The catalytic activity and selectivity of the artificial metalloproteins are expected to be controlled by substituents on the ligand and the active site structure. In fact, Cr^{III}(5,5'-*t*Bu_2-salophen)•apo-H64D/A71G Mb has indicated higher catalytic activity and selectivity in H_2O_2 dependent sulfoxidation than those of Cr^{III}(salophen)•apo-Mb. The crystal structure of Cr^{III}(3,3'-Me_2-salophen)•apo-A71G Mb shows that deep insertion of Cr^{III}(3,3'-Me_2-salophen) ligated to His64 decrease the catalytic reactivity.[19] We herein report the crystal structures of Fe^{III}(3,3'-Me_2-salophen)•apo-Mb and Fe^{III}(3,3'Me_2-salophen)•apo-A71G Mb and the effect of Ala71 mutation on cyanide binding (Scheme 1). The amino acid side chain at the

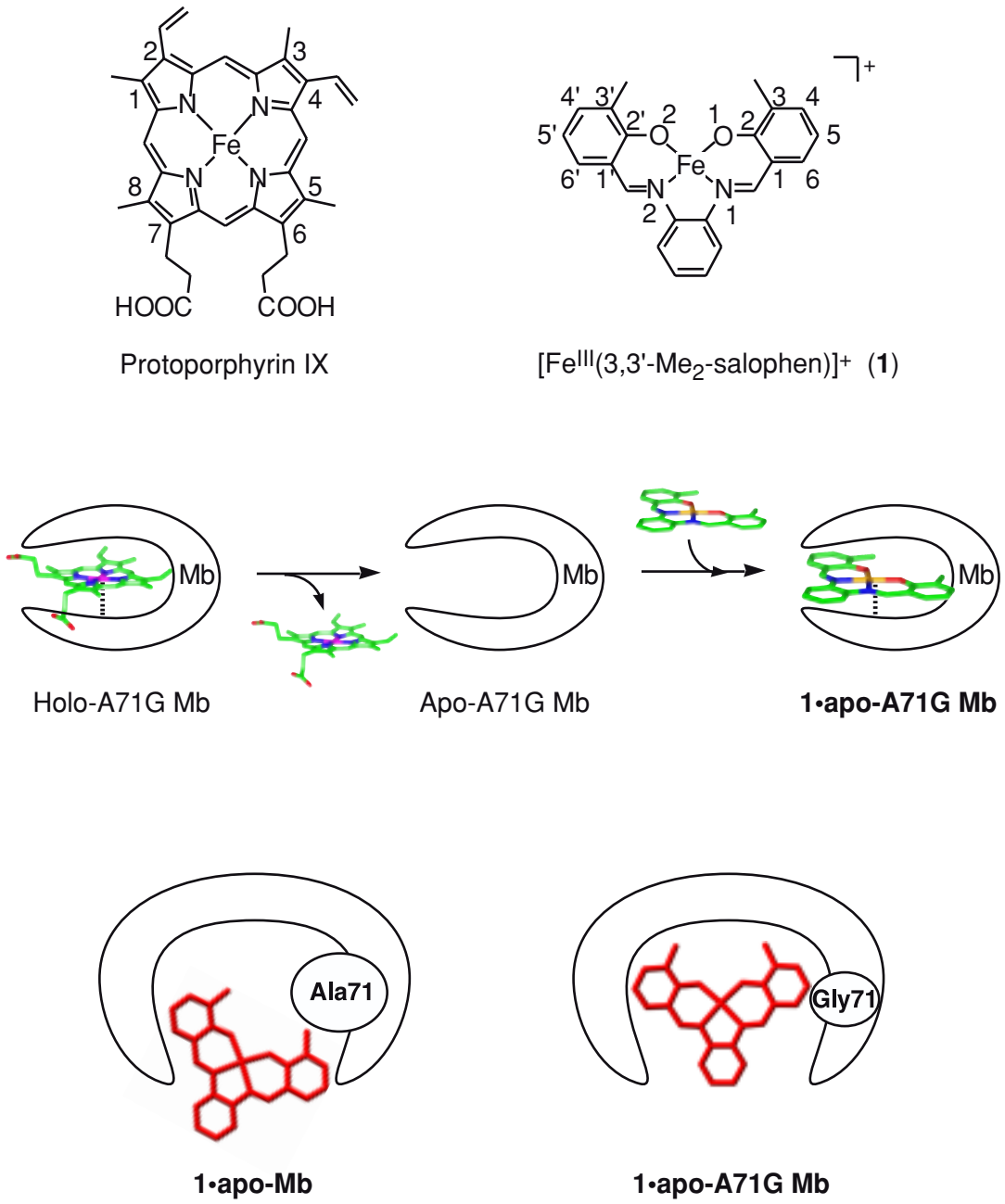

Scheme 1. Schematic drawing for the preparation of **Fe^{III}(3,3'-Me$_2$-salophen)(1)•apo-Mb** and mutational design at the position 71

position of 71 is very much effective on the cyanide binding kinetics because the steric repulsion between the side chain of Ala71 and the Schiff base ligand regulates the position

and stability of the Schiff base complex in the heme cavity.

Results and Discussion

Preparation and crystallization of **1•apo-A71GMb** and **1•apo-Mb** were carried out as described previously.[18,20] The structure of **1•apo-A71G Mb** was refined with the diffraction data of 1.6-Å resolution from a high quality crystal. The final R and R_{free} were 20.1 and 21.2, respectively, and the other X-ray data are summarized in Table 1. As shown in Figure 1, the iron complex **1** is fixed in the heme cavity by ligating to His93 with water molecule and has conserved six-coordinate geometry. Reported six-coordinate mono Lewis base adducts of Fe^{III}(Schiff base) complex are usually very unstable and the crystalline products were contaminated by a large amount of the corresponding μ-oxo dimer by standing for a period longer than 3h.[21] On the other hand, purified **1•apo-Mb** and **1•apo-A71G Mb** were stood under air for several weeks for crystallization and no conversion of the iron (III) complexes to the dimer was observed.

The coordination sphere around the iron atom shows a distorted octahedral geometry, e.g. N1–Fe–O2, N2–Fe–O1, and N1–Fe–N2 are 172.7°, 157.3°, and 81.5°, respectively. The Nε atom of proximal His93 ligates to the iron with a Fe–N distance of 2.30 Å to be slightly longer than those of $[Fe^{III}$(3-EtO-salen)(5-Ph-Im)$(H_2O)]^+$ (2.13 Å) and met-Mb (2.17 Å).[21,22] The distance between the iron and a coordinated water (2. 40 Å) is also longer than those of $[Fe^{III}$(3-EtO-salen)(5-Ph-Im)$(H_2O)]^+$ (2.21 Å)[21] and met-Mb (2.10 Å)[22] and the ligated water makes a hydrogen bond with the Nε atom of distal His64 (2.92 Å). Systematic studies of metal-Schiff base complexes have shown that the metal to imine nitrogen bond distance is sensitive to the spin-state of the metal ion. In iron (III) complexes the metal to imine nitrogen distances are in a range of *ca*. 2.06–2.10 Å for the high-spin state and in a range of *ca*. 1.93–1.96 Å for the low-spin cases. The iron-nitrogen bonds, Fe–N1 (2.15 Å) and Fe–N2 (1.99 Å), in **1•apo-A71G Mb** suggest the metal ion to be in the high-spin state, and it is consistent with the ESR results.[23] The Schiff base ligand

Table 1. Summary of X-ray data from the crystals of **1•apo-Mb** and **1•apo-A71GMb**.

	1•apo-A71GMb	**1•apo-Mb**
Data collection		
Space group	$P2_12_12_1$	$P2_12_12_1$
Unit cell (Å)		
a	33.3	33.1
b	57.6	58.8
c	75.3	75.6
Wavelength (Å)	1.5418 (CuKα)	1.5418 (CuKα)
Resolution (Å)	40.0-1.6 (1.66-1.60)	40.0-2.1 (2.18-2.10)
Total observations	323196	73324
Unique reflections	19256	8790
Completeness (%)	97.0 (91.2)	96.1 (94.0)
Rmerge (%)	9.7 (31.5)	7.4 (23.2)
I/σ (I)	41.9 (6.8)	19.6 (4.4)
Molecules per asymmetric unit	1	1
Refinement statistics		
Resolution (Å)	24.9-1.6	
Number of reflections		
Working set	17951	
Test set	923	
R-factor (%)		
Working set	19.9	
Test set	21.0	
R.m.s.deviation		
Bonds (Å)	0.005	
Angles (°)	1.8	
Dihedrals (°)	17.6	
Improper (°)	0.68	
B-factor (Å^2)		
Overall	24.8	
Ramachandran plot (%)		
Most favored	90.5	
Additional allowed	9.5	
Generously allowed	0.0	
Disallowed	0.0	
Final model		
Number of residues	154	
Fe^{III}(3,3'-Me_2-salophen)	1	
Water molecules	193	
Phosphate ions	6	

is stabilized its position by π-π and CH-π interactions with Phe43, Leu89, and Ile99 as

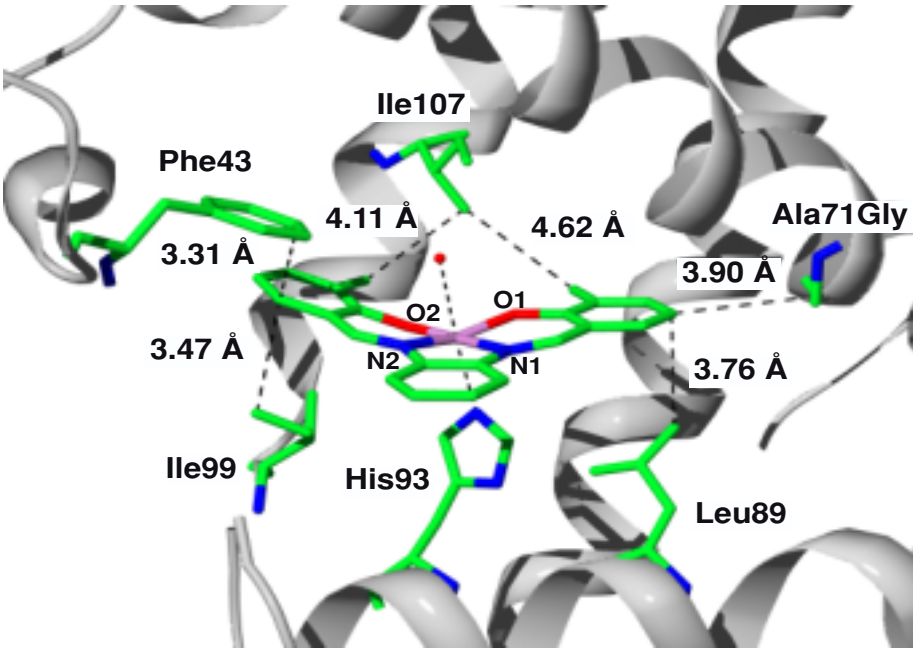

Figure 1. The crystal structure and close contacts in the active site of **1•apo-A71G Mb**.

observed in the crystal structure of Cr^{III}(3,3'-Me2-salophen)•apo-A71G Mb.[19] The results indicate the importance of the ligand structure in the metal complexes for the insertion in the protein matrix.

The **1•apo-Mb** structure is problematic, while it provides useful insights into the nature of binding. The protein portion in the crystal structure of **1•apo-Mb** is well resolved and it is similar to that of the native Mb, however, the electron density of the salophen ligand, the iron atom, and the imidazole ring of His93 appear to be disordered. The results suggest that **1** and the ligated imidazole of His93 are moving around in the protein or take several conformations. Therefore, the steric hindrance between the side chain of Ala71 and the Schiff base ligand prevents **1** to be uniquely fixed in the heme cavity. In fact, the C5 atom in **1** is close to the Cα atom of Ala71Gly with a distance of 3.90 Å as shown in Figure 2. Apparently, Gly at the position 71 plays a crucial role for the fixation of the Schiff base ligand in the Mb heme cavity. The crystal structure of **1•apo-A71G Mb** also shows that the 3- and 3'-methyl groups in the ligand are in Van der Waals contact with

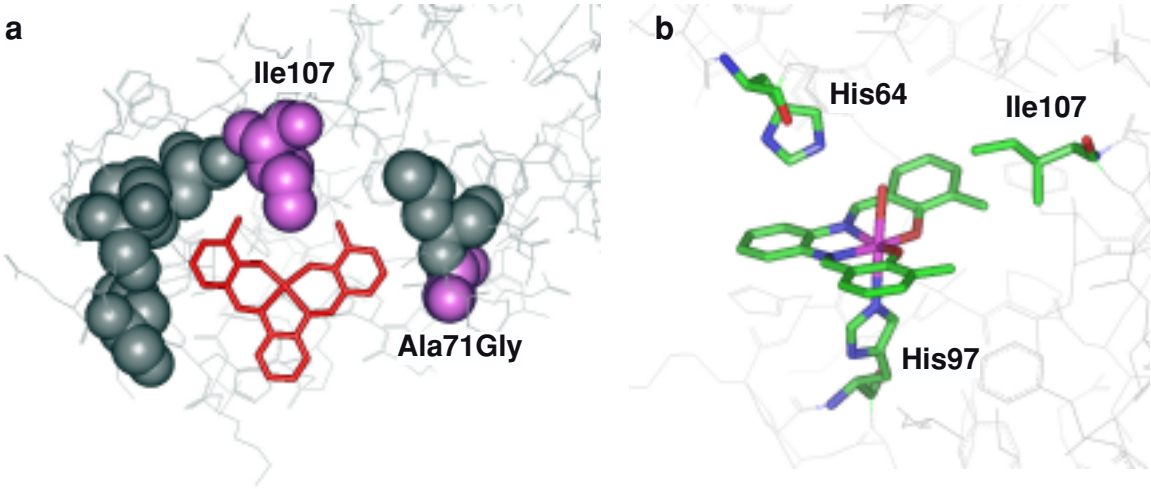

Figure 2. Top (**a**) and side (**b**) views of amino acid residues surrounding **1** of **1•apo-A71G Mb**.

Ile107, which limits the penetration depth of **1** into the heme pocket as observed in Cr^{III}(3,3'-Me_2-salophen)•apo-A71G Mb.[19]

Finally, we have evaluated cyanide binding to **1•apo-A71G Mb** and **1•apo-Mb** at pH 7.0. Figure 3 shows that the spectral change of **1•apo-A71G Mb** upon the addition of 100 equiv. KCN. New absorption appeared at 443 nm with a distinct isosbestic point at 403 nm. These spectral changes are caused by the cyanide binding to the iron in **1•apo-A71G Mb** confirmed by the EPR spectrum of the product.[23] Interestingly, the cyanide association rate constant of **1•apo-A71G Mb** (475 $M^{-1}s^{-1}$) is 216-fold larger than that of **1•apo-Mb** (2.2 $M^{-1}s^{-1}$). Most of cyanide is protonated at neutral pH (pKa ~9), and the crucial step for cyanide association has been shown to be the deprotonation of HCN in the distal heme pocket. The 160-fold decrease in the association rate upon the His64 to Leu mutation in Mb was attributed to the loss of a general base (His64).[24] The crystal structure of **1•apo-A71G Mb** shows that the geometry of His64–coordinated water–iron atom is almost identical to that of met-Mb (Figure 2b). On the other hand, **1** in apo-Mb appears to be deviated from the ideal geometry because **1** is disordered in the heme pocket while the location of distal histidine (His64) is well resolved in the crystal structure. Thus, His64 in

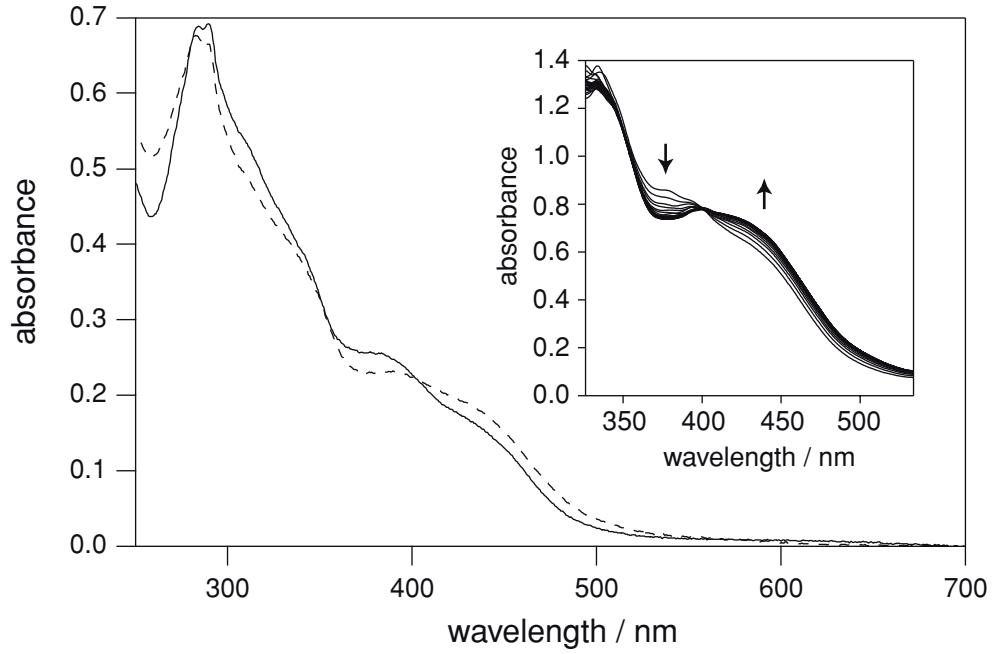

Figure 3. UV-vis spectral changes of **1•apo-A71GMb** (solid) upon the addition of 100 equiv. KCN (**1•apo-A71GMb**: 10 μM in 10 mM Tris/HCl buffer at pH 7.0) (broken). Time dependent spectral changes of the same reaction are shown in *insert* (every 130 msec).

1•apo-Mb could be a less effective base to assist the cyanide binding than His64 in **1•apo-A71G Mb**.

In summary, we have determined the crystal structures of **1•apo-Mb** and **1•apo-A71G Mb**. We also found that the Ala71 to Gly mutation considerably improved the cyanide association. The results also provide examples for the stabilization of a non-natural cofactor by the amino acid replacement.

Experimental Section

Materials. Reagents were purchased from TCI, Wako, Nacalai Tesque, and Aldrich and used without further purification. The expression vector for wild type of sperm whale Myoglobin (Mb) is a gift from John Olson (Rice University).[25] The expression and purification of Mb were performed according to a method described by Springer *et al*. with

some modification. Apo-myoglobin (apo-Mb) was prepared using an acid-butanone method.[26]

Preparation of iron (III) Schiff base complex (1). 3,3'-Me_2-salophen and its iron (III) complex (**1**) were prepared by literature methods.[27,28] To an ethanol solution of *o*-phenylenediamine (0.28 g, 2.6 mmol) was added 3-Me-salicylaldehyde (0.6 ml, 4.9 mmol). This mixture was refluxed for 3 h. When the mixture stood for 3 h, precipitation of an orange solid occurred and then the precipitate was collected by filtration. Dissolution of the precipitate in hot methanol followed by cooling afforded *N*,*N*'-bis(3-methylsalicyldene)-1,2-phenylenediamine, 3,3'-Me_2-salophen, as orange needle crystals (Yield: 80%). ^{1}H NMR ($CDCl_3$): δ 13.20 (s, 2H), 8.62 (s, 2H), 7.36-7.30 (m, 2H), 7.26-7.17 (m, 6H), 6.83 (t, J = 7.5 Hz, 2H), 2.29 (s, 6H). 3,3'-Me_2-salophen (0.37 g, 1.1 mmol) was dissolved in ethanol (15 ml), to which was added slowly an ethanol solution (10 ml) of $Fe^{III}Cl_3 \cdot 6H_2O$ (0.3 g. 1.1 mmol). The solution was stirred for 1h under air. The resulting precipitate was collected by filtration, and dried under vacuum to give [Fe^{III}(3,3'-Me_2-salophen)(**1**)•Cl] as a black powder (Yield: 58%). ESI-TOF MS: [**1**]$^+$ m/z 398.04 (calc. 398.07).

Reconstitution of apo-Mb with 1. To a methanol solution of **1•Cl** (12 ml, 25 mM) was added $AgBF_4$ (1.2 ml, 367 mM) in methanol. The mixture was stirred at 50 ˚C for 3 h, and then precipitated AgCl and excess of Ag^+ remaining in the solution were removed by celite filtration. The resulting solution containing **1•BF_4** was diluted by methanol upto 10 mM. The methanol solution of **1•BF_4** (1 ml, 10 mM) was slowly added to an aqueous solution of apo-Mb (14 ml, 0.3 mM in 10 mM Tris/HCl buffer, pH 7.0) and gently stirred at 4 ˚C for 10 min. The mixture was dialyzed against 10 mM Bis-tris buffer (pH 6.0) at 4 ˚C for 6 h. After the dialysis, the mixture was passed through Sephadex G-25 equilibrated with 10 mM Tris/HCl buffer (pH 7.0), and then purified with HiTrap™ CM FF on an ÄKTA explorer 100 FPLC system (Amersham Biosciences) with a linear gradient of 10-500 mM Tris/HCl buffer (pH 7.0). **1•apo-Mb** was purified in 20% yield. ESI-TOF MS: [**1•apo-Mb**]$^+$ m/z 17728.6 ± 1.6 (calc. 17728.2), UV-vis. (10 mM Tris/HCl buffer, pH7.0)

λ/nm (ε / M^{-1} cm^{-1}): 282(51000), 289.5 (47200), 326.5 (23100), 376 (15400).

Reconstitution of apo-A71GMb with 1. The reconstitution was also carried out by the same manner of apo-Mb and **1•apo-A71GMb** was isolated in yield of 3%. ESI-TOF MS: [**1•apo-A71GMb**]$^+$ *m*/*z* 17715.7 ± 0.5 (calc. 17715.2), UV-vis. (10 mM Tris/HCl buffer, pH7.0) λ/nm (ε / M^{-1} cm^{-1}): 289.5 (78500), 384.5 (29800).

Crystallization, X-ray data collection, and crystallographic refinement. Crystallization of **1•apo-Mb** and **1•apo-A71GMb** were carried out by a previous method with some modification.[20,29] The complexes were crystallized at 4 °C with the sitting-drop vapor diffusion method using freshly prepared and purified protein complexes. Drops of 6 μl solution containing approximately 9 mg/ml protein and sodium-phosphate buffer (1.4 M sodium phosphate buffer, pH 6.8) were equilibrated against a 1000 μl reservoir solution containing the same buffer in two-fold higher concentration (2.8 M). The crystals grew for three to four weeks at 4 °C to a maximum size of $0.2 \times 0.2 \times 2$ mm^3. **1•apo-A71GMb** was also crystallized under the same conditions. X-ray data of **1•apo-A71GMb** were collected at 100 K using a Rigaku R-AXIS VII detector system and Rigaku FR-E. X-ray data of **1•apo-Mb** were collected from the crystals at 100 K using a Rigaku R-AXIS IV detector system and Rigaku RU-300 rotating-anode generator with double focusing-mirror monochromated Cu *K*α radiation. Both of the collected data sets were processed with *DENZO* and *SCALEPACK*. The crystal parameters and data-collection statistics are given in Table 1.

The Cr^{III}(3,3'Me_2-salophen)•apo-A71GMb structure with deletion of the Cr^{III}(3,3'Me_2-salophen) moiety was used as an initial model for the refinement of **1•apo-A71GMb.** The refinement was carried out with a program *CNS* and manual model building with a program TURBO–FRODO. A statistically random selection of about 5% of the total reflection data was excluded from the refinement and the results were used to calculate the free *R* factor (R_{free}) as a monitor of model bias. After rigid-body refinement, positional refinement, and B-factor refinement, **1** was positioned manually on an omit |Fo|–|Fc| map in the

heme cavity. Subsequent several cycles of positional refinement, simulated-annealing refinement, and B-factor refinement with intermittent manual model correction brought the final R factor and the R_{free} to 20.1% and 21.2%, respectively. The model was subjected to quality analysis during the various refinement stages with omit maps and *PROCHECK*. The refinement statistics are summarized in Table 1.

An initial model for **1•apo-A71GMb** was constructed by deleting **1** from **1•apo-A71GMb.** The refinement was also performed with a program *CNS*. Even after several cycles of refinement (*R*-factor 21.3% and R_{free} 24.8%), the electron density corresponding to **1** was not clear. The refinement statistics are summarized in Table 1.

Physical measurements. Elemental analyses were performed at the Research Center for Molecular Materials, Institute for Molecular Science. UV-vis spectra were recorded on a SHIMADZU UV-2400PC UV-VIS spectrophotometer. The ^{1}H NMR spectra were recorded on a JEOL JNM-EX 270 spectrometer.

Atomic absorption spectroscopy. The iron concentration in **1•apo-Mb** and **1•apo-A71GMb** were determined by using a Polarizing Zeeman-effect atomic absorption spectrophotometer Z-5710 (HITACHI) operating in graphite furnace mode using a Fe hollow cathode lamp. Iron ion was detected at 248.3 nm with a slit width of 0.2 nm. $Fe^{III}(NO_3)_3$ in 0.1 mol/l•HNO_3 (99.8 mg/l, Wako) was used as a calibration standard.

EPR measurements. EPR spectra were recorded on an E500 X-band CW-EPR (Bruker). A cryostat (ITC503, Oxford) was used for the observation at 5 K. EPR spectra of **1•apo-Mb** and **1•apo-A71GMb** (0.6 mM, 10 mM Tris/HCl buffer, pH 7.0) and their cyanide bound derivatives were measured at 5 K. The cyanide bound samples were prepared by the addition of 100 equiv. of KCN (0.1 M, 10 mM Tris/HCl buffer, pH 7.0) to **1•apo-Mb** and **1•apo-A71G Mb** solutions (0.6 mM, 10 mM Tris/HCl buffer, pH 7.0). The reaction mixtures were then flash frozen by liquid nitrogen.

Mass spectrometry. ESI-TOF Mass analyses were performed on a Micromass LCT. Typical parameters are as follows; capillary voltage: 3 kV, cone voltage: 60 V, source

temperature: 60 °C, flow-rate: 5 μl min^{-1}. CsI (1 mg/ml) in 50% H_2O/CH_3CN was used for mass scale calibration. All sample were dialyzed against 5 mM ammonium acetate buffer (pH 6.7) at 4 ˚C for 6 h and diluted to 10 mM with the same buffer.

Kinetic measurements for cyanide binding. The cyanide binding to reconstituted Mbs was measured at 395-408 nm on a UNISOKU stopped-flow spectrophotometer in 10 mM Tris/HCl buffer (pH 7.0) under psuedo-first-order conditions. The binding rate constants were given by the slope of a plot of the observed rates *versus* cyanide concentration.

References

(1) Bayley, H. *Curr. Opin. Biochem.* **1999**, *10*, 94-103.

(2) Benson, D. E.; Wisz, M. S.; Hellinga, H. W. *Curr. Opin. Biochem.* **1998**, *9*, 370-376.

(3) Lu, Y.; Berry, S. M.; Pfister, T. D. *Chem. Rev.* **2001**, *101*, 3047-3080.

(4) Qi, D.; Tann, C.-M.; Haring, D.; Distefano, M. D. *Chem. Rev.* **2001**, *101*, 3081-3111.

(5) Sigman, D. S.; Bruice, T. W.; Mazumder, A.; Sutton, C. L. *Acc. Chem. Res.* **1993**, *26*, 98-104.

(6) Hellinga, H. W.; Richards, F. M. *J. Mol. Biol.* **1991**, *222*, 763-785.

(7) Wisz, M. S.; Garrett, C. Z.; Hellinga, H. W. *Biochemistry* **1998**, *37*, 8269-8277.

(8) Ozaki, S.; Roach, M.; Matsui, T.; Watanabe, Y. *Acc. Chem. Res.* **2001**, *34*, 818-825.

(9) Davies, R. R.; Distefano, M. D. *J. Am. Chem. Soc.* **1997**, *119*, 11643-11652.

(10) Ermacora, M. R.; Delfino, J. M.; Cuenoud, B.; Schepartz, A. *Proc. Natl. Acad. Sci. USA* **1992**, *89*, 6383-6387.

(11) Hamachi, I.; Shinkai, S. *Eur. J. Org. Chem.* **1999**, 539-549.

(12) Hayashi, T.; Hisaeda, Y. *Acc. Chem. Res.* **2002**, *35*, 35-43.

(13) Lin, C.-C.; Lin, C.-W.; Chan, A. S. C. *Tetrahedron: Asymmetry* **1999**, *10*, 1887-1893.

(14) Neya, S.; Tsubaki, M.; Hori, H.; Yonetani, T.; Funasaki, N. *Inorg. Chem.* **2001**, *40*, 1220-1225.

(15) Wilson, M. E.; Whitesides, G. M. *J. Am. Chem. Soc.* **1978**, *100*, 306-307.

(16) Sigman, J. A.; Kwok, B. C.; Lu, Y. *J. Am. Chem. Soc.* **2000**, *122*, 8192-8196.

(17) Matsui, T.; Ozaki, S.-i.; Watanabe, Y. *J. Am. Chem. Soc.* **1999**, *121*, 9952-9957.

(18) Ohashi, M.; Koshiyama, T.; Ueno, T.; Yanase, M.; Fujii, H.; Watanabe, Y. *Angew. Chem. Int. Ed.* **2003**, *42*, 1005-1008.

(19) Watanabe, Y. *The final structure will be submitted somewhere.*

(20) Wagner, U. G.; Muller, N.; Schmitzberger, W.; Falk, H.; Kratky, C. *J. Mol. Biol.*

1995, *247*, 326-337.

(21) Kennedy, B. J.; Brain, G.; Horn, E.; Murray, K. S.; Snow, M. R. *Inorg. Chem.* **1985**, *24*, 1647-1653.

(22) Takano, T. *J. Mol. Biol.* **1977**, *110*, 537-568.

(23). The ESR spectra of the reaction mixtures containing the iron (III) complexes and apo-Mb were measured at 5 K in 10 mM Tris/HCl buffer (pH 7.0). The EPR spectrum of **1** and apo-Mb (1:1.2) shows typical high-spin iron (III) signals at g = 4.25 and 8. These signals are very similar to those of [Fe^{III}(3-EtO-salen)(5-Ph-imd)(H_2O)]BPh_4•0.5H_2O in CH_2Cl_2. Furthermore, these high-spin signal were disappeared by the addition of 100 equiv. KCN and new three signals occurred at 1.8–2.5 assigned to the low-spin species.

(24) Brancaccio, A.; Cutruzzola, F.; Allocatelli, C. T.; Brunori, M.; Smerdon, S. J.; Wilkinson, A. J.; Dou, Y.; Keenan, D.; Ikeda-Saito, M.; Brantley, R. E. J.; Olson, J. S. *J. Biol. Chem.* **1994**, *269*, 13843-13853.

(25) Springer, B. A.; Sligar, S. G. *Proc. Natl. Acad. Soc.* **1987**, *84*, 8961-8965.

(26) Ascoli, F.; Fanelli, M.; Antonini, E. *Methods Enzymol* **1981**, *76*, 72-87.

(27) Ciringh, Y.; Gordon-Wylie, S. W.; Norman, R. E.; Clark, G. R.; Weintraub, S. T.; Horwitz, C. P. *Inorg. Chem.* **1997**, *36*, 4968-4982.

(28) Gullotti, M.; Casella, L.; Pasini, A.; Ugo, R. *J. Chem. Soc., Dalton Trans.* **1977**, 339-345.

(29) Neya, S.; Funasaki, N.; Sato, T.; Igarashi, N.; Tanaka, N. *J. Biol. Chem.* **1993**, *268*, 8935-8942.

Chapter 2.

Regulation of Cyanide Binding to Fe^{III}(Schiff Base)•Apo-Myoglobin by the Schiff Base Ligand Structure

Introduction

Metal ions play important roles in controlling biological functions of proteins and enzymes by constructing their active sites. The coordination environment of the active site is the primary factor for defining their biological functions. For example, ribonucleotide reductase (RNR) and methane monooxygenase share a similar dinuclear ion site, while a small difference in their coordination structures results in these two nonheme enzymes being responsible for very different biological functions. Therefore, it is possible for metalloenzymes to alter their biological functions by changing their active site structures including the nature of metal ligands. It also implies that the rational design of metalloenzymes could be possible if we really understand the structure-function relationship. In fact, several rational designs of metalloenzymes have been reported.[1-3] Heme proteins, especially, have been a target for rational design by site-directed mutagenesis or modification of the heme prosthetic group, since there have been many fundamental studies on heme proteins and enzymes including their model systems. Amino acids located near the heme are considered to regulate their functions as well as the fixation of the heme in the protein cavity. Thus, it has been reported that environmental change around the heme brings a major change in the function and stability of native heme proteins. For example, Ozaki *et al*. have converted Mb into a peroxidase-like enzyme by alternation of the heme distal pocket by site-directed mutagenesis.[4] Further, Neya and Hayashi have improved oxygen affinity of Mb by the reconstitution of apo-Mb with porphyrin isomers, due to the geometric strain on the iron (II) atom in the trapezoidal coordination core of porphyrin isomers.[5-7]

On the other hand, we have reported a new strategy for the construction of artificial metalloproteins by noncovalent insertion of metal complex catalysts into an apo-Mb cavity, i.e., the utilization of both proximal histidine (His93) as the axial ligand for the metal complexes and hydrophobic interaction between metal ligands and the heme cavity (metal binding site). For example, we have prepared Fe^{III}(Schiff base)•apo-Mbs and Cr^{III}(Schiff

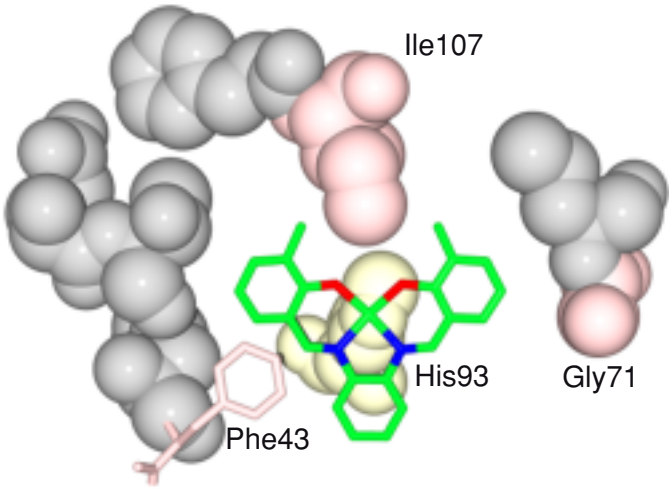

Figure 1. Crystal structure of Cr^{III}(3, 3'-Me_2-salophen)•apo-A71G Mb

base)•apo-Mbs and solved their crystal structures. Furthermore, reactivity and stability of those metalloproteins were shown to be regulated by changing the protein structure of the metal binding site. In the case of Fe^{III}(Schiff base)•apo-Mb, the binding affinity of Fe^{III}(Schiff base) for apo-Mb was increased by the replacement of alanine 71 to glycine.[8] On the other hand, distal histidine (H64) in Mb was replaced with aspartic acid for providing a polar substrate binding site in Cr^{III}(Schiff base)•apo-Mb. The resulting Cr^{III}(5, 5'-*t*-Bu_2-salophen)•apo-H64D/A71G Mb was capable to catalyze asymmetric sulfoxidation of thioanisole.[9]

The crystal structure of Cr^{III}(3,3'-Me_2-salophen)•apo-A71G Mb shows the ligation of proximal histidine (H93) to the Cr^{III} ion.[10] At the same time, two methyl groups in the ligand interact with Ile107 to stabilize the Cr^{III}(3, 3'-Me_2-salophen) in the heme cavity (Fig. 1). According to these interactions, Cr^{III}(3, 3'-Me_2-salophen) is located in the heme cavity, where the heme was originally locate. Superimposition of the structures of Cr^{III}(3,3'-Me_2-salophen)•apo-A71G Mb and native Mb clearly shows that the Cr^{III} ion stays *ca*. 1 Å deeper in the heme cavity due to the two methyl-Ile107 interaction. The heme binding site structure in Cr^{III}(3,3'-Me_2-salophen)•apo-A71G Mb suggest the introduction of substitu-

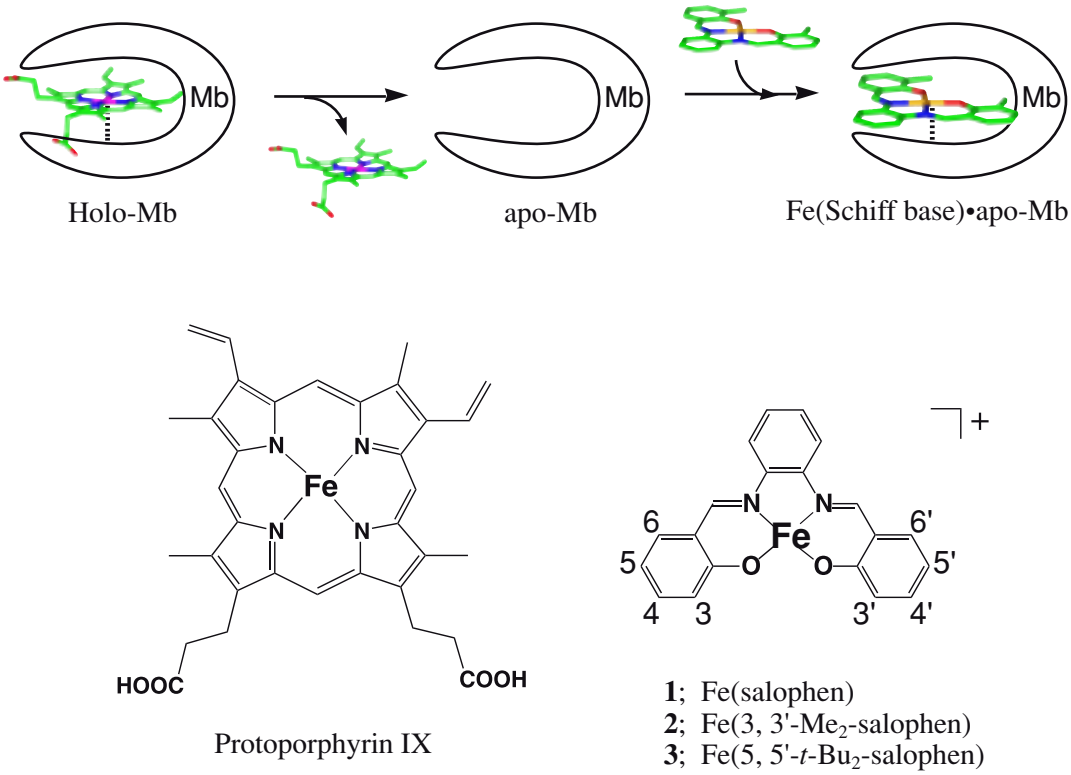

Figure 2. Preparation of Fe^{III}(salophen)-derivatives•apo-Mb

ents on the salophen ligand could causes the change in the position and orientation of Cr^{III}(salophen) in apo-Mb. The relocation of the metal complexes in the heme cavity is expected to affect the change of catalytic activities of the metal complexes.

In this chapter, the author describes the design and screening of salophen ligands in order to improve the thermal stability and cyanide binding property of Fe^{III}(salophen)•apo-Mb (Fig. 2). The 3, 3'- or 5, 5'- positions of salophen were modified with methyl (Me) or tertiary butyl (*t*-Bu) groups. The thermal stability of a series of Fe^{III}(salophen)-derivatives•apo-Mb was examined by measuring melting temperature (T_m). The effect of the modification of the salophen ligand on cyanide binding was examined by stopped flow analysis.

Table 1. Absorption maxima (λ_{max}) of **1–3•apo-Mbs** and their cyanide complexes.

	λ_{max} nm ($\varepsilon \times 10^3$ mol^{-1}cm^{-1})					
1•apo-Mb[a]	282 (50.9)	289.5 (47.2)	326.5 (23.1)	376 (15.4)		
1•apo-Mb-CN^{-}[b]	282	289	337	387.5	450	
2•apo-Mb[a]	283.5 (65.9)	289 (65.2)	324.5 (41.8)	380.5 (22.1)		
2•apo-Mb-CN^{-}[b]	283.5	289.5	307	339.5	390	449
3•apo-Mb[a]	282.5 (155)	291 (130)	341.5 (38.7)	410 (24.7)		
3•apo-Mb-CN^{-}[b]	282.5	291	345.5	399.5	460.5	
1 in buffer[c]	305.5 (34.1)	338 (31.4)	434 (21.5)			

[a] 10 mM Tris/HCl (pH7.0) buffer. [b] 100eq of KCN. [c] 0.17% methanol in 10 mM Tris/HCl (pH7.0) buffer.

Results and Discussion

Preparation of Fe^{III} Schiff base•apo-Mb.

The heme is fixed in the Mb cavity by three factors; hydrophobic interaction of the heme ligand with the cavity (50 %), proximal histidine ligation to the heme iron (25 %), and hydrogen bonds between the heme side chains and amino acid residues (25 %).[11] Thus, the design of Schiff base ligands is important to increase its binding affinity to an apo-Mb cavity. In order to examine the effect of Schiff base ligands on the binding affinity, Fe^{III}(salophen)-derivatives were synthesized. Salophen and its derivatives were synthesized by reactions of salicylaldehyde derivatives and 1,2-phenylenediamine and the corresponding iron(III) complexes were obtained by their reactions with iron(III) chloride in ethanol. Reconstitution of apo-Mb with Fe^{III}(salophen)-derivatives was carried out according to a method reported with some modification.[9] In order to accelerate the ligand-exchange reaction of Fe^{III}(salophen)Cl with apo-Mb, the chloride ion was removed by

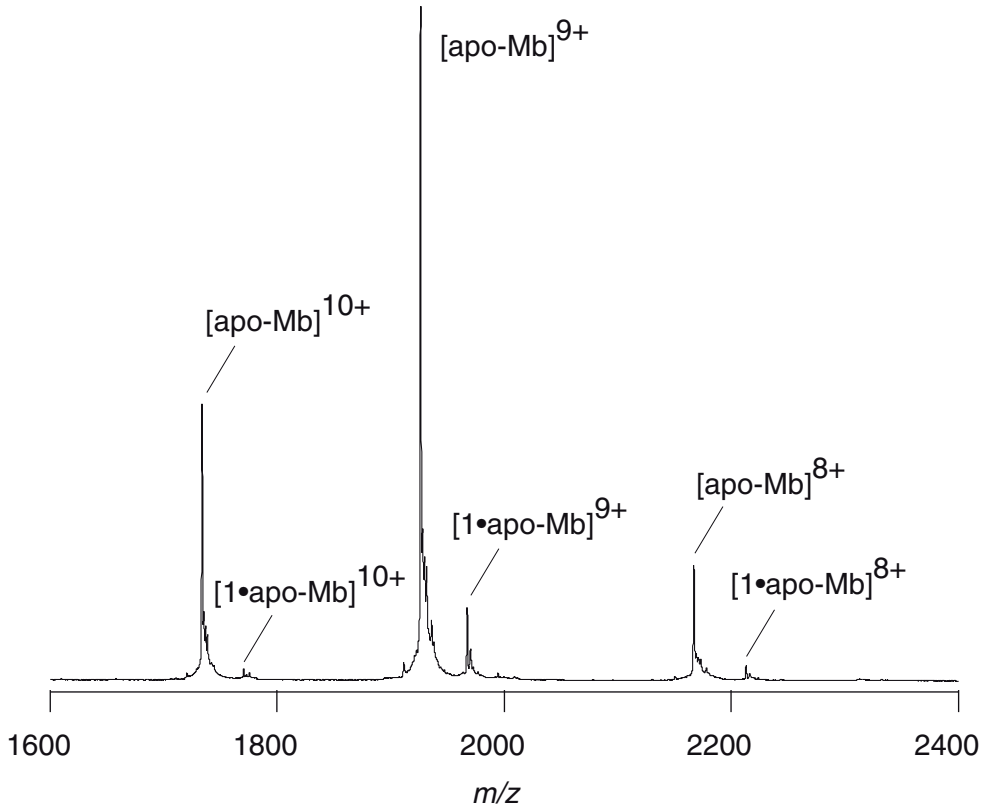

Figure 3. ESI-TOF mass spectrum of **1•apo-Mb**

$AgBF_4$ in methanol.[12] The resulting methanol solution of $[Fe^{III}(salophen)]^+$ was mixed with an aqueous solution of apo-Mb (10 mM Tris/HCl, pH 7.0). After removal of methanol by the dialysis, Fe^{III}(salophen)•apo-Mb was purified by G-25 and CM52 column chromatography. The final yields of **1•apo-Mb**, **2•apo-Mb**, and **3•apo-Mb** are 28, 20, and 11 %, respectively. We failed the isolation of Fe^{III}(3,3'-*t*-Bu_2-salophen)•apo-Mb. UV-vis spectra of Fe^{III}(salophen)-derivatives•apo-Mbs are listed in Table 1. The absorption maxima of **1•apo-Mb** are observed at 282, 289.5, 326.5, and 376 nm which are not observed for **1** without apo-Mb under the same conditions (Table 1).

ESI-TOF MS measurement.

Electrospray ionization-time of flight mass spectrometry (ESI-TOF MS) was measured to confirm the 1:1 complex formation of purified Fe^{III}(salophen)-derivatives•apo-Mbs.

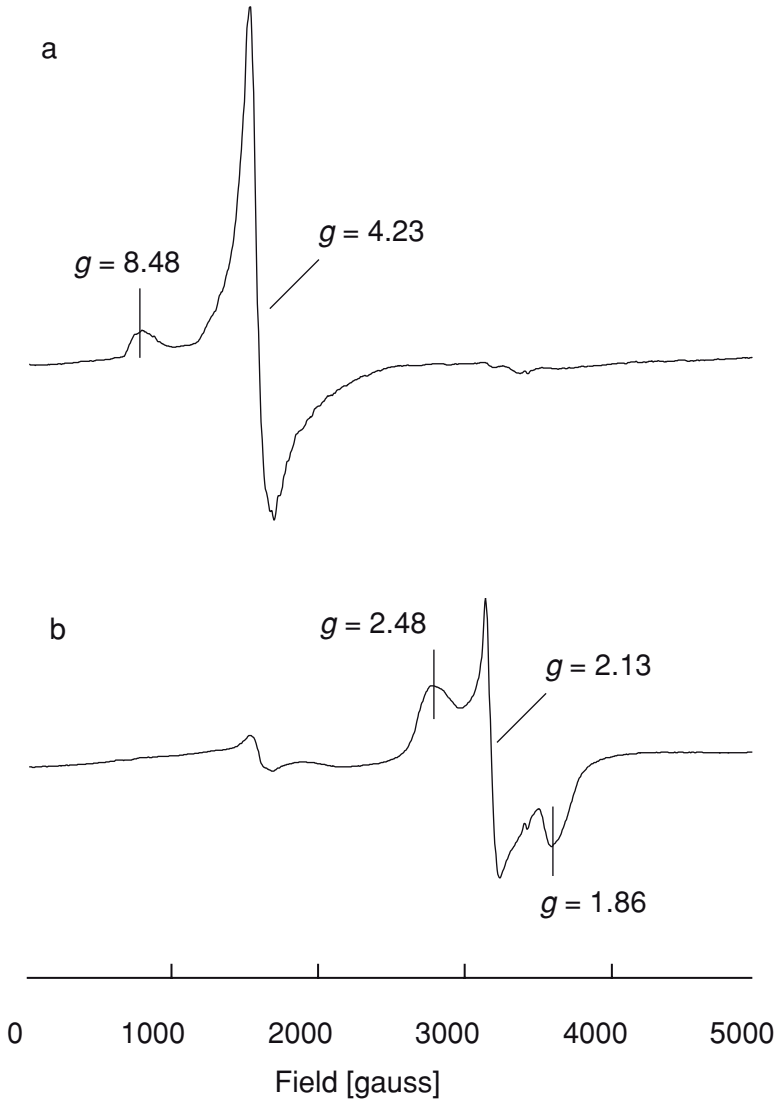

Figure 4. The EPR spectrum of **1**·**apo-Mb** (0.6 mM) (**a**). Addition of 100 equiv. of KCN to the solution of **a** at 5 K in 10 mM Tris/HCl (pH 7.0) caused spectral change to **b**.

1•apo-Mb ions bearing multiple charges were observed in the ESI-TOF mass spectrum and the averaged molecular mass deconvoluted from these peaks is 17700.9 ± 0.2, consistent with the expected mass value for **1•apo-Mb** (calc. 17700.2) (Fig. 3). ESI-TOF mass spectra of **2•apo-Mb** and **3•apo-Mb** also showed 1:1 complex formation. Almost identical ESI-TOF mass was also observed for **2•apo-A71G Mb** whose crystal structure has

Table 2. EPR g values of Fe^{III}(salophen)-derivatives•apo-Mbs[a] and their complexes with CN^-.

	Fe^{III}(salophen)-derivatives• apo-Mb		Cyanide complex[b]		
1•apo-Mb	8.48	4.23	2.48	2.13	1.86
2•apo-Mb	8.38	4.25	2.48	2.12	1.89
3•apo-Mb	8.13	4.24	2.44	2.14	1.90

[a]Conditions: [Fe] = 0.6 mM in10 mM Tris/HCl (pH7) at 5K. [b]100 equiv KCN was added to Fe^{III}(salophen)-derivative•apo-Mb.

been solved at 1.45 Å resolution.

EPR spectra.

ESR spectra of the reaction mixtures of Fe^{III}(salophen)-derivatives and apo-Mb were measured at 5 K in 10 mM Tris/HCl buffer (pH 7) (Fig. 4 and Table 2). The EPR spectrum of **1** and apo-Mb (1:1.2) shows typical high-spin iron (III) signals at g = 4.23 and 8.48 (Fig. 4a) and almost identical spectra for **2•** and **3•apo-Mb** are also obtained (Table 3). These spectra are very similar to those of $[Fe^{III}$(3-EtO-salen)(5-Ph-imd)$(H_2O)]BPh_4$•$0.5H_2O$ in CH_2Cl_2.[13] On the other hand, the EPR spectrum of **1** without apo-Mb in the same buffer solution is silent, because of the dimmer formation. These results suggest that the high-spin signals of the Fe^{III}(salophen)-derivatives are attributed to Fe^{III}(salophen) bound to imidazole of apo-Mb. Furthermore, these high-spin signals were disappeared by the addition of 100 equiv. of KCN with concomitant appearance of new three signals at 1.8–2.5 assigned to low-spin species (Figure 4b and Table 2). A similar spectral change from the high-spin to the low-spin state by the addition of KCN has also been reported for holo-Mb.[14]

The binding affinity of 1, 2, and 3 for apo-Mb.

The binding affinity of Fe^{III}(salophen)-derivatives to apo-Mb was compared by measuring competitive binding of the derivatives to apo-Mb. The binding affinity of biomolecular

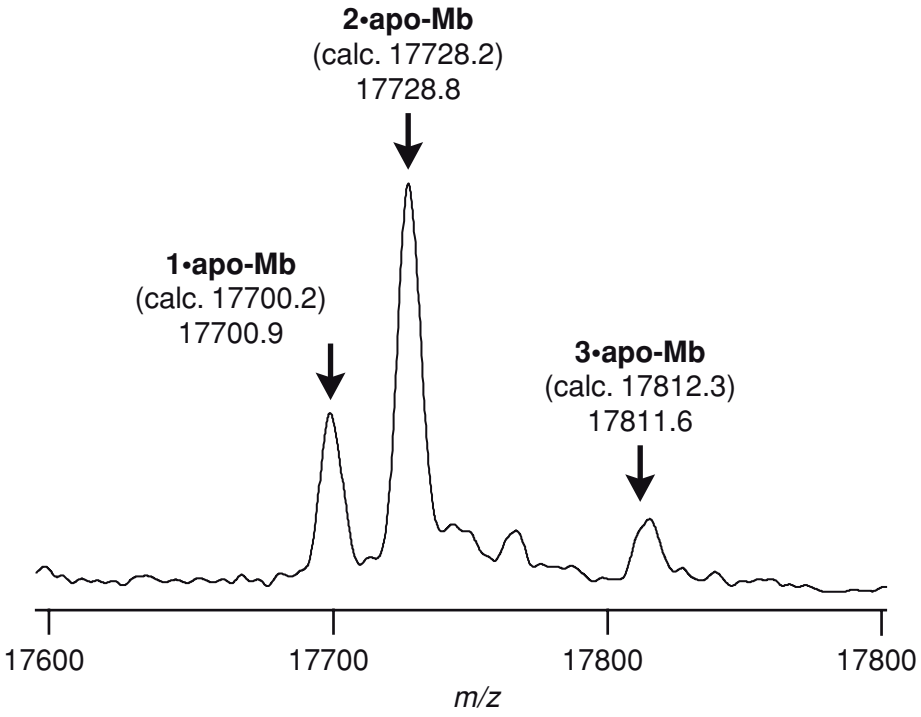

Figuer 5. The ESI-TOF mass spectrum of apo-Mb reconstituted by a mixture of **1**, **2**, and **3**.

composites such as a DNA-protein complex has been estimated by a relative peak intensity of those complexes in ESI-TOF mass spectra.[15] In order to compare the affinity of Fe^{III}(salophen)-derivatives and apo-Mb, a mixture of **1**, **2**, and **3** in methanol was mixed with an aqueous solution of apo-Mb (5 mM ammonium acetate buffer, pH 6.4) and the resulting solution was directly submitted to a ESI-TOF MS (Fig. 5). The mass spectrum of the solution gave three peaks corresponding to **1•**, **2•**, and **3•apo-Mb** and relative peak intensity was in the order of **2** > **1** > **3**, suggesting the same order for the binding affinity. The results suggest that substituents on the Schiff base ligand are very effective on the complexation with apo-Mb.

Thermal stability.

In order to investigate an effect of Schiff base ligand structure on the thermal stability of Fe^{III}(salophen)-derivatives•apo-Mbs, melting temperature of purified Fe^{III}(salophen)-

Table 3. Melting temperature (T_m) of Fe^{III}(salophen)-derivatives•apo-Mbs.

	Tm ˚C	*ΔTm* ˚C
1•apo-Mb	68.1	0.9
2•apo-Mb	69.7	2.5
3•apo-Mb	67.0	-0.2
Holo-Mb	85.3	18.1
apo-Mb	67.2	–

derivatives•apo-Mbs was determined by circular dichroism spectral measurements (Table 3).[11] The apo-Mb shows a melting temperature at 67.2 °C and those of reconstituted Mbs with **1** and **2** are higher than that of apo-Mb, 68.1 (ΔT_m = 0.9 °C) and 69.7 °C (ΔT_m = 2.5 °C), respectively. In contrast, the thermal stability of **3•apo-Mb** was slightly lower than apo-Mb (67.0 °C, ΔT_m = –0.2 °C). The order of the thermal stability of Fe^{III}(salophen)-derivatives•apo-Mbs is, therefore, **2** > **1** > **3**. The results are good agreement with the relative peak intensity in the ESI-TOF mass spectrum of **1•**, **2•**, and **3•apo-Mb**. These differences in the thermal stability of Fe^{III}(salophen)-derivatives•apo-Mbs could be explained on the basis of the X-ray crystal structure of **2•apo-A71G Mb**. According to the crystal structure of **2•apo-A71G Mb** (Fig. 1), **2** is located in the heme pocket by avoiding steric repulsion of the ligand and amino acid residue surrounding **2**, such as Phe43, Gly71, and Ile107 (Fig. 1). Even in the crystal structure of Cr^{III}(3,3'-Me_2-salophen)•apo-A71G Mb, the location of the Cr complex is almost the same. Therefore, we expect the structures of **1•** and **2•apo-Mb** might be very similar to **2•apo-A71G Mb**. Higher thermal stability of **2•apo-Mb** than **1•apo-Mb** is readily attributed to the hydrophobic interaction between two methyl groups in **2** and Ile107 of apo-Mb. In contract, the thermal stability of **3•apo-Mb** is the lowest in the three apo-Mb complexes. Introduction of two *t*-Bu

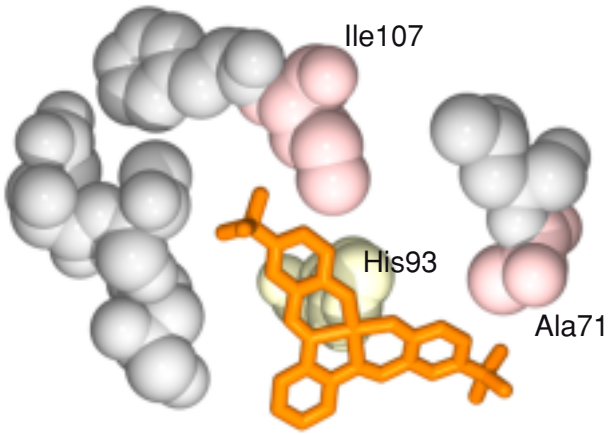

Figuer 6. Calculated structure of **3•apo-Mb** by Insight II/Discover 3 with ESFF force field.

groups on the C5 and C5' positions of salophen must cause steric repulsion if we place **3** into apo-Mb as observed for **2•apo-A71G Mb**. Thus, the orientation of **3** in apo-Mb must be different form that of **2•apo-A71G Mb**. According to a calculated structure of **3•apo-Mb** by Insight II/Discover 3, two *tert*-buthyl groups at C5 and C5' on salophen prevent the deep insertion of **3** into apo-Mb cavity (Fig. 6). Therefore, these results imply that the position and size of substituted hydrophobic groups on the metal complex are very important for the complexation with protein and stability of the composite.

Kinetics of cyanide binding.

In order to investigate whether or not we could control the reactivity of Fe^{III}(salophen)•apo-Mb by the modification of the salophen ligand, cyanide binding to Fe^{III}(salophen)•apo-Mb was studied by stopped-flow measurements. The absorption spectral changes of **1•apo-Mb** in the reaction with KCN are shown in Figure 7 (inset). Within 1 min after the mixing, new peaks appeared at 337 and 387.5 nm with isosbestic point at 333 nm. The absorption spectral change corresponds to the formation of CN bound **1•apo-Mb** as characterized by EPR spectroscopy. The cyanide binding rate for **1•apo-Mb** is 100 and 30-fold faster than those of **2•apo-Mb** and **3•apo-Mb**, respectively (Table 4). In the case of holo-Mb, the rate-determining step for cyanide binding is known to be the

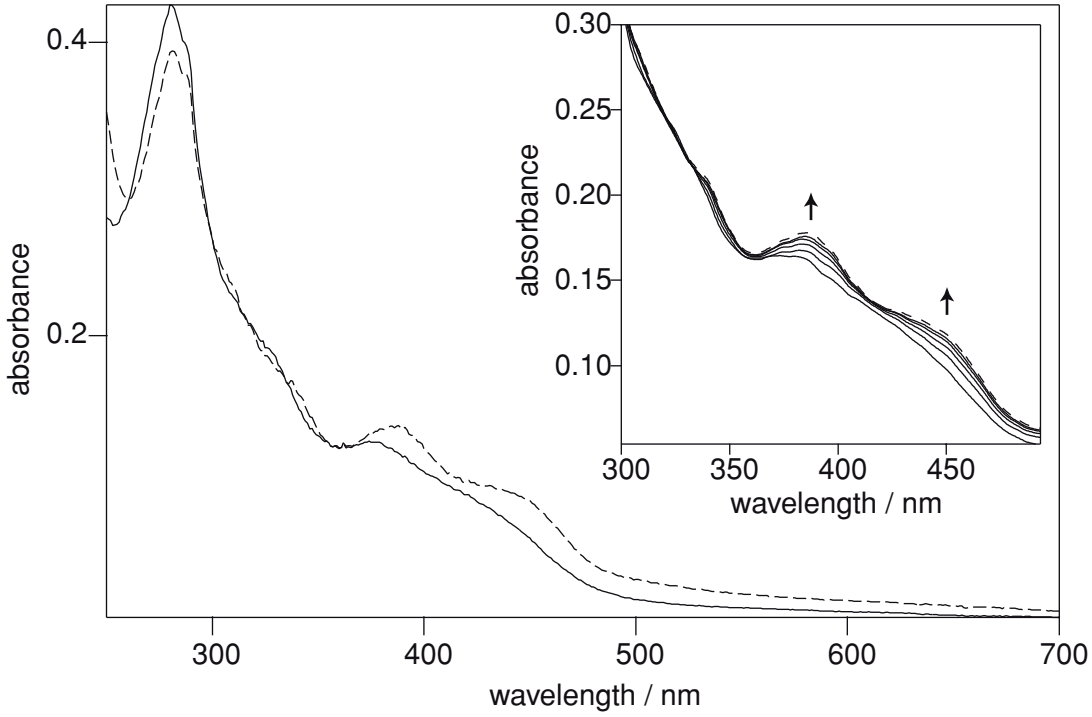

Figure 7. UV-vis spectra of **1**·**apo-Mb** and cyanide treated **1**·**apo-Mb**: 9 μM of **1**·Mb in 10 mM Tris/HCl (pH 7.0) (solid line); 100 equiv. of cyanide treated **1**·**apo-Mb** at in 10 mM Tris/HCl (pH 7.0) (dot line); Inset shows rapid scan spectra of 100 equiv. of cyanide treated **1**·**apo-Mb** measured at every 14 msec interval.

Table 4. Kinetic parameters of cyanide binding to Fe^{III}(salophen)-derivatives•apo-Mbs.

	1•apo-Mb	**2•apo-Mb**	**3•apo-Mb**	holo-Mb
k_{on}	202.0	2.216	7.313	3010

deprotonation of HCN by distal residues, since the major form of cyanide is protonated at neutral pH (pKa ~9).[16] Actually, 160-fold decrease in k_{CN} upon the mutation of histidine 64 in Mb with leucine (H64L Mb) was attributed to the loss of a general base.[16] In the case of Fe^{III}(salophen)-derivatives•apo-Mb, both orientation and location of each iron (III) complex are expected to be different due to the substituents at the C3, C3', C5, and C5' posi-

tions. Therefore, orientation and distance of distal histidine (His64) to the iron ion in **1•**, **2•**, and **3•apo-Mb** are different. These differences could perturb the relative basicity of distal histidine in **1•**, **2•**, and **3•apo-Mb**.

In summary, we have investigated the effects of ligand modification on function and stability of Fe^{III}(salophen)-derivatives•apo-Mb. The substituents on the Schiff base ligand play important two roles. The hydrophobic interactions as well as the minimization of steric hindrance of the ligand regulate the location and orientation of the metal complex in the protein matrix. The different orientation and location of the complexes affect the reactivity of the metal complexes such as cyanide binding. Those results suggested that the design of Schiff base ligand is very important for the preparation of artificial metalloenzymes.

Experimental Section

Materials. Reagents were purchased from Wako, Nacalai Tesque, and Aldrich and used without further purification. The expression vector for wild type of sperm whale Myoglobin (Mb) is a gift from John Olson (Rice University).[17] Expression and purification of Mb were performed according to a method described by Springer *et al*. with some modification. Apomyoglobin (apo-Mb) was prepared using an acid-butanone method.[18]

Preparation of iron (III) Schiff base complexes. Schiff base ligands and their iron (III) complexes were prepared by literature methods[19-22] and described in chapter 1 of part I. The yield, mass data, and ^{1}H NMR of each Schiff base ligand and the corresponding iron (III) complexes are as follows; **salophen-H_2**; yield: 87%, MS: 317.1 (calc. 316.1), ^{1}H NMR ($CDCl_3$): δ 13.02 (s, 2H), 8.64 (s, 2H), 7.40-7.33 (m, 6H), 7.26-7.23 (m, 2H), 7.04 (d, *J* = 8.1 Hz, 2H), 6.92 (t, *J* = 7.5 Hz, 2H). **3, 3'-Me_2-salophen-H_2**; yield: 80%, MS: 345.1 (calc. 344.1); ^{1}H NMR ($CDCl_3$): δ 13.20 (s, 2H), 8.62 (s, 2H), 7.36-7.30 (m, 2H), 7.26-7.17 (m, 6H), 6.83 (t, *J* = 7.5 Hz, 2H), 2.29 (s, 6H). **5, 5'-*t*-Bu_2-salophen-H_2**; yield: 82%, MS: 429.2 (calc. 428.2), ^{1}H NMR ($CDCl_3$): δ 12.85 (s, 2H), 8.64 (s, 2H), 7.41 (dd, *J*

= 8.7, 2.7 Hz, 2H), 7.35 (s, 2H), 7.34-7.30 (m, 2H), 7.25-7.19 (m, 2H), 6.99 (d, *J* = 8.6 Hz, 2H), 1.29 (s, 18H). **1•Cl**; yield: 30%, MS: 370.02 (calc. 370.04). **2•Cl**; yield: 58%, MS: 398.01 (calc. 398.07). **3•Cl**; yield: 59%, MS: 482.09 (calc. 489.17).

Preparation of iron (III) Schiff base complex•apo-Mb. To **1•Cl** (12 ml, 25 mM) in methanol was added a methanol solution of $AgBF_4$ (1.2 ml, 367 mM). The mixture was stirred at 50 ˚C for 3 h and then precipitated AgCl and Ag^+ ion were removed by celite filtration. The eluent containing **1•BF$_4$** was diluted with methanol to 10 mM. The methanol solution of **1•BF$_4$** (1 ml, 10 mM) was slowly added to an apo-Mb solution (14 ml, 0.3 mM in 10 mM Tris/HCl buffer, pH 7.0) and gently stirred at 4˚C for 10 min. The mixture was dialyzed against 10 mM Bis-tris buffer (pH 6.0) at 4 ˚C for 6 h. After the dialysis, the mixture was passed through Sepadex G-25 equilibrated with 10 mM Tris/HCl buffer (pH 7.0), and then purified with HiTrap™ CM FF on an ÄKTA explorer 100 FPLC system (Amersham Biosciences) with linear gradient (10-500 mM Tris/HCl buffer, pH 7.0). **1•apo-Mb**; yield: 28%, ESI-TOF MS: [**1•apo-Mb**]$^+$ m/z 17700.9 (calc. 17700.2), UV-vis. (10 mM Tris/HCl buffer, pH 7.0) λ/nm (ε M^{-1} cm^{-1}): 282(50950), 289.5 (47160), 326.5 (23130), 376 (15400). 2•apo-Mb and 3•apo-Mb were also prepared by the same method. **2•apo-Mb**; yield: 20%, ESI-TOF MS: [**2•apo-Mb**]$^+$ m/z 17728.8 (calc. 17728.2), UV-vis (10 mM Tris/HCl buffer, pH7.0) λ/nm (ε M^{-1} cm^{-1}): 283.5 (65895), 289 (65230), 324.5 (41790), 380.5 (22050). **3•apo-Mb**; yield: 11%, ESI-TOF MS: [**3•apo-Mb**]$^+$ m/z 17811.6 (calc. 17812.3), UV-vis. (10 mM Tris/HCl buffer, pH 7.0) λ/nm (ε M^{-1} cm^{-1}): 282.5(154550), 291(130270), 341.5(38680), 410(24700).

Physical measurements. Elemental analyses were performed by the Research Center for Molecular Materials, Institute for Molecular Science. UV-vis spectra were recorded on a SHIMADZU UV-2400PC UV-VIS spectrophotometer. ^{1}H NMR spectra were recorded on a JEOL JNM-EX 270 spectrometer.

Atomic absorption spectroscopy. Iron concentration in Fe^{III}(salophen)-derivatives•apo-Mb was determined by a Polarizing Zeeman-effect atomic absorption spectrophotometer

Z-5710 (HITACHI) operating in graphite furnace mode using an Fe hollow cathode lamp. Iron ion was detected at 248.3 nm with a slit width of 0.2 nm. $Fe^{III}(NO_3)_3$ in 0.1 mol/l•HNO_3 (99.8 mg/l, Wako) was used as a calibration standard.

EPR measurements. EPR spectra were recorded on an E500 X-band CW-EPR (Bruker). A cryostat (ITC503, Oxford) was used for the observation at 5 K. EPR absorption spectra of iron (III) schiff base complex•apo-Mb (0.6 mM, 10 mM Tris/HCl buffer, pH 7.0) and their cyanide bound derivatives were measured at 5 K. The cyanide bound samples were prepared by addition of 100 equiv. of KCN (0.1 M, 10 mM Tris/HCl buffer, pH 7.0) to a solution of iron (III) schiff base complex•apo-Mb (0.6 mM, 10 mM Tris/HCl buffer, pH 7.0). The reaction mixture was then frozen by liquid nitrogen.

Mass spectrometry. ESI-TOF mass analyses were performed on a Micromass LCT instrument. Typical parameters are as follows, capillary voltage: 3 kV, cone voltage: 60 V, source temperature: 60 °C, flow-rate: 5 μl min^{-1}. CsI (1 mg/ml) in 50% H_2O/CH_3CN was used for mass scale calibration. All samples were dialyzed against 5 mM ammonium acetate buffer (pH 6.7) at 4 ˚C for 6 h and diluted to 10 mM by the same buffer solution.

Kinetic measurements for the association of cyanide. Reactions of holo-Mb and reconstituted Mbs with cyanide were measured at 395-408 nm on a UNISOKU stopped-flow apparatus in 10 mM Tris/HCl buffer (pH 7.0). The association rate constants were given by the slope of a plot of the observed rates *versus* cyanide concentration.

Analysis of thermal stability. Circular dichroism spectra were recorded on a JASCO model J-720 spectropolarimeter that was equipped with a JASCO model PTC-348WI Peltiert cooling temperature controller. Spectropolarimeter and water bath were operated under computer control. Protein samples (2.5 μM in 1 mM Tris/HCl buffer, pH 7.0) were placed into a quartz cell (1 cm path length), and ellipticity was recorded at 222 nm from 25 to 95 ˚C with a heating rate of 50 ˚C/h. The midpoint melting temperature (T_m) was determined from the first derivative of the resulting ellipticity *versus* temperature plot.

MD calculations. The X-ray structure of sperm whale myoglobin was obtained from the

Brookhaven Protein Data Bank (1DUK.pdb). All calculations were carried out by using InsightII/Discover program with an ESFF force field.

Reference

(1) Watanabe, Y. *Curr. Opin. Chem. Biol*. **2002**, *6*, 208-216.

(2) Hayashi, T.; Hisaeda, Y. *Acc. Chem. Res*. **2002**, *35*, 35-43.

(3) Benson, D. E.; Wisz, M. S.; Hellinga, H. W. *Proc. Natl. Acad. Sci. USA* **2000**, *97*, 6292-6297.

(4) Ozaki, S.; Roach, M.; Matsui, T.; Watanabe, Y. *Acc. Chem. Res*. **2001**, *34*, 818-825.

(5) Hayashi, T.; Dejima, H.; Matsuo, T.; Sato, H.; Murata, D.; Hisaeda, Y. *J. Am. Chem. Soc*. **2002**, *124*, 11226-11227.

(6) Neya, S.; Funasaki, N.; Hori, H.; Imai, K.; Nagatomo, S.; Iwase, T.; Yonetani, T. *Chem. Lett*. **1999**, 989-990.

(7) Neya, S.; Nakamura, M.; Imai, K.; Funasaki, N. *Chem. Pharm. Bull*. **2001**, *49*, 345-346.

(8) Chapter 1 in this part

(9) Ohashi, M.; Koshiyama, T.; Ueno, T.; Yanase, M.; Fujii, H.; Watanabe, Y. *Angew. Chem. Int. Ed*. **2003**, *42*, 1005-1008.

(10) Ueno, T.; Koshiyama, T.; Ohashi, M.; Kono, M.; Kondo, K.; Szuki, A.; Yamane, T.; Watanabe, Y. in preparation.

(11) Hunter, C. L.; Lloyd, E.; Eltis, L. D.; Rafferty, S. P.; Lee, H.; Smith, M.; Mauk, A. G. *Biochemistry* **1997**, *36*, 1010-1017.

(12) Gullotti, M.; Casella, L.; Pasini, A.; Ugo, R. *J. Chem. Soc., Dalton Trans*. **1977**, 339-345.

(13) Kennedy, B. J.; Brain, G.; Horn, E.; Murray, K. S.; Snow, M. R. *Inorg. Chem*. **1985**, *24*, 1647-1653.

(14) Paul, M. A. G.; Andrew, J. T. *J. Am. Chem. Soc*. **1990**, *112*, 5003-5011.

(15) Kapur, A.; Beck, J. L.; Brown, S. E.; Dixon, N. E.; Sheil, M. M. *Protein Sci*. **2002**, *11*, 147-157.

(16) Brancaccio, A.; Cutruzzola, F.; Allocatelli, C. T.; Brunori, M.; Smerdon, S. J.;

Wilkinson, A. J.; Dou, Y.; Keenan, D.; Ikeda-Saito, M.; Robert. E. Brantley, J.; Olson, J. S. *J. Biol. Chem.* **1994**, *269*, 13843-13853.

(17) Springer, B. A.; Sligar, S. G. *Proc. Natl. Acad. Soc.* **1987**, *84*, 8961-8965.

(18) Ascoli F; Fanelli MR; E., A. *Methods Enzymol* **1981**, *76*, 72-87.

(19) Chen, H.; Cronin, J. A.; Archer, R. D. *Macromolecules* **1994**, *27*, 2174-2180.

(20) Ciringh, Y.; Gordon-Wylie, S. W.; Norman, R. E.; Clark, G. R.; Weintraub, S. T.; Horwitz, C. P. *Inorg. Chem.* **1997**, *36*, 4968-4982.

(21) Fitzsimmons, B. W.; Smith, A. W.; Larkworthy, L. F.; Rogers, K. A. *J. Chem. Soc., Dalton Trans.* **1973**, 676-680.

(22) Gerloch, M.; Lewis, J.; Mabbs, F. E.; Richards *J. Chem. Soc (A)* **1968**, 112-116.

Chapter 3.

Preparation of Artificial Metalloenzymes by Noncovalent Insertion of Cr^{III}(Schiff Base) Complexes into Apo-Myoglobin Mutants*

* *Angew. Chem. Int. Ed.* **2003**, *42*, 1005-1008.

Preparation of Artificial Metalloenzymes by Insertion of Chromium(III) Schiff Base Complexes into Apo-Myoglobin Mutants.

Masataka Ohashi, Tomomi Koshiyama, Takafumi Ueno, Manabu Yanase, Hiroshi Fujii, and Yoshihito Watanabe Regulation of Cyanide Binding to Fe^{III}(Schiff Base)•Apo-Myoglobin by the Schiff Base Ligand Structure

Introduction

Construction of artificial metalloenzymes is one of the most important subjects in bioinorganic chemistry, because metalloenzymes catalyze chemical transformation with high selectivity and reactivity under mild conditions.[1-4] There are several reports on protein design; introduction of metal binding sites,[1,3,5-8] design of substrate binding cavities,[9-12] chemical modification of prosthetic groups,[13-16] and covalent attachment of metal cofactors.[2,17-20] Especially, the covalent modification of proteins has been proved to be a powerful tool for the generation of new metalloenzymes, while the efficiency of the modification is very much dependent on the position and reactivity of the cysteinyl thiol functional group.[2] In this chapter, we describe a novel strategy for the preparation of artificial metalloenzymes by noncovalent insertion of metal complex catalysts into protein cavities. The resulting semi-synthetic metalloenzymes, apo-Myoglobin (apo-Mb) reconstituted with Cr^{III} Schiff base complexes, are able to catalyze enantioselective sulfoxidation.

Results and Discussion

Manganese (III) and chromium (III) Schiff base complexes are known as catalysts for various oxidations in organic solvents.[21,22] Jacobsen and Katsuki have already reported many examples of asymmetric oxidations catalyzed by chiral Mn Schiff base complexes.[23,24] In our case, symmetric complexes, $[M^{III}(salophen)]^+$ [**M•1**, M=Mn and Cr, salophen (**1**) =N,N'-bis(salicylidene)-1,2-phenylenediamine], are employed to insert into a chiral cavity of apo-Mb (Scheme 1). In addition, the 5 and 5' positions of salophen are substituted by *tert*-buthyl group, 5,5'-tBu$_2$-salophen (**2**), in order to improve the binding affinity to apo-Mb; i.e., the binding affinity of heme in apo-Mb is provided by hydrophobic interaction and the ligand size[25] and we found that similar factors are applicable for metal complexes to be inserted.

For the creation of artificial metalloenzymes, apo-Mb is an excellent candidate since reconstitution of apo-Mb with heme has been well studied.[13,26-28] We have already demon-

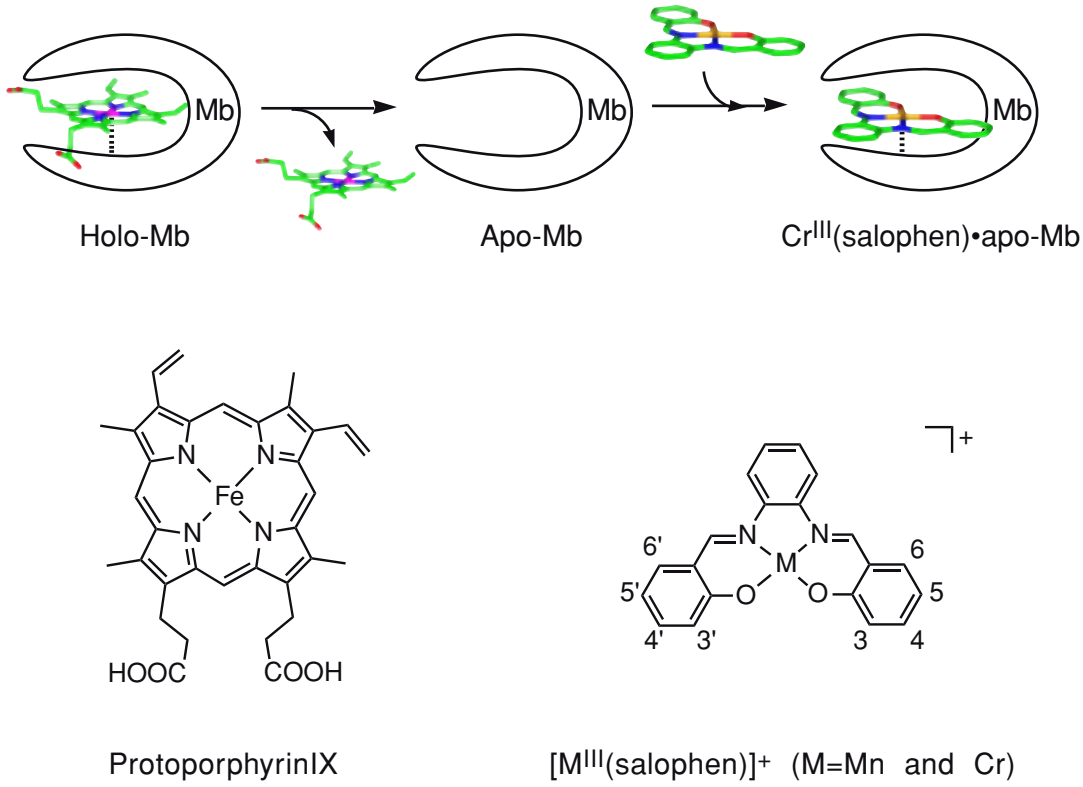

Scheme 1. Insertion of a salophen complex into apo-Mb.

strated that the catalytic selectivity and reactivity of Mb as a peroxygenase are controlled by appropriate site-directed mutagenesis in the active site.[10,11,29] On the basis of these results, we have designed a suitable apo-Mb mutant for the reconstitution with Schiff base complexes by using Insight II/Discover 3. A designed protein structure, **Cr•2•apo-H64D/A71GMb**, is shown in Figure 1b. If we assume that **Cr•2** binds to His93 as observed for the heme, the replacement of His-64 to Asp (H64D) will provide an increased access of substrates and oxidants to a vacant distal site above the Cr^{III} center.[11] At the same time, the alanyl sidechain at the position 71 in Mb is expected to be located very much close to the 4 and 5 positions of **Cr•2** (Figure 1). Thus, alanine71 was replaced to Gly in order to improve the binding affinity of **Cr•2** in the active site.

The reconstitution of apo-Mb with **Cr•2** was carried out by applying a method for modified hemes;[28] to an apo-Mb solution in 10mM Tris/HCl (pH 7.0) was added dropwise

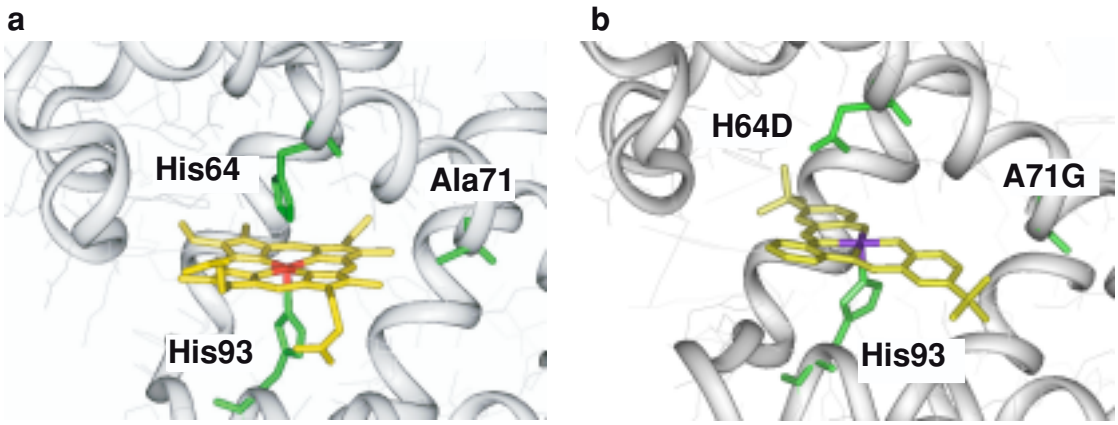

Figure 1. Comparison of the crystal structure of wild-type Mb (PDB code 2MBW) (**a**) and a proposed structure of **Cr•2•apo-H64D/A71GMb** calculated by Insight II/Discover 3 (ESFF force field) (**b**).

0.9 equiv. of [**Cr•2**$(H_2O)_2$]•BF_4 dissolved in MeOH (0.7 mM). The mixture was dialyzed against 10mM Bis-Tris/HCl (pH 6.0) and then loaded on Sephadex G-25. The final purification was done by CM52 column with a linear gradient of 10–100 mM Tris/HCl buffer, pH 7.0 and isolated yield of **Cr•2•apo-Mb** was 15 %. The isolated yield of **Cr•2•apo-H64D/A71GMb** (4.3 %) was 15 and 2-fold larger than that of **Cr•1•apo-H64D/A71GMb** (0.3 %) and **Cr•2•apo-H64DMb** (2.4 %), respectively. On the other hand, any effort for the preparation of **Mn•1•apo-H64D/A71GMb** was failed. These results imply that metal ions and ligand structure are very important for the binding affinity to the Mb mutants.

Figure 2a shows the deconvoluted electrospray ionization time-of-flight (ESI-TOF) mass spectrum of purified **Cr•2•apo-Mb** in 5 mM ammonium acetate. Two peaks are readily assigned to **Cr•2•apo-Mb** (measured: 17808.3 ± 1.1 Da, calculated: 17808.6 Da) and a small portion of apo-Mb (measured: 17330.0 ± 0.1 Da, calculated: 17330.1 Da), respectively. Appearance of a small peak corresponding to apo-Mb is also observed for purified heme bound Mb (holo-Mb) under the same condition, indicating the binding affinity of **Cr•2** to be comparable to that of heme. In order to confirm that **Cr•2** is incorpo

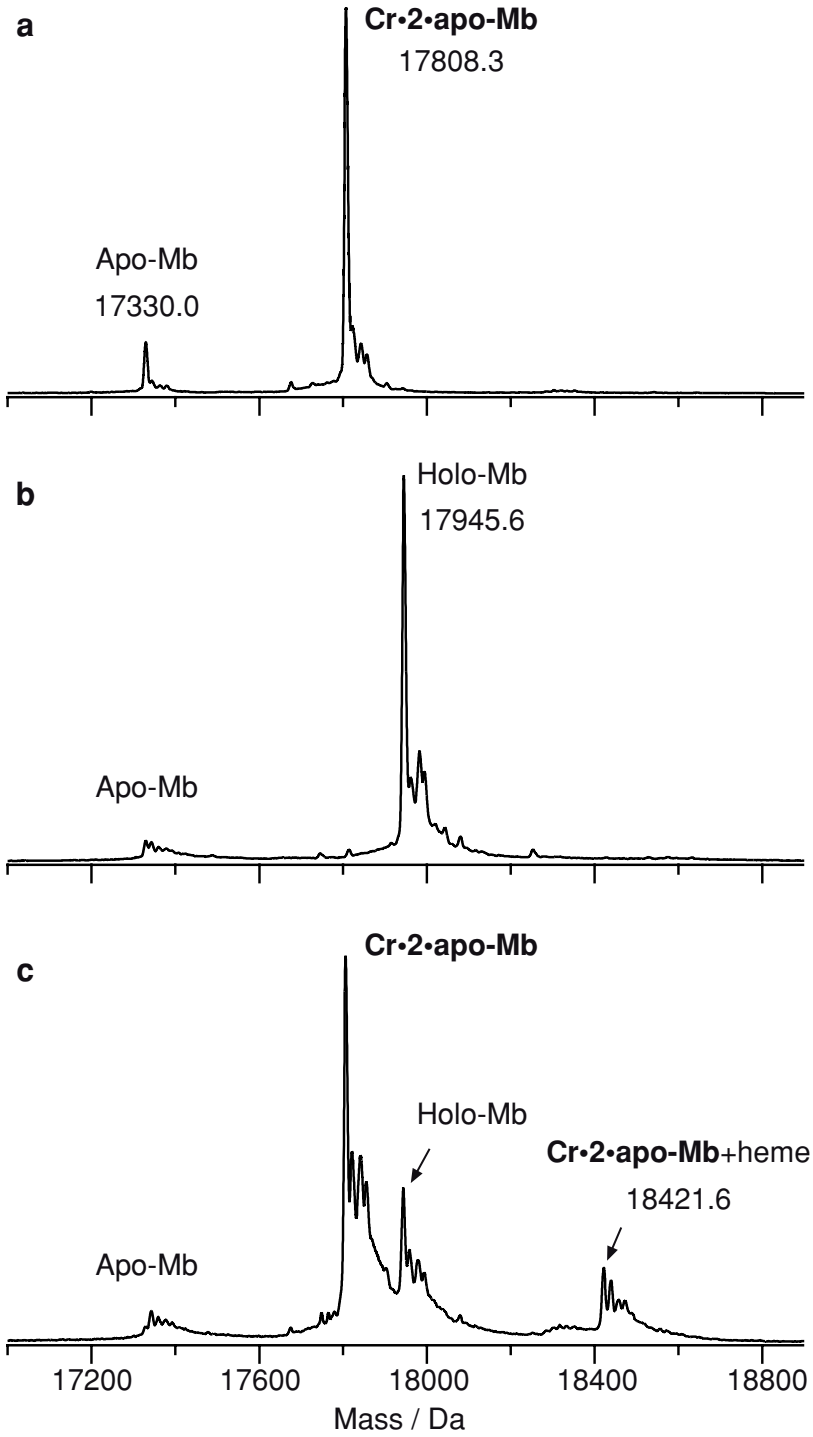

Figure 2. Deconvoluted ESI-TOF mass spectra of **Cr•2•apo-Mb** (**a**), apo-Mb + 2 equiv. hemin (**b**), and **Cr•2•apo-Mb** + 2 equiv. hemin (**c**) in 5 mM ammonium acetate. Sample preparation for (**b**) and (**c**); to purified **Cr•2•apo-Mb** (10 μM) and apo-Mb (10 μM), respectively, was added 2 equiv. hemin (1 mM, DMF solution), and then the mixtures were stirred for 10 min and then dialyzed against 5 mM ammonium acetate for 8 h at 4 °C.

rated in the position of heme, the following experiments were performed. In the first experiment, a mixture of apo-Mb and 2 equiv. of hemin was applied for ESI-TOF MS measurement and holo-Mb was observed as the main peak (measured: 17945.6 ± 0.1 Da, calculated: 17946.6 Da) (Figure 2b). On the other hand, to a purified **Cr•2•apo-Mb** in 5mM ammonium acetate was added a DMF solution of 2 equiv. of hemin. The ESI-TOF mass spectrum of the resulting solution is shown in Figure 2c. New peaks assigned to holo-Mb and **Cr•2•apo-Mb**+heme (measured: 18421.6 ± 0.3 Da, calculated: 18424.7 Da) were appeared as small peaks compared with that of **Cr•2•apo-Mb**. If the Cr^{III} complex binds on the surface of apo-Mb, we expect to observe **Cr•2•apo-Mb**+heme as the major peak since the incorporation of heme into apo-Mb is very rapid and the mutation of His64 and Ala71 should not be effective for the reconstitution. In addition, preliminary result of X-ray crystallographic analysis of Cr(3,3'-Me_2-salophen)•apo-A71GMb shows the chromium (III) ion binds to the Nε atom of imidazole in His 93.[30] Thus, we concluded that the His 93 coordination is crucial for **Cr•2** to locate in the active site of Mb.

The H_2O_2-dependent sulfoxidation of thioanisole was examined at 35 °C and pH 5.0 (Table 1). The rate and enantiomeric excess of the sulfoxidation was determined by HPLC analysis (Daicel OD chiral-sensitive column).[9] **Cr•1•apo-H64D/A71GMb** and **Cr•2•apo-H64D/A71GMb** exhibit the highest sulfoxidation activity and **Cr•2•apo-H64DMb** is the lowest. **Cr•1•apo-H64D/A71GMb** and **Cr•2•apo-H64D/A71GMb** showed *ca*. 6-fold rate increase *over* **Cr•2**. In addition, **Cr•2•apo-H64D/A71GMb** gave (*S*)-methylphenyl sulfoxide with a 13%ee while the sulfoxidation catalyzed by **Cr•2** proceeded with no enantiomeric discrimination. The other mutants show lower enantioselectivity than that of **Cr•2•apo-H64D/A71GMb**. As a control experiment, the sulfoxidation by Cr•2•bovin serum albumin (BSA) was done[31] and the enantioselectivity and rate were very low compared with that of **Cr•2•apo-H64D/A71GMb** (Table 1) because of nonspecific binding ability of **Cr•2** to BSA and the absence of histidine coordination to the Cr^{III} complex. This indicates that an apo-Mb mutated cavity and His93 coordination to the Cr^{III} atom are im-

Table 1. Thioanisole sulfoxidation activity.[a]

	Rate[b]	% ee
Cr•2•apo-Mb	46	4.3(*R*)
Cr•2•apo-A71GMb	54	6(*S*)
Cr•2•apo-H64DMb	27	0.3(*S*)
Cr•1•apo-H64D/A71GMb	83	8.3(*S*)
Cr•2•apo-H64D/A71GMb	78	13(*S*)
Cr•2•BSA	12	0.5(*S*)
Cr•2 in buffer	13	0

[a] Sulfoxidation was carried out in sodium acetate buffer (50 mM, pH 5.0) at 35 °C in the presence of complex (10 μM), thioanisole (1 mM), and H_2O_2 (1 mM). [b] The unit for rate is 10^{-3} turnover per minute.

portant to improve the enantioselectivity and rate of the sulfoxidation. Furthermore, EPR spectrum of **Cr•2•apo-H64D/A71GMb** oxidized by *m*-chloroperbenzoic acid at 5 K (pH 7.0) shows a signal at $g = 1.97$ to be assigned to an oxochromium (V) species.[32] Thus, the unstable active species in the catalytic sulfoxidation is expected to be the oxochromium (V) formed in the Mb cavity. While the enantioselectivity is still low, the results clearly demonstrate that asymmetric reactions can be achieved if we use protein cavities even though symmetric metal complexes are employed.

In summary, we have demonstrated the insertion of symmetric metal complexes into the active site of apo-Mb by binding to His93 and the semi-synthesized metalloenzymes catalyze the enantioselective sulfoxidation by utilizing the chiral protein cavity. Although the semi-synthetic metalloenzymes still exhibit low reactivity and enantioselectivity, our experiments suggest the possibility of this method for the design of artificial

metalloenzymes. Refinement of the crystal structure and further design to improve the reactivity and selectivity of the metalloenzymes are currently under progress.

Experimental Section

Materials. The mutants were constructed by cassette mutagenesis. Expression and purification of the mutants were performed as reported previously.[33] Ligand **1**, **2** and their Cr(III) complexes were synthesized by methods described in literatures.[34,35] **[Cr•2(H_2O)$_2$]BF_4** ESI-TOF MS: **Cr•2** $(CH_3CN)_2$ 560 (calc. 560); UV-vis: 480nm (ε /$M^{-1}cm^{-1}$ 0.93×10^4), 337 (2.35×10^4), **[Cr•1(H_2O)$_2$]BF_4** ESI-TOF MS: **Cr•1** $(CH_3CN)_2$ 448 (calcd. 449); UV-vis: 469nm (ε /$M^{-1}cm^{-1}$ 1.04×10^4), 334 (2.54×10^4); **Cr•2•apo-Mb** ESI-TOF MS: 17808.3 ± 1.1 (calc.17808.3); UV-vis: 485nm (ε /$M^{-1}cm^{-1}$ 1.02×10^4), 341 (2.45×10^4), 270 (3.75×10^4). **Cr•2•apo-A71GMb** ESI-TOF MS:17793.9 ± 0.9 (calc.17794.3); UV-vis: 483nm (ε /$M^{-1}cm^{-1}$ 1.02×10^4), 341 (2.88×10^4), 281 (4.38×10^4). **Cr•2•apo-H64DMb** ESI-TOF MS: 17786.0 ± 0.6 (calc.17786.2) ; UV-vis: 474nm (ε /$M^{-1}cm^{-1}$ 0.95×10^4), 338 (2.39×10^4), 321 (2.41×10^4), 282 (3.52×10^4). **Cr•2•apo-H64D/A71GMb** ESI-TOF MS: 17772.1 ± 0.3 (calc.17772.2) ; UV-vis: 471nm (ε /$M^{-1}cm^{-1}$ 1.02×10^4), 339 (2.61×10^4), 280 (4.18×10^4). **Cr•1•apo-H64D/A71GMb** ESI-TOF MS: 17658.2 ± 0.7 (calc.17660.1) ; UV-vis: 460nm (ε /$M^{-1}cm^{-1}$ 1.18×10^4), 320 (1.2×10^3), 282nm (2.3×10^3).

Determination of the chromium ion concentration. The concentration of Cr ion in the purified enzymes was determined by inductively coupled plasma atom emission spectrometry (ICPAES). The spectra were recorded on a SEIKO SPS 7000 that was calibrated with $K_2Cr_2O_7$ in 0.1 mol/l•HNO_3 (100.3 mg/l, Wako).

ESI-TOF MS. ESI-TOF mass spectra were measured on a LCT (Micromass, UK). Typical parameters; capillary: 3 kV, cone: 60 V, source temperature: 60 °C, flow-rate: 5 μl min^{-1}, and mass scale calibration: CsI (1 mg/ml) in 50% H_2O/CH_3CN. All samples were dialyzed against 5 mM ammonium acetate for 8–10 h at 4 °C.

EPR. EPR spectra were recorded at 5 K on a Bruker E500 operating at X band with an Oxford helium cryostat. The sample was prepared by addition of 100 equiv. of *m*-chloroperbenzoic acid (1 M in MeOH) to a purified **Cr•2•apo-H64D/A71GMb** (1 mM in 10 mM Tris/HCl at pH 7.0). The reaction mixtures were then frozen in liquid nitrogen.

References

(1) Lu, Y.; Berry, S. M.; Pfister, T. D. *Chem. Rev.* **2001**, *101*, 3047-3080 and references in this review.

(2) Qi, D.; Tann, C.; Haring, D.; Distefano, M. D. *Chem. Rev.* **2001**, *101*, 3081-3111 and references in this review.

(3) Benson, D. E.; Wisz, M. S.; Hellinga, H. W. *Curr. Opin. Biochem.* **1998**, *9*, 370-376.

(4) Velde, F. v. d.; Rantwijk, F. v.; Sheldon, R. A. *Trends Biotech.* **2001**, *19*, 73-80.

(5) Sigman, J. A.; Kwok, B. C.; Lu, Y. *J. Am. Chem. Soc.* **2000**, *122*, 8192-8196.

(6) Braha, O.; Walker, B.; Cheley, S.; Kasianowicz, J. J.; Song, L.; Gouaux, J. E.; Bayley, H. *Chem. Biol.* **1997**, *4*, 497-505.

(7) Miyawaki, A.; Llopis, J.; Heim, R.; McCaffery, J. M.; Adams, J. A.; Ikura, M.; Tsien, R. Y. *Nature* **1997**, *388*, 882-887.

(8) Pinto, A. L.; Hellinga, H. W.; Caradonna, J. P. *Proc. Natl. Acad. Sci. USA* **1997**, *94*, 5562-5567.

(9) Ozaki, S.; Yang, H.; Matsui, T.; Goto, Y.; Watanabe, Y. *Tetrahedron: Asymmetry* **1999**, *10*, 183-192.

(10) Hara, I.; Ueno, T.; Ozaki, S.; Itoh, S.; Lee, K.; Ueyama, N.; Watanabe, Y. *J. Biol. Chem.* **2001**, *276*, 36067-36070.

(11) Kato, S.; Yang, H.; Ueno, T.; Ozaki, S.; George N. Phillips, J.; Fukuzumi, S.; Watanabe, Y. *J. Am. Chem. Soc.* **2002**, *124*, 8506-8507.

(12) Ozaki, S.; Ortiz de Montellano, P. R. *J. Am. Chem. Soc.* **1995**, *117*, 7056-7064.

(13) Neya, S.; Funasaki, N. *J. Biol. Chem.* **1988**, *263*, 8810-8815.

(14) Hayashi, T.; Hitomi, Y.; Ando, T.; Mizutani, T.; Hisaeda, Y.; Kitagawa, S.; Ogoshi, H. *J. Am. Chem. Soc.* **1999**, *121*, 7747-7750.

(15) Hu, Y.; Tsukiji, S.; Shinkai, S.; Oishi, S.; Hamachi, I. *J. Am. Chem. Soc.* **2000**, *122*, 241-253.

(16) Monzani, E.; Alzuet, G.; Casella, L.; Redaelli, C.; Bassani, C.; Sanangelantoni, A.

M.; Gullotti, M.; Gioia, L. D.; Santagostin, L.; Chillemi, F. *Biochemistry* **2000**, *39*, 9571-9582.

(17) Davies, R. R.; Distefano, M. D. *J. Am. Chem. Soc.* **1997**, *119*, 11643-11652.

(18) Ma, S. K.; Lu, Y. *J. Inorg. Biochem.* **1999**, *74*, 217.

(19) Ermacora, M. R.; Delfino, J. M.; Cuenoud, B.; Schepartz, A. *Proc. Natl. Acad. Sci. USA* **1992**, *89*, 6383-6387.

(20) Sigman, D. S.; Bruice, T. W.; Mazumder, A.; Sutton, C. L. *Acc. Chem. Res.* **1993**, *26*, 98-104.

(21) Samsel, E. G.; Srinivasan, K.; Kochi, J. K. *J. Am. Chem. Soc.* **1985**, *107*, 7606-7617.

(22) Srinivasan, K.; Michaud, P.; Kochi, J. K. *J. Am. Chem. Soc.* **1986**, *108*, 2309-2320.

(23) Jacobsen, E. N. In *Comprehensive organometallic chemistry II*; Abel, E. W., Stone, F. G. A., Wilkinson, G., Eds.; Pergamon: New York, 1995; Vol. 12, pp 1097-1135.

(24) Katsuki, T. *Coord. Chem. Rev.* **1995**, *140*, 189-214.

(25) Hunter, C. L.; Lloyd, E.; Eltis, L. D.; Rafferty, S. P.; Lee, H.; Smith, M.; Mauk, A. G. *Biochemistry* **1997**, *36*, 1010-1017.

(26) Hayashi, T.; Hisaeda, Y. *Acc. Chem. Res.* **2002**, *35*, 35-43.

(27) Hamachi, I.; Shinkai, S. *Eur. J. Org. Chem.* **1999**, 539-549.

(28) Tamura, M.; Asakura, T.; Yonetani, T. *Biochim. Biophys. Acta.* **1973**, *295*, 467-479.

(29) Ozaki, S.; Roach, M.; Matsui, T.; Watanabe, Y. *Acc. Chem. Res.* **2001**, *34*, 818-825.

(30) A preliminary result of 1.8 Å resolution crystal structure of Cr^{III}(3,3'-Me_2-salophen)•apo-A71G Mb shows the distance of 2.12 Å between the Cr^{III} ion and the Nε atom of imidazole in His93. While we do not have the crystal stracture of **Cr•2•apo-Mb**, we believe that it possess the same coordination structure. We are undergoing the final refinement of the X-ray crystal structure to be submitted else where.

(31) **Cr•2•BSA** was synthesized by the reported procedure.[36] The Cr atom and protein concentrations were determined by ICPAES and BCA method,[37] respectively, and

the protein-chromium ratio has been found to be 1:0.3. The catalytic reaction was carried out under the conditions described in Table 1 except for the concentration ([Cr] = 10 μM).

(32) Srinivasan, K.; Kochi, J. K. *Inorg. Chem.* **1985**, *24*, 4671-4679.

(33) Springer, B. A.; Egeberg, K. D.; Sligar, S. G.; Rohlfs, R. J.; Mathews, A. J.; Olson, J. S. *J. Biol. Chem.* **1989**, *264*.

(34) Chen, H.; Cronin, J. A.; Archer, R. D. *Macromolecules* **1994**, *27*, 2174-2180.

(35) Coggon, P.; Mcphail, A. T.; Mabbs, P. E.; Richards, A.; Thornley, A. S. *J. Chem. Soc. (A)* **1970**, 3296-3303.

(36) H. Y. Shrivastava, B. U. Nair, *Biochem. Biophys. Res. Commun.* **2000**, *270*, 749-754.

(37) P. K. Smith, R. I. Krohn, G. T. Hermanson, A. K. Mallia, F. H. Gartner, M. D. Provenzano, E. K. Fujimoto, N. M. Goeke, B. J. Olson, D. C. Klenk, *Anal. Biochem.* **1985**, *150*, 76-85.

PART III

CONSTRUCTION OF ORGANOMETALLOPROTEINS:

In situ Synthesis of Organometalloproteins

Introduction

As biocatalysts, the enzymes are responsible for a variety of chemical reactions in the biological systems. If we are able to design proteins and enzymes having desired reactivities, many synthetic processes will be replaced to enzymic systems, even in industrial scale processes. Many approaches have been developed for the construction of novel proteins based on the native protein scaffolds.[1-6] Among them, chemical modification of either protein or functional groups could introduce diverse functions that are different from those of natural enzymes and cannot be easily incorporated by genetic methods.[6-13] The use of proteins in organometallic chemistry has been a growing area in these couple of years.[14,15] One of the advantage to use proteins in this field is the resulting organometallic proteins are water soluble, thus, reactions by organometallic catalysts will proceed in aqueous solutions. In addition, a variety of metal ligands such as cysteine, histidine, aspartic acid, tyrosine, and so on are available either on the surface or inside of proteins. For example, Whitesides *et al*. investigated a possible use of proteins as chiral supports for rhodium catalysts.[13] They prepared a cationic Rh^{I}-complex of a biotin-linked diphosphine ligand and the complex was attached to avidin by using extremely strong binding affinity of biotin to avidin, a globular protein (Fig. 1).

Recently, we have reported a new method for the preparation of artificial metalloenzymes.[16] Our strategy is the removal of heme from holo-myoglobin (Mb) and then the insertion of a symmetric Cr^{III} Schiff base complex, which is known as an oxidation catalyst in organic solvent,[17] into the empty cavity of apo-Mb as shown in Scheme 1a. The binding affinity of the complex to the apo-Mb cavity and catalytic activity for enantioselective sulfoxidation was improved by a combination of site-directed mutagenesis of Mb with modification of the Schiff base ligand structure.[16] The X-ray crystal structures of artificial metalloproteins, **M^{III}(3,3'-Me_2-salophen)•apo-A71GMb (M=Fe and Cr)** indicate that the Schiff base complexes are captured in the heme pocket of apo-Mb by specific hydrophobic interaction in the active site and the metal coordination to

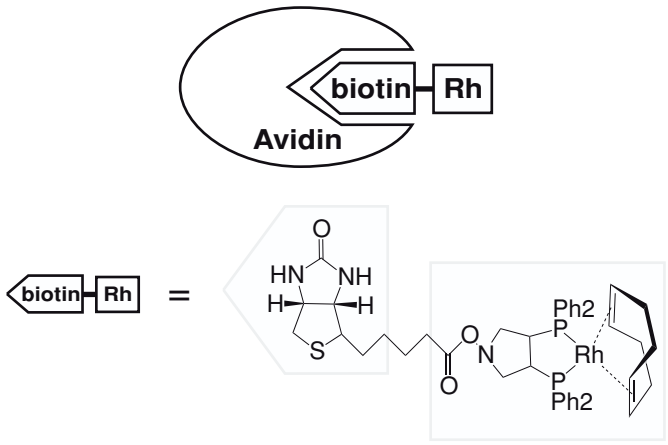

Figure 1. Schematic image of an avidin–biotin–Rh complex composite

imidazole of His93.[18] In this Part, the author describes the synthesis of organometalloproteins by utilizing a noncovalently binding of Ru complexes to apo-Mb (Scheme 1b). At the same time, a vacant site of the protein is used for the synthesis of metal complexes, i.e., organometalloprotein are planned to construct by mixing all components in one portion. Thus, we call this method as "*in situ* synthesis of organometalloproteins." In order to evaluate the "*in situ* synthesis," we have employed electrospray ionization-time of flight mass spectrometry (ESI-TOF MS). ESI-TOF MS has been used to characterize noncovalent complexes of small substrates and biomacromolecules.[19,20] As the components organometalloproteins the author has used apo-Mb, apo-H64D Mb, dichloro(*p*-cymene)ruthenium(II) dimer (**1**), and a series of diamine ligands as shown in Figure 2.

Results and Discussion

In order to compare the ability of self formation of Ru-amine complexes and its binding affinity in the heme cavity of apo-Mb or apo-H64D Mb, **1** and a diamine ligand (2 equiv. each) in methanol were mixed with an aqueous solution (5 mM ammonium acetate, pH6.4) of apo-Mb or apo-H64D Mb (1 equiv.). The reaction solution was directly submitted to ESI-TOF MS for the identification of product(s). Figure 3 shows typical examples

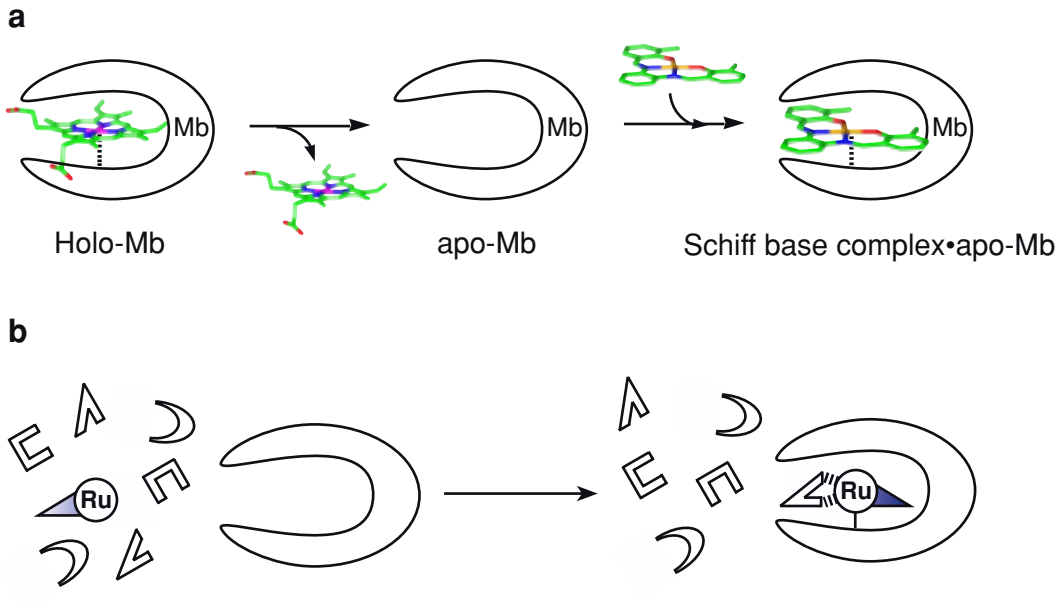

Scheme 1. Schematic drawings of preparation of **M(Schiff base)•apo-Mbs** (**a**) and *in situ* synthesis of orgaometalloproteins (**b**).

of ESI-TOF mass spectra. The spectrum for a mixture of **1**, diamine (**2**), and apo-Mb shows a peak corresponding to Ru^{II}(*p*-cymene)•apo-Mb along with intact apo-Mb. Replacement of apo-Mb to apo-H64D Mb gave the same results. Even in the cases of Ru/diamine**3** and Ru/diamine**4**, the same results were observed. On the other hand, a mixture of apo-Mb, **1**, and diamine **5** or **11**, afforded a mass peak corresponding to Ru(**5**)• or Ru(**11**)•apo-Mb. These are also the cases for apo-H64D Mb. Apparently, aliphatic diamine-Ru complexes and aromatic diamine-Ru complexes show different behaviors. Thus, we have summarized relative intensities of Ru^{II}(*p*-cymene)•apo-Mb (or apo-H64D Mb) over apo-Mb (or apo-H64D Mb) observed in the Ru/diamine (**2**-**4**)/apo-Mb (or apo-H64D Mb) system in Figure 4. Relative intensities of Ru(**5**-**11**)•apo-Mb (or apo-H64D Mb) over apo-Mb (or apo-H64D Mb) are also shown in Figure 5. Very interestingly, Ru(**7**) and Ru(**9**) afforded their protein complexes exclusively with apo-H64D Mb. Ru(**11**) complex shows quite unique properties for its interaction with apo-Mb. While the other Ru com-

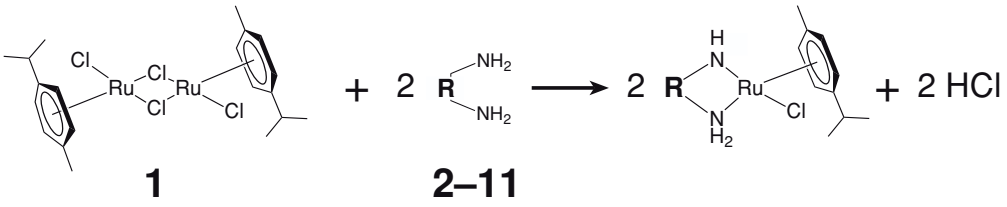

Dichloro(*p*-cymene)ruthenium(II) Dimer

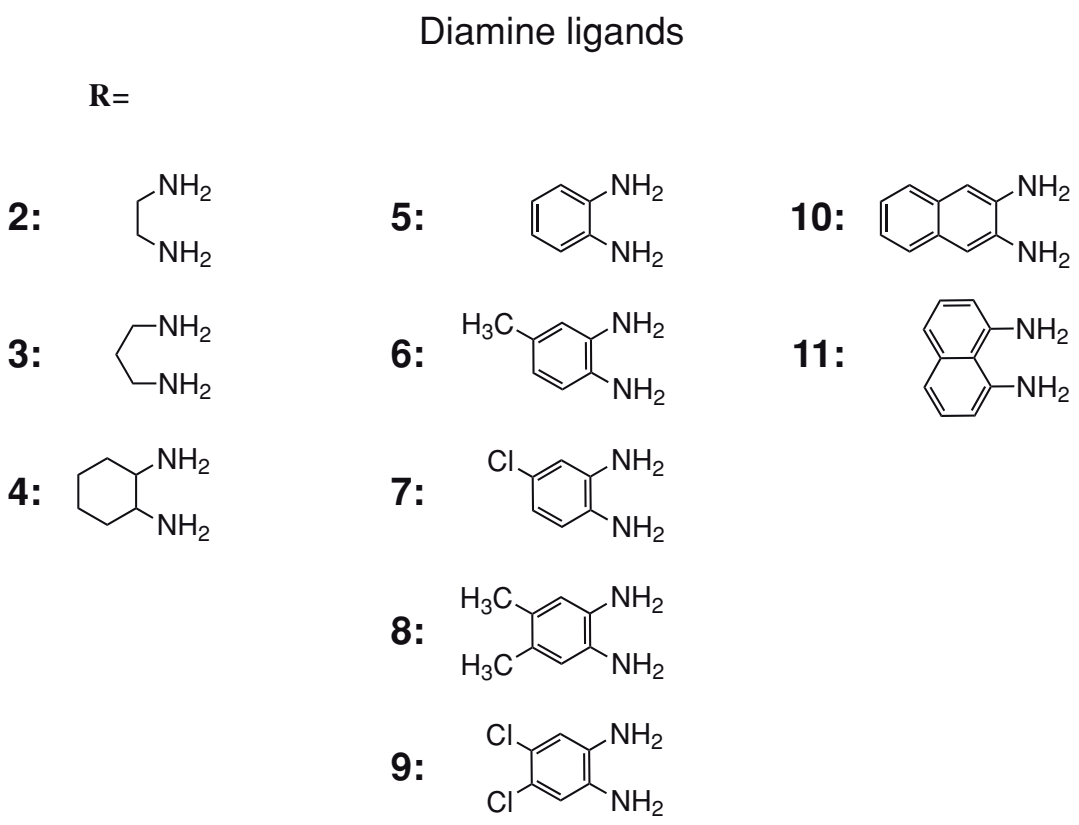

Figure 2. Structures of a Ru complex and diamine ligands.

plexes gave 1:1 complexes with apo-Mb and apo-H64D Mb, complexation of **1**, diamine **11,** and apo-Mb gave a mixtured Ru(**11**)•apo-Mb and [Ru(**11**)]$_2$•apo-Mb as evidenced by the ESI-TOF MS spectra shown in Figure 3E and F. Appearence of the 2:1 complexes in the ESI-TOF MS spectra suggests these 2:1 complexes are stable enough even in the ionization process for the mass measurement. In the cases of Fe^{III}(3,3'-Me_2-salophen)•apo-

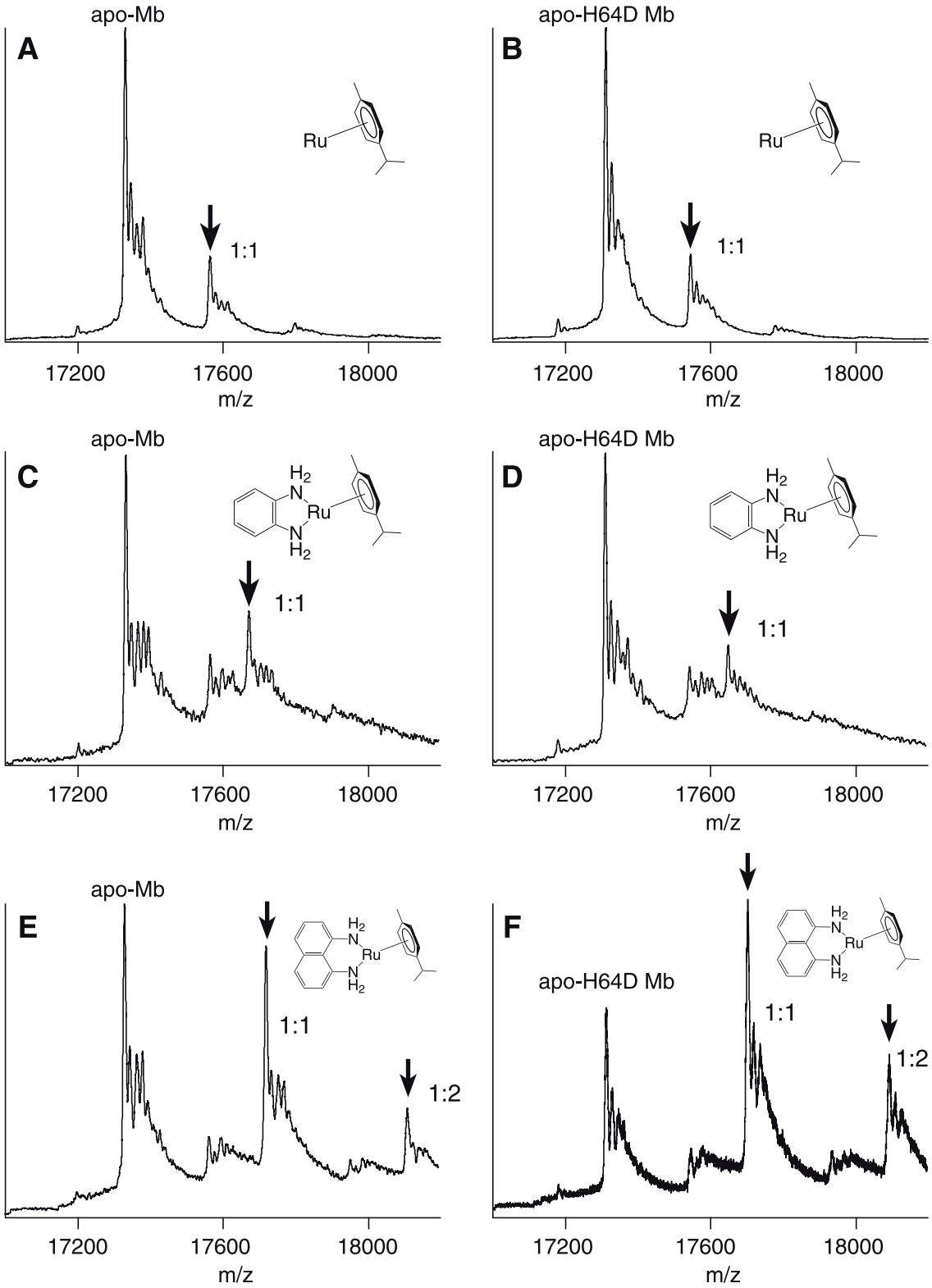

Figure 3. ESI-TOF MS spectra of **1**, amine ligand and apo-Mb or apo-H64D Mb mixture, 10 μM protein dissolved in 5 mM ammonium acetate (pH 6.4) buffer, A; Ru-amine**2**•apo-Mb, B; Ru-amine**2**•apo-H64D Mb, C; Ru-amine**5**•apo-Mb, D; Ru-amine**5**•apo-H64D Mb, E; Ru-amine**11**•apo-Mb, F; Ru-amine**11**•apo-H64D Mb

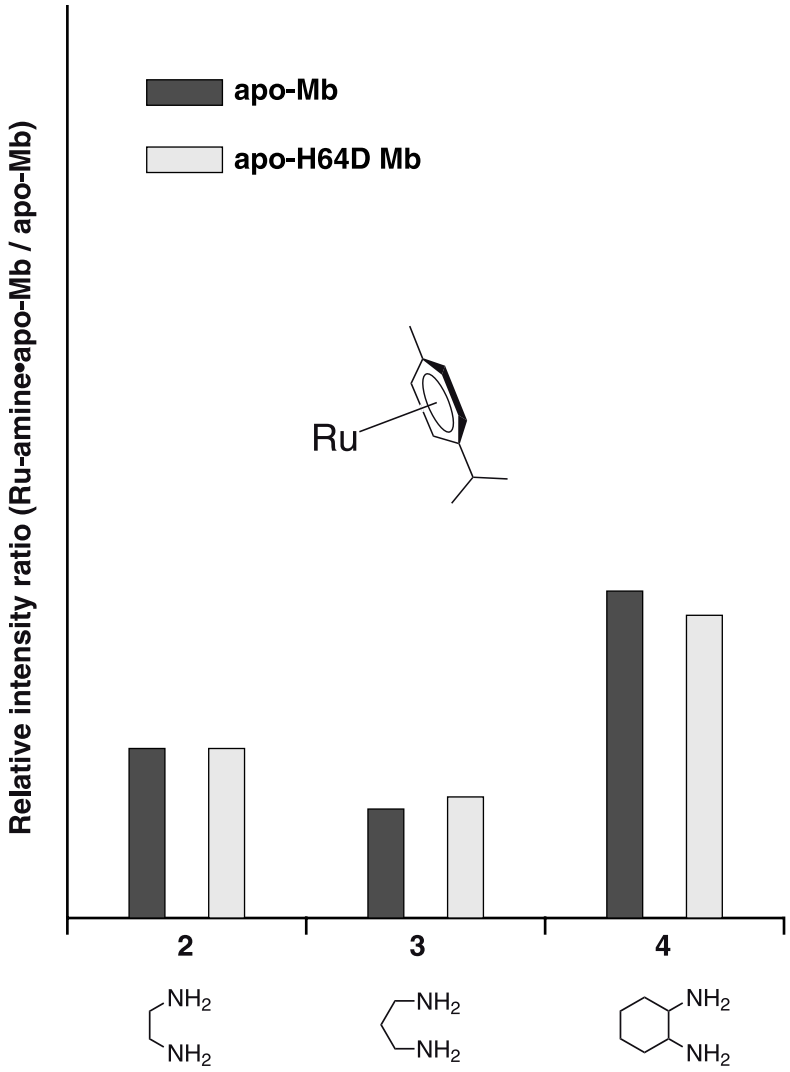

Figure 4. Relative intensity of Ru-(**2**–**4**)•apo-Mb and Ru-(**2**–**4**)•apo-H64D Mb over apo-Mb or apo-H64D Mb in the ESI-TOF mass spectra.

A71G Mb and Cr^{III}(3,3'-Me_2-salophen)•apo-A71G Mb, the ESI-TOF MS spectra of these two complexes show two peaks corresponding to the complexes and apo-A71G Mb even though the samples are purified. Thus, the binding affinity of the second molecule of Ru(**11**) in the 2:1 complex is as strong as the affinity of M(3,3'-Me_2-salophen)•apo-A71G Mb (M=Fe^{III}, Cr^{III}) where M(3,3'-Me_2-salophen) complexes are inserted in the heme cavity of apo-A71G Mb (Fig. 6).[21,22] On the basis of there results, one may consider that two

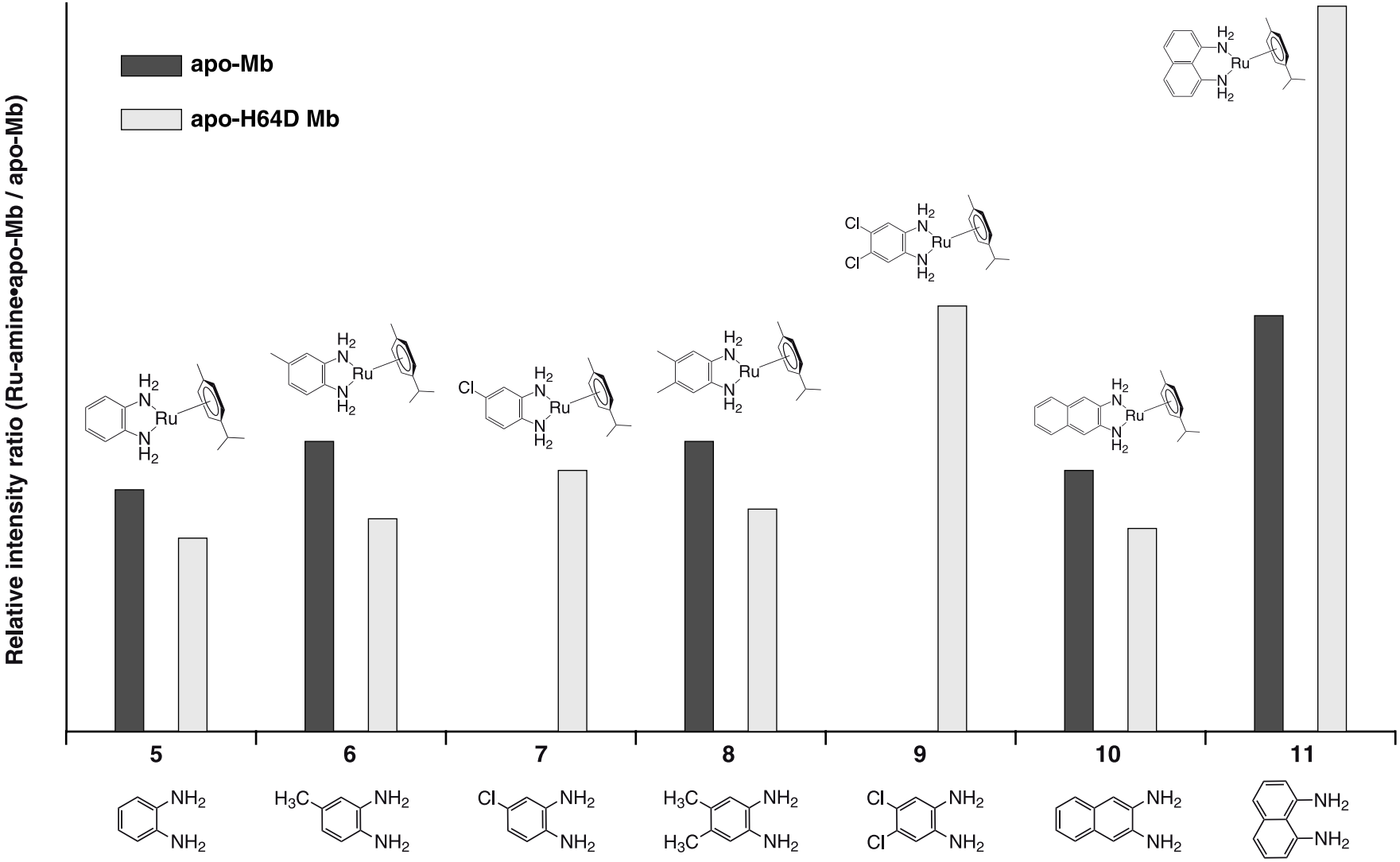

Figure 5. Relative intensity of Ru-(**5–11**)•apo-Mb and Ru-(**5–11**)•apo-H64D Mb over apo-Mb orapo-H64D Mbin the ESI-TOF mass spectra.

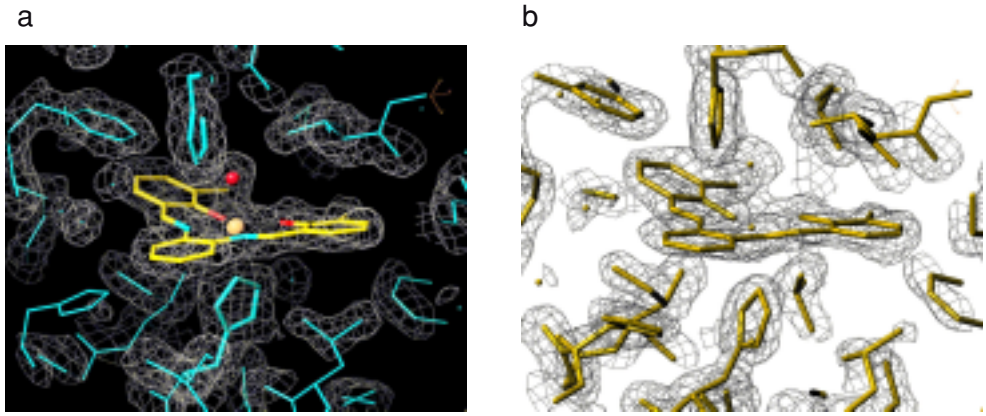

Figure 6. X-ray crstal structures of Cr^{III}(3,3'-Me_2-salophen)•apo-A71G Mb (**a**) and Fe^{III}(3,3'-Me_2-salophen)•apo-A71G Mb (**b**)

Ru(**11**) complexes could be inserted in the heme cavity. However, the heme cavity of apo-Mb and apo-H64D Mb is not spacious enough to accomodate two Ru(**11**) complexes at the same time, suggesting one molecule of the Ru(**11**) complex must be bound on a protein surface of apo-H64D Mb. There are several example of metal complexes bound on protein surfaces. For example, Gray *et al*. and Marchetti *et al*. have prepared a number of Co^{III}(Schiff base) or $Rh^{I}(CO)_2$(acac) bound on the surface of Mb or human serum albumin.[23,24]

Exclusive formation of Ru-diamine•apo-Mbs when **R** in diamine is aromatic groups suggests that the aromatic diamines (**5**–**11**) were incorporated in the heme cavity of apo-Mb while aliphatic diamines (**2**–**4**) failed to be incorporated. These results indicate that apo-Mb could discriminate aliphatic compounds from aromatic compound in the "*in situ*" reconstitution of organometallic proteins.

In summary, the author has investigated the specific interaction of Ru-amine complexes with apo-Mb and apo-H64D Mb by using an ESI-TOF mass screening method. The binding affinity of Ru-amine complexes to apo-Mb or apo-H64D Mb was improved by highly hydrophobic aromatic diamine ligands **5**–**11**. A similar trend was also observed in Fe^{III}(Schiff base)•apo-Mb described in chapter 2 on part II. Therefore, the hydrophobic

interaction between organometallic complexes and proteins is important for the construction of stable organometalloproteins. The screening method which is based on relative peak intensity of ESI-TOF mass spectra can be applicable to many other protein-organometallic complexes to estimate the binding affinity.

Experimental Section

Materials. Reagents were purchased from TCI, Wako, Nacalai Tesque, Aldrich, and used without further purification. The expression vector for wild type of sperm whale Myoglobin (Mb) is a gift from John Olson (Rice University).[25] The expression and purification of Mb were performed according to a method described by Springer *et al*. with some modification. Apomyoglobin (apo-Mb) was prepared using an acid-butanone method.[26]

Preparation of Ru-amine mixtures. The each Ru-amine complexes were prepared by following method. To the methanol solution of dichloro(*p*-cymene)Ru^{II} (100 μl, 5 mM) was added methanol solution of diamine ligand (50 μl, 20 mM). The mixture was stirred for 1 min at R.T. and stood for overnight at R.T.

Preparation of Ru-amine•apo-Mb. Apo-Mb and apo-H64D Mb were dialyzed against 10 mM ammonium acetate buffer (pH 6.7) at 4 ˚C for 12 h. The methanol solution of Ru-amine (6 μl, 10 mM) was added into apo-Mb and apo-H64D Mb (1.4 ml, 20 mM) respectively. The mixture solution was stood at 4 ˚C for 3 h. The resulting solutions were diluted to 10 μM with the water and filtrated with PTFE filter to remove precipitates.

ESI-TOF mass screening. ESI-TOF mass analyses were performed on a Micromass LCT. Typical parameters were as follows; capillary voltage: 3 kV, cone voltage: 30 V, source temperature: 60 °C, the flow-rate: 5 μl min^{-1}. CsI (1 mg/ml) in 50% H_2O/CH_3CN was used for mass scale calibration.

Reference

(1) DeGrado, W. F. *Chem. Rev.*, **2001**, *101*, 3025-3026.

(2) Bayley, H. *Curr. Opin. Biochem.* **1999**, *10*, 94-103.

(3) Benson, D. E.; Wisz, M. S.; Hellinga, H. W. *Curr. Opin. Biochem.* **1998**, *9*, 370-376.

(4) Lu, Y.; Berry, S. M.; Pfister, T. D. *Chem. Rev.* **2001**, *101*, 3047-3080.

(5) Qi, D.; Tann, C.; Haring, D.; Distefano, M. D. *Chem. Rev.* **2001**, *101*, 3081-3111.

(6) Sigman, D. S.; Bruice, T. W.; Mazumder, A.; Sutton, C. L. *Acc. Chem. Res.* **1993**, *26*, 98-104.

(7) Davies, R. R.; Distefano, M. D. *J. Am. Chem. Soc.* **1997**, *119*, 11643-11652.

(8) Ermacora, M. R.; Delfino, J. M.; Cuenoud, B.; Schepartz, A. *Proc. Natl. Acad. Sci. USA* **1992**, *89*, 6383-6387.

(9) Hamachi, I.; Shinkai, S. *Eur. J. Org. Chem.* **1999**, 539-549.

(10) Hayashi, T.; Hisaeda, Y. *Acc. Chem. Res.* **2002**, *35*, 35-43.

(11) Lin, C. C.; Lin, C. W.; Chan, A. S. C. *Tetrahedron: Asymmetry* **1999**, *10*, 1887-1893.

(12) Neya, S.; Tsubaki, M.; Hori, H.; Yonetani, T.; Funasaki, N. *Inorg. Chem.* **2001**, *40*, 1220-1225.

(13) Wilson, M. E.; Whitesides, G. M. *J. Am. Chem. Soc.* **1978**, *100*, 306-307.

(14) Cornils, B.; Herrmann, W. A., Eds. *Aqueous-Phase Organometallic Catalysts Concepts and Applications*; Wiley-VCH: New York, 1998.

(15) Joo, F., Ed. *Aqueous Organometallic Catalysis*; Kluwer Academic Publishers: London, 2001; Vol. 23.

(16) Ohashi, M.; Koshiyama, T.; Ueno, T.; Yanase, M.; Fujii, H.; Watanabe, Y. *Angew. Chem. Int. Ed.* **2003**, *42*, 1005-1008.

(17) Srinivasan, K.; Kochi, J. K. *Inorg. Chem.* **1985**, *24*, 4671-4679.

(18) Watanabe, Y. *The final structure will be submitted somewhere*.

(19) Przybyski, M.; Glocker, M. O. *Angew. Chem. Int. Ed.* **1996**, *35*, 806-826.

(20) Wan, K. X.; Shibue, T.; Gross, M. L. *J. Am. Chem. Soc.* **2000**, *122*, 300-307.

(21) Ueno, T.; Koshiyama, T.; Ohashi, M.; Kono, M.; Kondo, K.; Szuki, A.; Yamane, T.; Watanabe, Y. in preparation.

(22) Ueno, T.; Ohashi, M.; Kono, M.; Kondo, K.; Szuki, A.; Yamane, T.; Watanabe, Y. in preparation.

(23) Blum, O.; Haiek, A.; Cwikel, D.; Dori, Z.; Meade, T. J.; Gray, H. B. *Proc. Natl. Acad. Sci. USA* **1998**, *95*, 6659-6662.

(24) Marchetti, M.; Mangano, G.; Paganelli, S.; Botteghi, C. *Tetrahedron Lett.* **2000**, *41*, 3717-3720.

(25) Springer, B. A.; Sligar, S. G. *Proc. Natl. Acad. Soc.* **1987**, *84*, 8961-8965.

(26) Ascoli, F.; Fanelli, M.; Antonini, E. *Methods Enzymol* **1981**, *76*, 72-87.

PART IV

SUMMARY AND CONCLUSION

In the present thesis, the author has aimed to construct artificial metalloproteins by noncovalent insertion of metal complexes into protein cavities. In order to control functions of the resulting artificial metalloproteins, both site-directed mutagenesis of protein cavities and modification of metal complex ligands were carried out.

Part II describes the construction of artificial metalloenzyme by noncovalent insertion of metal-Schiff base complexes into the heme cavity of apo-myoglobin and its mutants. Chapter 1 describes effects of the mutation at the position 71 in Mb on thermal stability and the cyanide association rate of Fe^{III}(Schiff base)•apo-Mb. Substituent effects of Schiff base ligand on the thermal stability and cyanide association rate of Fe^{III}(Schiff base)•apo-Mb were examined in chapter 2. In chapter 3, Cr and Mn Schiff base complexes were employed for the construction of artificial monooxygenase.

Fe^{III}(3,3'-Me_2-salophen)•apo-Mb and **Fe^{III}(3,3'-Me_2-salophen)•apo-A71G Mb** were crystallized for the structural analysis. The crystal structure of **Fe^{III}(3,3'-Me_2-salophen)•apo-A71G** shows that the 3- and 3'-methyl group in the salophen ligand are in Van der Waals contact with Ile107. In contract, **Fe^{III}(3,3'-Me_2-salophen)•apo-Mb** structure shows the electron density of the salophen ligand, the iron atom, and the imidazole ring of His93 appears to be disordered. These results suggest that Gly at the position 71 plays a crucial role for the fixation of the Schiff base ligand in the heme cavity of Mb. Furthermore, the cyanide association rate constant of **Fe^{III}(3,3'-Me_2-salophen)•apo-A71GMb** is 216-fold larger than that of **Fe^{III}(3,3'-Me_2-salophen)•apo-Mb**. These results indicated that the Ala71 to Gly mutation considerably improved the cyanide association.

The substituents on Schiff base ligand also influenced the thermal stability and cyanide association rate of Fe^{III}(Schiff base)•apo-Mb. The author has employed three types of Fe^{III}(Schiff base); Fe^{III}(salophen) (**1**), Fe^{III}(3,3'-Me_2-salophen) (**2**), and Fe^{III}(5,5'-*t*-Bu_2-salophen) (**3**). Each Fe^{III}(Schiff base)•apo-Mb showed different thermal stability (**2** > **1** > **3**) and cyanide association rate (**1** > **3** > **2**). These results indicate that the Schiff base ligand plays important two roles. The hydrophobic interactions as well as the minimiza-

tion of steric hindrance of the ligand regulate the location and orientation of the metal complex in the protein matrix. The different orientation and location of the complexes affect the reactivity of the metal complexes such as cyanide binding.

Symmetric Cr^{III}(5,5'-*t*-Bu_2-salophen) was also inserted into the heme cavity of apo-Mb and its mutants by the ligation to His93. The resulting semi-synthesized metalloenzymes catalyze enantioselective sulfoxidation in water by utilizing the chiral protein cavity. Although the semi-synthetic metalloenzymes still exhibit low reactivity and enantioselectivity, these experiments promise the possibility of this method for the design of artificial metalloenzymes.

Part III is aimed to apply our strategy to the construction of organometalloproteins. The complexation and binding affinity of Ru-amine complexes with apo-Mb or apo-H64D Mb were estimated by relative intensity of the Ru complex–apo-Mb composites in ESI-TOF mass spectra. ESI-TOF MS measurements indicate the formation of Ru-amine•apo-Mb complexes. Futher, the comparison of relative peak intensities of a series of Ru complexes in ESI-TOF MS suggested that the hydrophobicity of the diamine ligand is important to stabilize the Ru-amine complex in the apo-Mb cavity.

Throughout the work in Part II, the author has demonstrated the strategy for the construction of artificial metalloenzymes by the noncovalent insertion of metal complexes into the apo-Mb cavity. In addition, thermal stability and activity of the artificial metalloenzymes are controlled by protein mutation or chemical modification of the metal complex ligand. The studies in Part III suggest that it is possible to construct organometalloproteins and the resulting organometalloproteins are expected to be new biomaterials having novel properties.

ACKNOWLEDGMENT

The present thesis is a summary of the author's studies from 2000 to 2002 at Department of Structural Molecular Science, the Graduate University for Advanced Studies. This work is generously supported by Institute for Molecular Science and Graduate School of Science, Nagoya University and carried out under the supervision of Prof. Yoshihito Watanabe. The author wishes to express his cordial gratitude to Prof. Yoshihito Watanabe for his continual direction, stimulating discussion, and hearty encouragement. The author also owes his accomplishment of the studies to the discerning advice and helpful discussion by Dr. Takafumi Ueno. The author wishes to thank Miss Tomomi Koshiyama, Mr. Satoshi Abe, and Mr. Toshimitsu Tsuruga (Nagoya University) for their help as collaborators.

The author is really grateful to Prof. John S. Olson (Rice University) for providing cDNA of sperm whale myoglobin, Prof. Takashi Yamane, Mr. Masaharu Kono, and Mr. Kazuyoshi Kondo (Nagoya University) for X-ray crystalstructure analyses, and Prof. Saburo Neya and Prof. Hiroshi Fujii for their useful suggestion for EPR measurements.

This work would not have been possible without help of the members and co-workers in the Prof. Watanabe's research group. The author is deeply indebted to Drs. Seiji Ogo, Manabu Yanase, Hidetaka Nakai, Shiro Yoshioka, Kazuharu Suzuki, Isao Hara, Hui-Jun Yang, Ryo Yamahara, Akira Odani, Shun Hirota, and Yukari Fujimoto for valuable suggestion and unfailing encouragement. Acknowledgments are also due to Mrs. Misako Tanizawa and Mrs. Akiyo Ota for their office work and heartfelt kindness.

Finally, the author would express his sincere gratitude to his parents for their supports, generous understanding, and affectionate encouragement.

Nagoya, January 2003

大橋雅卓

Masataka Ohashi

LIST OF PUBLICATIONS

1. Preparation of Artificial Metalloenzymes by Insertion of Chromium(III) Schiff Base Complexes into Apo-Myoglobin Mutants
   Masataka Ohashi, Tomomi Koshiyama, Takafumi Ueno, Manabu Yanase, Hiroshi Fujii, and Yoshihito Watanabe
   Angew. Chem. Int. Ed. **2003**, *42*, 1005-1008.

OTHER PUBLICATIONS

1. Ammonium Dichlorobis(dimethylglyoximato)iridate(III)
   Masataka Ohashi, Hidetaka Yuge,and Takeshi Ken Miyamoto
   Acta Crystallographica Section C **2000**, *56*, E38-E39.

2. Role of Iron in Particulate Methane Monooxygenase from *Methylosinus trichosporium* OB3b
   Masayuki Takeguchi, Masataka Ohashi, and Ichiro Okura
   BioMetals **1999**, *12*, 123-129.

3. The Role of Ala71 in Apo-Myoglobin on Schiff Base Binding and Cyanide Association to Fe^{III}(Schiff Base)•Apo-Myoglobins
   Takafumi Ueno, Masataka Ohashi, Masaharu Kono, Kazuyoshi Kondo, Atsuo Szuki, Takashi Yamane, and Yoshihito Watanabe
   in preparation.

4. Regulation of Cyanide Binding to Fe^{III}(Schiff Base)•Apo-Myoglobin by the Schiff Base Ligand Structure

Masataka Ohashi, Takafumi Ueno, Masaharu Kono, Kazuyoshi Kondo, Atsuo Szuki, Takashi Yamane, and Yoshihito Watanabe

in preparation.

5. Structure Determination of an Artificial Metalloprotein: Cr^{III}(3,3'-Me_2-Salophen)•Apo-A71G Myoglobin

Takafumi Ueno, Tomomi Koshiyama, Masataka Ohashi, Masaharu Kono, Kazuyoshi Kondo, Atsuo Szuki, Takashi Yamane, and Yoshihito Watanabe

in preparation.

Semisynthetic Metalloenzymes

Preparation of Artificial Metalloenzymes by Insertion of Chromium(III) Schiff Base Complexes into Apomyoglobin Mutants**

*Masataka Ohashi, Tomomi Koshiyama, Takafumi Ueno, Manabu Yanase, Hiroshi Fujii, and Yoshihito Watanabe**

Construction of artificial metalloenzymes is one of the most important subjects in bioinorganic chemistry, because metalloenzymes catalyze chemical transformations with high selectivity and reactivity under mild conditions.[1–4] There are several reports on protein design: introduction of metal binding sites,[1,3,5–8] design of substrate binding cavities,[9–12] chemical modification of prosthetic groups,[13–16] and covalent attachment of metal cofactors.[2,17–20] In particular, the covalent modification of proteins is a powerful tool for the generation of new metalloenzymes, while the efficiency of the modification is very much dependent on the position and reactivity of the cysteinyl thiol functional group.[2] Herein, we describe a novel strategy for the preparation of artificial metalloenzymes by noncovalent insertion of metal-complex catalysts into protein cavities. The resulting semisynthetic metalloenzymes, apo-myoglobin (apo-Mb) reconstituted with Cr^{III} Schiff base complexes, are able to catalyze enantioselective sulfoxidation.

Manganese(III) and chromium(III) Schiff base complexes are known to be catalysts for various oxidations in organic solvents.[21,22] Jacobsen,[23] and Katsuki[24] have already reported many examples of asymmetric oxidations catalyzed by chiral Mn Schiff base complexes. In our case, symmetric complexes, $[M^{III}(salophen)]^+$ (M·**1**; M = Mn, Cr; H_2 salophen

[*] Prof. Dr. Y. Watanabe, T. Koshiyama
Department of Chemistry
Graduate School of Science
Nagoya University
Nagoya 464-8602 (Japan)
Fax: (+81) 52-789-2953
E-mail: yoshi@nucc.cc.nagoya-u.ac.jp
M. Ohashi
Department of Structural Molecular Science
The Graduate University for Advanced Studies
Okazaki 444-8585 (Japan)
Dr. T. Ueno
Research Center for Materials Science
Nagoya University
Nagoya 464-8602 (Japan)
Dr. M. Yanase
Institute for Molecular Science
Okazaki 444-8585 (Japan)
Prof. Dr. H. Fujii
Center for Integrative Bioscience and Institute for Molecular Science
Okazaki 444-8585 (Japan)

[**] This work was supported by a Grant-in-Aid for Scientific Research 11490036 and 1122828 (to Y.W.), 13740384 (to T.U.). We also thank Prof. T. Yamane, Prof. A. Suzuki, and Mr. M. Kono at Nagoya University for valuable guidance and help with the X-ray crystallographic analysis.

  1433-7851/03/4209-1005 $ 20.00+.50/0

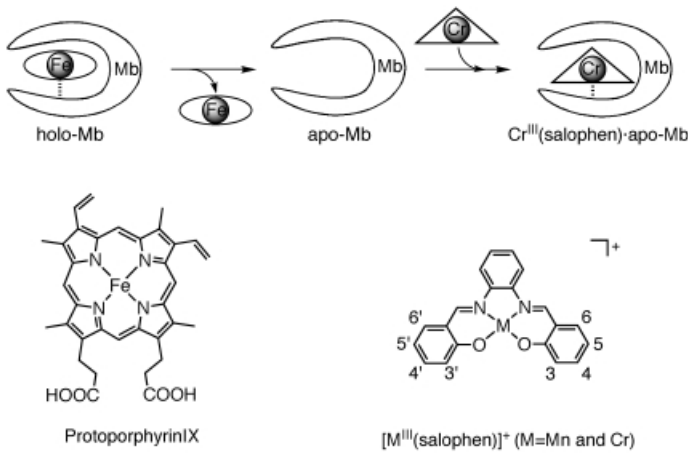

Figure 1. Insertion of a salophen complex into apo-Mb.

(**1**) = *N*,*N*′-bis(salicylidene)-1,2-phenylenediamine) are inserted into a chiral cavity of apo-Mb (Figure 1). In addition, the 5- and 5′- positions of salophen are substituted by a *tert*-butyl group, 5,5′-*t*Bu$_2$-salophen (**2**) to improve the binding affinity to apo-Mb, that is, the binding affinity of heme in apo-Mb is provided by the hydrophobic interaction, and the ligand size.[25] We found that similar factors are important for metal complexes to be inserted into the Mb cavity.

For the creation of artificial metalloenzymes, apo-Mb is an excellent candidate, since reconstitution of apo-Mb with heme has been well studied.[13,26–28] We demonstrated that the catalytic selectivity and reactivity of Mb as a peroxygenase are controlled by appropriate site-directed mutagenesis in the active site.[10,11,29] On the basis of these results, we have designed a suitable apo-Mb mutant for the reconstitution with Schiff base complexes by using the Insight II/Discover 3 program. A designed protein structure, Cr·**2**·apo-H64D/A71GMb, is shown in Figure 2b. If we assume that Cr·**2** binds to His 93 as observed for heme, the replacement of His 64 with Asp (H64D) will provide increased access of substrates and oxidants to a vacant distal site above the Cr^{III} center.[11] At the same time, the alanyl side chain at the position 71 in Mb is expected to locate very close to the 4- and 5- positions of Cr·**2** (Figure 2). Thus, Ala 71 was replaced with Gly (A71G) to improve the binding affinity of Cr·**2** in the active site.

The reconstitution of apo-Mb with Cr·**2** was carried out by applying a method used for modified hemes;[28] [Cr·**2**·2H$_2$O]BF$_4$ dissolved in MeOH (0.9 equiv, 0.7 mM) was added dropwise to an apo-Mb solution in Tris/HCl (10 mM, pH 7.0). The mixture was dialyzed against Bis-Tris/HCl (10 mM pH 6.0) and then loaded on Sephadex G-25. The final purification was performed on a CM52 column with linear gradient Tris/HCl buffer (10–100 mM pH 7.0), which gave a 15% yield of isolated Cr·**2**·apo-Mb. The yield of isolated Cr·**2**·apo-H64D/A71GMb (4.3%) was about 15-fold larger than that of Cr·**1**·apo-H64D/A71GMb (0.3%) and almost twice as large as that of Cr·**2**·apo-H64DMb (2.4%). In contrast, all efforts made to prepare Mn·**1**·apo-H64D/A71GMb failed. These results imply that the type of metal ion and the ligand structure are important factors that influence the binding affinity of the metal complexes with the Mb mutants.

The deconvoluted ESI-TOF mass spectrum of purified Cr·**2**·apo-Mb in ammonium acetate (5 mM; Figure 3a) shows two peaks, which are readily assigned to Cr·**2**·apo-Mb (measured: 17808.3 ± 1.1 Da, calcd: 17808.6 Da) and a small portion of apo-Mb (measured: 17330.0 ± 0.1 Da, calcd: 17330.1 Da), respectively. The appearance of a small peak corresponding to apo-Mb is also observed for purified heme-bound Mb (holo-Mb) under the same conditions, which indicates that the binding affinity of Cr·**2** is comparable to that of heme. To confirm that Cr·**2** is incorporated into the heme position, the following experiments were performed. In the first experiment, a mixture of apo-Mb and two equivalents of hemin was analyzed by ESI-TOF mass spectrometry (MS) and holo-Mb was observed as the main peak of the resulting spectrum (measured: 17945.6 ± 0.1 Da, calcd: 17946.6 Da; Figure 3b). In the second experiment, a solution of hemin (two equiv) in DMF was added to purified Cr·**2**·apo-Mb in ammonium acetate (5 mM). The ESI-TOF mass spectrum of the resulting solution (Figure 3c) shows peaks assigned to holo-Mb and Cr·**2**·apo-Mb + heme (measured: 18421.6 ± 0.3 Da, calcd: 18424.7 Da), which are smaller than the peaks of Cr·**2**·apo-Mb. If the Cr^{III} complex binds to the surface of apo-Mb, we expect to observe Cr·**2**·apo-Mb + heme as the major peak, since the incorporation of heme into apo-Mb is very rapid and the mutation of His 64 and Ala 71 should not be effective for the reconstitution. In addition, the preliminary results of an X-ray crystallographic analysis of

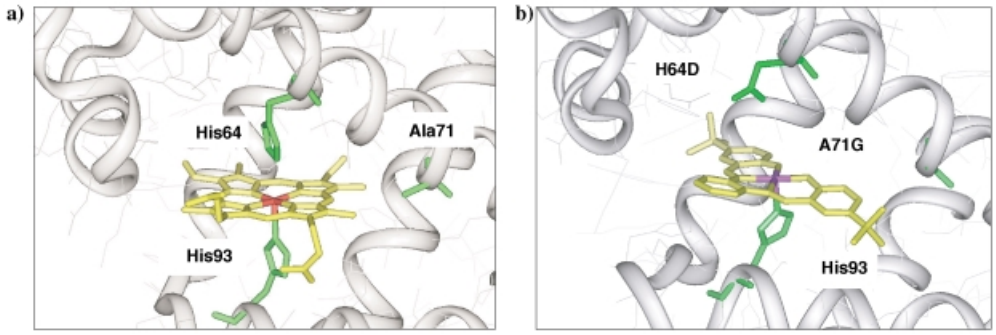

Figure 2. Comparison of a) the crystal structure of wild-type Mb (PDB code 2MBW) with b) a proposed structure of Cr·**2**·apo-H64D/A71GMb calculated by the Insight II/Discover 3 program (ESFF force field). The parts of apo-Mb that interact with Cr·**2** are shown in green, **2** is yellow, Cr is a) red or b) purple.

  1433-7851/03/4209-1006 $ 20.00+.50/0

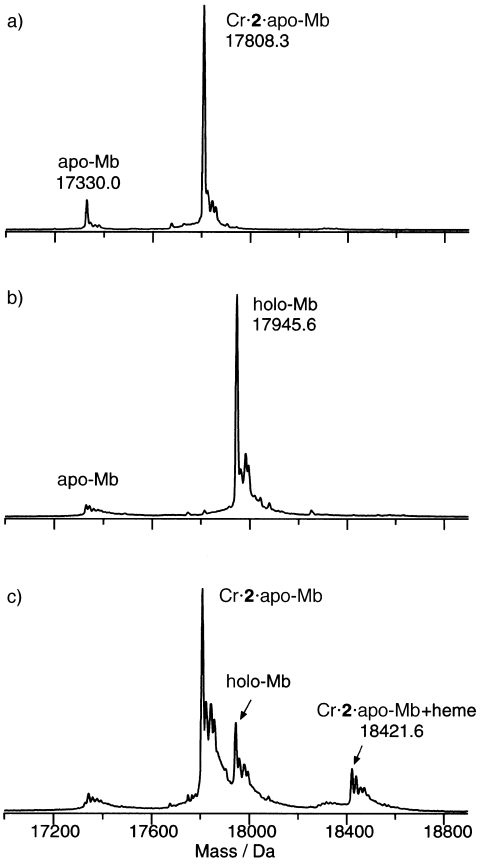

Figure 3. Deconvoluted ESI-TOF mass spectra of a) Cr·**2**·apo-Mb, b) apo-Mb with two equivalents of hemin, and c) Cr·**2**·apo-Mb with two equivalents of hemin in ammonium acetate (5 mM). Sample preparation for b) and c): two equivalents of hemin (1 mM, DMF solution) was added to purified Cr·**2**·apo-Mb (10 μM) and apo-Mb (10 μM), respectively. The mixtures were stirred for 10 min and then dialyzed against 5 mM ammonium acetate for 8 h at 4 °C.

Cr(3,3′-Me_2-salophen)·apo-A71GMb show that the Cr^{III} ion binds to the Nε atom of imidazole in His 93.[30] Thus, we concluded that the His 93 coordination is crucial for Cr·**2** to locate in the active site of Mb.

The H_2O_2-dependent sulfoxidation of thioanisole was examined at 35 °C and pH 5.0 (Table 1). The rate and enantiomeric excess of the sulfoxidation were determined by HPLC analysis (Daicel OD chiral-sensitive column).[9] Catalysts Cr·**1**·apo-H64D/A71GMb, and Cr·**2**·apo-H64D/A71GMb exhibit the highest sulfoxidation activities (entries 4 and 5), whereas Cr·**2**·apo-H64DMb has the lowest activity (entry 3). Catalysts Cr·**1**·apo-H64D/A71GMb and Cr·**2**·apo-H64D/A71GMb showed an approximately sixfold rate increase over Cr·**2** (entries 4,5 versus entry 7). Notably, Cr·**2**·apo-H64D/A71GMb gave (*S*)-methylphenyl sulfoxide with a 13 % *ee*, while the sulfoxidation catalyzed by Cr·**2** proceeded with no enantiomeric discrimination. The other mutants show lower enantioselectivity than that of Cr·**2**·apo-H64D/A71GMb. In a control experiment, the sulfoxidation by Cr·**2**·bovin serum albumin (BSA) was performed (Table 1, entry 6).[31] The enantioselectivity and rate were very low compared with those achieved with Cr·**2**·apo-H64D/A71GMb because of the nonspecific binding ability of Cr·**2** to BSA and the absence of histidine coordination to the Cr^{III} complex. This result indicates that the cavity of an apo-Mb mutant, and His 93 coordination to the Cr^{III} atom are important to improve the enantioselectivity and rate of the sulfoxidation. Furthermore, the EPR spectrum of Cr·**2**·apo-H64D/A71GMb oxidized by *m*-chloroperbenzoic acid at 5 K (pH 7.0) shows a signal at $g = 1.97$ assigned to an oxochromium(v) species.[32] Thus, the intermediate responsible for the catalytic sulfoxidation is expected to be the oxochromium(v) species formed in the Mb cavity. While the enantioselectivity is still low, the results clearly demonstrate that asymmetric reactions can be performed if we use protein cavities, even though symmetric metal complexes are employed.

In summary, we have demonstrated the insertion of symmetric metal complexes into the active site of apomyoglobin by binding to His 93, and that semisynthetic metalloenzymes catalyze enantioselective sulfoxidation by using the chiral protein cavity. Although the semisynthetic metalloenzymes still exhibit low reactivity and enantioselectivity, our experiments suggest the possible use of this method for the design of artificial metalloenzymes. Refinement of the crystal structure and further design to improve the reactivity and selectivity of the metalloenzymes are currently in progress.

Table 1: The different rates and enantiomeric excesses obtained in the sulfoxidation of thioanisole by using a range of catalysts based on chromium Schiff base complexes in a range of proteins.[a]

Entry	Catalyst	Rate[b]	*ee* [%]
1	Cr·**2**·apo-Mb	46	4.3 (*R*)
2	Cr·**2**·apo-A71GMb	54	6 (*S*)
3	Cr·**2**·apo-H64DMb	27	0.3 (*S*)
4	Cr·**1**·apo-H64D/A71GMb	83	8.3 (*S*)
5	Cr·**2**·apo-H64D/A71GMb	78	13 (*S*)
6	Cr·**2**·BSA	12	0.5 (S)
7	Cr·**2** in buffer	13	0

[a] Sulfoxidations were carried out in sodium acetate buffer (50 mM, pH 5.0) at 35 °C in the presence of a Mb complex (10 μM), thioanisole (1 mM), and H_2O_2 (1 mM). [b] The unit of the rate is 10^{-3} turnover min^{-1}.

Experimental Section

The mutants were constructed by cassette mutagenesis. Expression and purification of the mutants were performed as reported previously.[33] Ligands **1** and **2**, and their Cr^{III} complexes were synthesized by methods described in the references [34, 35].

[Cr·**2**·$2H_2O$]BF_4: ESI-TOF MS: Cr·**2**·$2CH_3CN$ 560 (calcd 560); UV/Vis: λmax (ε $M^{-1}cm^{-1}$) 480 (0.93×10^4), 337 nm (2.35×10^4).

[Cr·**1**·$2H_2O$]BF_4: ESI-TOF MS: Cr·**1**·$(CH_3CN)_2$ 448 (calcd 449); UV/Vis: λmax (ε $M^{-1}cm^{-1}$) 469 (1.04×10^4), 334 nm (2.54×10^4).

Cr·**2**·apo-Mb: ESI-TOF MS: 17808.3 ± 1.1 (calcd 17808.3);UV/Vis: λmax (ε $M^{-1}cm^{-1}$) 485 (1.02×10^4), 341 (2.45×10^4), 270 nm (3.75×10^4).

Cr·**2**·apo-A71GMb: ESI-TOF MS:17793.9 ± 0.9 (calcd 17794.3); UV/Vis: λmax (ε $M^{-1}cm^{-1}$) 483 (1.02×10^4), 341 (2.88×10^4), 281 nm (4.38×10^4).

Cr·**2**·apo-H64DMb: ESI-TOF MS: 17786.0 ± 0.6 (calcd 17786.2); UV/Vis: λmax (ε $M^{-1}cm^{-1}$) 474 (0.95×10^4), 338 (2.39×10^4), 321 (2.41×10^4), 282 nm (3.52×10^4).

  1433-7851/03/4209-1007 $ 20.00+.50/0

Cr·**2**·apo-H64D/A71GMb: ESI-TOF MS: 17772.1 ± 0.3 (calcd 17772.2); UV-Vis: λmax (ε $M^{-1}cm^{-1}$) 471 (1.02×10^4), 339 (2.61×10^4), 280 nm (4.18×10^4).

Cr·**1**·apo-H64D/A71GMb: ESI-TOF MS: 17658.2 ± 0.7 (calcd 17660.1); UV/Vis: λmax (ε $M^{-1}cm^{-1}$) 460 (1.18×10^4), 320 (1.2×10^3), 282 nm (2.3×10^3).

The concentration of Cr ion in the purified enzymes was determined by inductively coupled plasma atom emission spectrometry (ICPAES). The spectra were recorded on a SEIKO SPS 7000 that was calibrated with $K_2Cr_2O_7$ in 0.1 mol L^{-1} HNO_3 (100.3 mg L^{-1}, Wako).

ESI-TOF MS were measured on a LCT (Micromass, UK). Typical parameters: capillary, 3 kV; cone, 60 V; source temperature, 60 °C; flow-rate, 5 μL min^{-1}; mass scale calibration, CsI (1 mg mL^{-1}) in 50 % H_2O/CH_3CN. All samples were dialyzed against 5 mM ammonium acetate for 8–10 h at 4 °C.

EPR spectra were recorded at 5 K on a Bruker E500 (X band) with an Oxford helium cryostat. Samples were prepared by addition of 100 equivalents of *m*-chloroperbenzoic acid (1M in MeOH) to purified Cr·**2**·apo-H64D/A71GMb (1 mM in 10 mM Tris/HCl at pH 7.0). The reaction mixtures were then frozen in liquid nitrogen.

Received: July 15, 2002
Revised: November 19, 2002 [Z19733]

[1] Y. Lu, S. M. Berry, T. D. Pfister, *Chem. Rev.* **2001**, *101*, 3047 – 3080, and references therein.
[2] D. Qi, C.-M. Tann, D. Haring, M. D. Distefano, *Chem. Rev.* **2001**, *101*, 3081 – 3111, and references therein.
[3] D. E. Benson, M. S. Wisz, H. W. Hellinga, *Curr. Opin. Biotechnol.* **1998**, *9*, 370 – 376.
[4] F. v. d. Velde, F. v. Rantwijk, R. A. Sheldon, *Trends Biotechnol.* **2001**, *19*, 73 – 80.
[5] J. A. Sigman, B. C. Kwok, Y. Lu, *J. Am. Chem. Soc.* **2000**, *122*, 8192 – 8196.
[6] O. Braha, B. Walker, S. Cheley, J. J. Kasianowicz, L. Song, J. E. Gouaux, H. Bayley, *Chem. Biol.* **1997**, *4*, 497 – 505.
[7] A. Miyawaki, J. Llopis, R. Heim, J. M. McCaffery, J. A. Adams, M. Ikura, R. Y. Tsien, *Nature* **1997**, *388*, 882 – 887.
[8] A. L. Pinto, H. W. Hellinga, J. P. Caradonna, *Proc. Natl. Acad. Sci. USA* **1997**, *94*, 5562 – 5567.
[9] S. Ozaki, H.-J. Yang, T. Matsui, Y. Goto, Y. Watanabe, *Tetrahedron: Asymmetry* **1999**, *10*, 183 – 192.
[10] I. Hara, T. Ueno, S. Ozaki, S. Itoh, K. Lee, N. Ueyama, Y. Watanabe, *J. Biol. Chem.* **2001**, *276*, 36067 – 36070.
[11] S. Kato, H.-J. Yang, T. Ueno, S. Ozaki, J. George N. Phillips, S. Fukuzumi, Y. Watanabe, *J. Am. Chem. Soc.* **2002**, *124*, 8506 – 8507.
[12] S. Ozaki, P. R. Ortiz de Montellano, *J. Am. Chem. Soc.* **1995**, *117*, 7056 – 7064.
[13] S. Neya, N. Funasaki, *J. Biol. Chem.* **1988**, *263*, 8810 – 8815.
[14] T. Hayashi, Y. Hitomi, T. Ando, T. Mizutani, Y. Hisaeda, S. Kitagawa, H. Ogoshi, *J. Am. Chem. Soc.* **1999**, *121*, 7747 – 7750.
[15] Y.-Z. Hu, S. Tsukiji, S. Shinkai, S. Oishi, I. Hamachi, *J. Am. Chem. Soc.* **2000**, *122*, 241 – 253.
[16] E. Monzani, G. Alzuet, L. Casella, C. Redaelli, C. Bassani, A. M. Sanangelantoni, M. Gullotti, L. D. Gioia, L. Santagostin, F. Chillemi, *Biochemistry* **2000**, *39*, 9571 – 9582.
[17] R. R. Davies, M. D. Distefano, *J. Am. Chem. Soc.* **1997**, *119*, 11643 – 11652.
[18] S. K. Ma, Y. Lu, *J. Inorg. Biochem.* **1999**, *74*, 217.
[19] M. R. Ermacora, J. M. Delfino, B. Cuenoud, A. Schepartz, *Proc. Natl. Acad. Sci. USA* **1992**, *89*, 6383 – 6387.
[20] D. S. Sigman, T. W. Bruice, A. Mazumder, C. L. Sutton, *Acc. Chem. Res.* **1993**, *26*, 98 – 104.
[21] E. G. Samsel, K. Srinivasan, J. K. Kochi, *J. Am. Chem. Soc.* **1985**, *107*, 7606 – 7617.
[22] K. Srinivasan, P. Michaud, J. K. Kochi, *J. Am. Chem. Soc.* **1986**, *108*, 2309 – 2320.
[23] E. N. Jacobsen in *Comprehensive organometallic chemistry II, Vol. 12* (Eds.: E. W. Abel, F. G. A. Stone, G. Wilkinson), Pergamon, New York, **1995**, pp. 1097 – 1135.
[24] T. Katsuki, *Coord. Chem. Rev.* **1995**, *140*, 189 – 214.
[25] C. L. Hunter, E. Lloyd, L. D. Eltis, S. P. Rafferty, H. Lee, M. Smith, A. G. Mauk, *Biochemistry* **1997**, *36*, 1010 – 1017.
[26] T. Hayashi, Y. Hisaeda, *Acc. Chem. Res.* **2002**, *35*, 35 – 43.
[27] I. Hamachi, S. Shinkai, *Eur. J. Org. Chem.* **1999**, 539 – 549.
[28] M. Tamura, T. Asakura, T. Yonetani, *Biochim. Biophys. Acta* **1973**, *295*, 467 – 479.
[29] S. Ozaki, M. Roach, T. Matsui, Y. Watanabe, *Acc. Chem. Res.* **2001**, *34*, 818 – 825.
[30] A crystal structure of Cr(3,3′-Me_2-salophen)·apo-A71GMb with a resolution of 1.8 Å shows a distance of 2.12 Å between the Cr^{III} ion and the Nε atom of imidazole in His 93. While we do not have the crystal structure of Cr·**2**·apo-Mb, we believe that it has the same coordination structure. The final refinement of the X-ray crystal structure of Cr(3,3′-Me_2-salophen)·apo-A71GMb is being completed by our group.
[31] Cr·**2**·BSA was synthesized by using a reported procedure.[36] The Cr atom content was determined by ICPAES, and protein concentration was determined by the bicinchoninic acid (BCA) method,[37] the protein/chromium ratio was determined to be 1:0.3. Catalytic reactions were carried out under the conditions described in Table 1 except for the concentration ([Cr] = 10 μM).
[32] K. Srinivasan, J. K. Kochi, *Inorg. Chem.* **1985**, *24*, 4671 – 4679.
[33] B. A. Springer, K. D. Egeberg, S. G. Sligar, R. J. Rohlfs, A. J. Mathews, J. S. Olson, *J. Biol. Chem.* **1989**, *264*.
[34] H. Chen, J. A. Cronin, R. D. Archer, *Macromolecules* **1994**, *27*, 2174 – 2180.
[35] P. Coggon, A. T. Mcphail, P. E. Mabbs, A. Richards, A. S. Thornley, *J. Chem. Soc. A* **1970**, 3296 – 3303.
[36] H. Y. Shrivastava, B. U. Nair, *Biochem. Biophys. Res. Commun.* **2000**, *270*, 749 – 754.
[37] P. K. Smith, R. I. Krohn, G. T. Hermanson, A. K. Mallia, F. H. Gartner, M. D. Provenzano, E. K. Fujimoto, N. M. Goeke, B. J. Olson, D. C. Klenk, *Anal. Biochem.* **1985**, *150*, 76 – 85.

  1433-7851/03/4209-1008 $ 20.00+.50/0